UNITED NATIONS EDUCATIONAL, SCIENTIFIC AND CULTURAL ORGANIZATION
INTERNATIONAL ATOMIC ENERGY AGENCY
INTERNATIONAL CENTRE FOR THEORETICAL PHYSICS
I.C.T.P., P.O. BOX 586, 34100 TRIESTE, ITALY, CABLE: CENTRATOM TRIESTE

H4.SMR/1058-19

WINTER COLLEGE ON OPTICS

9 - 27 February 1998

Modern Optical Coherence Theory

A. Friberg

Royal Institute of Technology, Stockholm, Sweden

Winter College on Optics
ICTP Trieste, 9-28 Feb 1998

MODERN OPTICAL COHERENCE THEORY

Lecture 1: Preliminaries and Elementary Coherence Phenomena

Lecture 2: Coherent Modes, Partially Coherent Beams, and Focusing

Lecture 3: Propagation, Generalized Radiometry, Coherence Transport, Twist, and Spectral Shifts

Ari T. Friberg
Royal Institute of Technology
Department of Physics II – Optics
S-100 44 Stockholm
Sweden
Tel. ++46 8 790 7296
Fax. ++46 8 789 6672
Email ari.friberg@optics.kth.se

GENERAL REFERENCES ON COHERENCE:

Born, M. and Wolf, E., *Principles of Optics* (Pergamon Press, Oxford and New York, 6th ed., 1980), chapt. X.

Glauber, R. J., "Optical coherence and photon statistics" in *Quantum Optics and Electronics*, Les Houches 1964, C. DeWitt, A. Blandin and C. Cohen-Tannoudji, eds., (Gordon and Breach, New York, 1965), pp. 63-108.

Goodman, J. W., *Statistical Optics* (Wiley, New York, 1985).

Mandel, L. and Wolf, E., "Coherence properties of optical fields", *Rev. Mod. Phys.* 37, pp. 231-287 (1965).

Mandel, L. and Wolf, E., *Optical Coherence and Quantum Optics* (Cambridge University Press, Cambridge, 1995).

Perina, J., *Coherence of Light* (Reidel, Boston, second ed., 1985).

COHERENCE

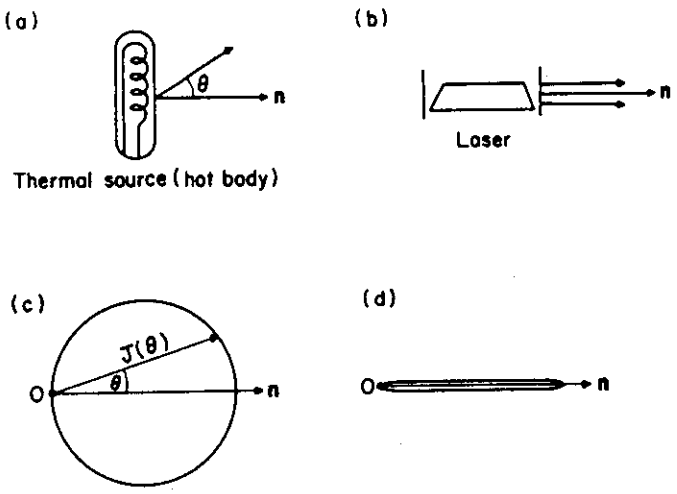

Polar diagrams of radiant intensity $J(\theta)$:

(c) From thermal source (d) From laser

FIG. 2. Comparison of the angular distribution of radiant intensity from a thermal source and from a laser.

- thermal
- spontaneous emission
- random (chaotic)

- laser
- stimulated emission
- non-random (orderly)

- market crowd
- marching soldiers

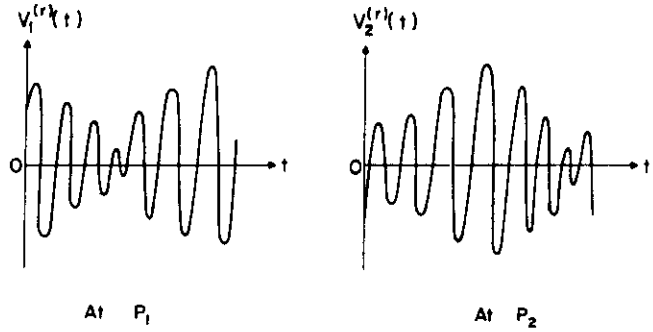

FIG. 3. Illustrating the temporal behavior of the field variable $V^{(r)}(t)$ at two points $P_1(r_1)$ and $P_2(r_2)$ in space.

- interferometry
  - Young
  - Michelson
- correlation functions

[E. Wolf, J. Opt. Soc. Am. 68, 7-17 (1978)]

DOUBLE SLIT (YOUNG)

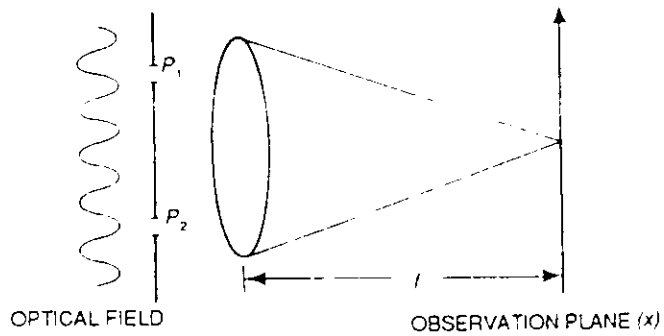

Fig. 10.1 Schematic diagram of the experimental arrangement.

Airy pattern

$$\left| \frac{2J_1(x)}{x} \right|^2 .$$

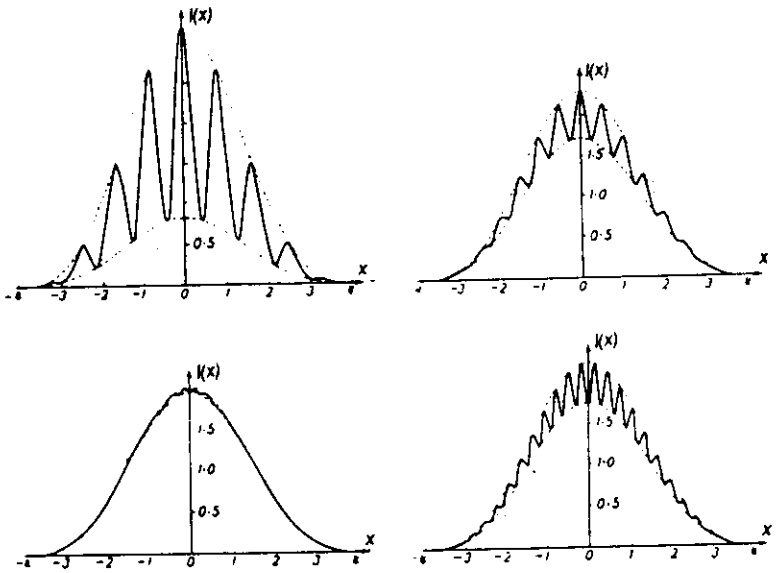

Fig. 10.3 Intensity plots of typical results of Fig. 10.2.

Fringe visibility

$$V = \frac{I_{max} - I_{min}}{I_{max} + I_{min}} .$$

$$I(P) = I_1 + I_2 + 2\sqrt{I_1 I_2}\,|\gamma_{12}| \cos \Phi_{12}$$

$|\gamma_{12}| = V$

Φ_{12} ↑ path difference

INTERFERENCE LAW

(quasi-monochromatic light)

COMPLEX ANALYTIC SIGNAL

(D. Gabor, 1946)

$$E(t) = \int_{-\infty}^{\infty} \tilde{E}(\omega) e^{-i\omega t} d\omega$$

↓ reality $\Rightarrow$ $\tilde{E}(-\omega) = E^*(\omega)$

ANALYTIC SIGNAL

$$\boxed{V(t) \equiv \int_{0}^{\infty} \tilde{E}(\omega) e^{-i\omega t} d\omega}$$

- $E(t) = 2 \mathrm{Re}\, V(t)$
- $V(t) V^*(t) = \frac{1}{2} \overline{E^2(t)}$
- analytic in lower $z = t + is$ complex half-space
- $$\begin{cases} \mathrm{Im}\, V(t) = \frac{1}{\pi} P \int_{-\infty}^{\infty} \frac{\mathrm{Re}\, V(t')}{t' - t} dt' \\ \mathrm{Re}\, V(t) = -\frac{1}{\pi} P \int_{-\infty}^{\infty} \frac{\mathrm{Im} V(t')}{t' - t} dt' \end{cases}$$

(Hilbert transforms)

- non-causal

CORRELATION FUNCTIONS

$V = V^{(r)} + i V^{(i)}$ complex

$V(\underline{r}, t) \longleftrightarrow$ at $\underline{r}$ random function

at $\underline{r}, t$ random variable

↑ mean
variance
skewness
curtosis ...

- ENSEMBLE AVERAGE
- TIME AVERAGE

} ERGODIC

self $p(V)$ probability

$$\iint p(V)\, d^2V = 1$$

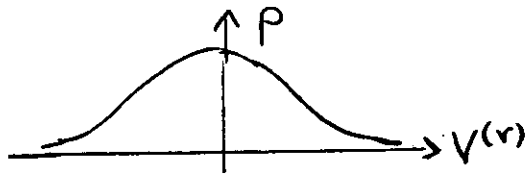

$$\langle V \rangle = \iint V p(V)\, d^2V = 0 \quad \text{(in optics)}$$

$$\langle |V|^2 \rangle = \iint V^* V\, p(V)\, d^2V$$

⋮

$\left(d^2V = dV^{(r)} dV^{(i)} \right)$

self $\quad p_1(V) = p(V)$

mutual $\quad p_2(V_1, V_2)$

$$\langle V_1^* V_2 \rangle = \iiint V_1^* V_2 \, p_2(V_1, V_2) \, d^2V_1 \, d^2V_2$$

$$\vdots$$

$$\langle \underbrace{V_1^* V_2^* \cdots V_m^*}_{m} \; \underbrace{V_{m+1} \cdots V_{m+n}}_{n} \rangle = \Gamma^{(m,n)}$$

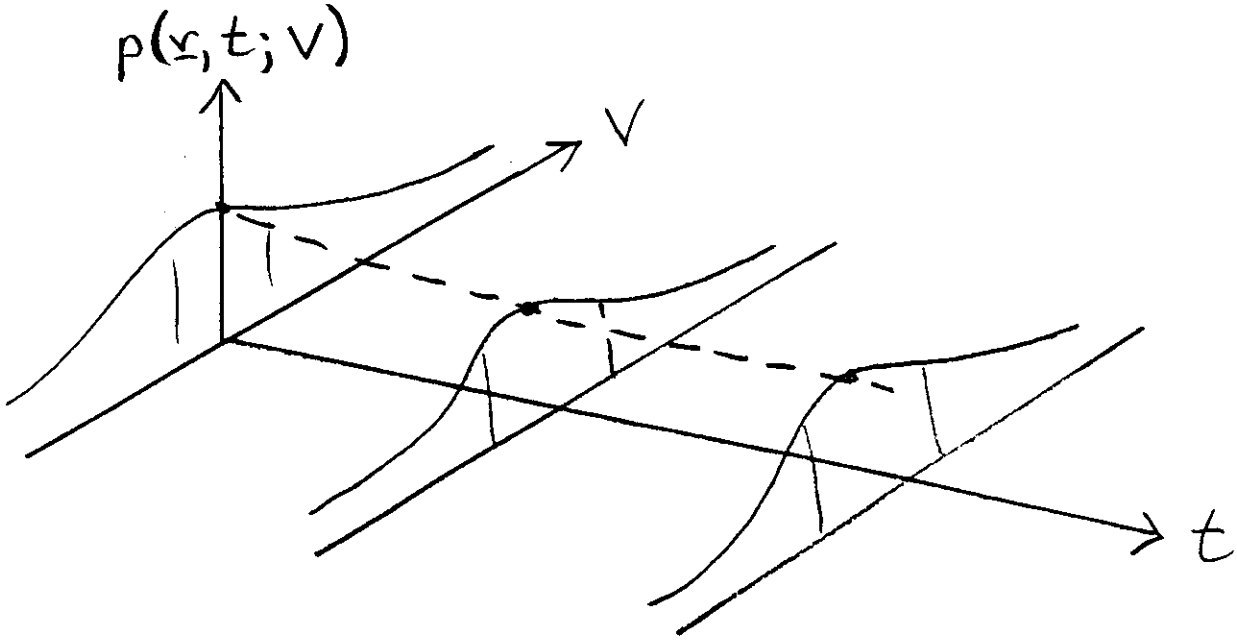

$$\{ p_n(r_1 t_1 V_1, \cdots, r_n t_n V_n), \; n = 1, 2, 3, \cdots \}$$

STATIONARY FIELDS

$$\Gamma^{(1,1)}(\underline{r}_1 t_1, \underline{r}_2 t_2) = \Gamma(\underline{r}_1, \underline{r}_2, \tau) \qquad \tau = t_2 - t_1$$

$$\Gamma(\underline{r}_1, \underline{r}_2, \tau) = \left\langle V^*(\underline{r}_1, t) V(\underline{r}_2, t+\tau) \right\rangle_{\substack{\text{time} \\ \text{ensemble}}}$$

$$= \lim_{T\to\infty} \frac{1}{2T} \int_{-T}^{T} V^*(\underline{r}_1, t') V(\underline{r}_2, t'+\tau)\, dt'$$

$$= \iiint V_1^* V_2\, p_2(r_1, t_1, V_1; r_2, t_1+\tau, V_2)\, d^2V_1\, d^2V_2$$

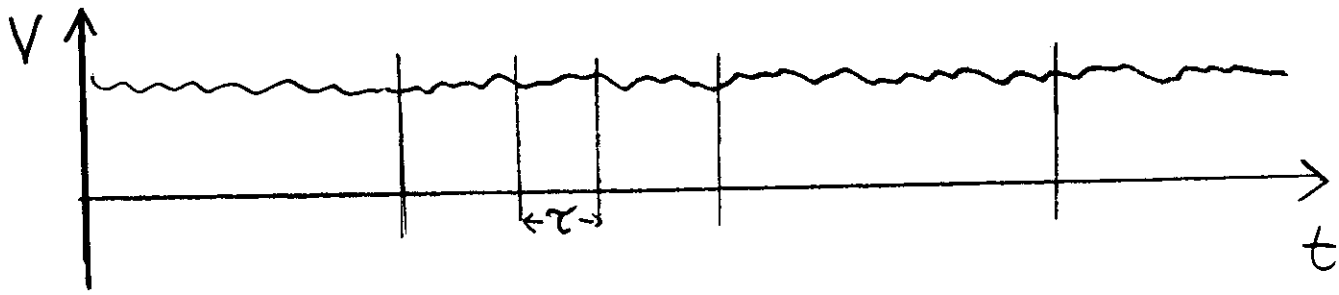

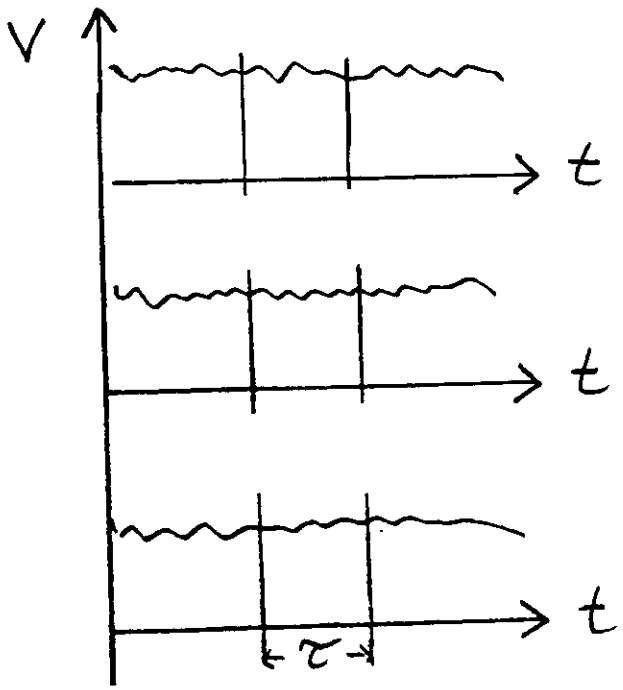

Obs:

Harmonic function

$V(t) = v e^{-i\omega t}$

is not ergodic!

(In nature all functions are ergodic.)

SPACE-TIME COHERENCE

✧ scalar theory
✧ stationary & ergodic field

$V(\mathbf{r},t)$	COMPLEX ANALYTIC SIGNAL (only positive frequencies)
$\Gamma(\mathbf{r}_1,\mathbf{r}_2;\tau)=\langle V^*(\mathbf{r}_1,t)V(\mathbf{r}_2,t+\tau)\rangle$	MUTUAL COHERENCE FUNCTION
$I(\mathbf{r})=\Gamma(\mathbf{r},\mathbf{r};0)=\langle \lvert V^*(\mathbf{r},t)\rvert^2\rangle$	(AVERAGED) OPTICAL INTENSITY
$\gamma(\mathbf{r}_1,\mathbf{r}_2;\tau)=\dfrac{\Gamma(\mathbf{r}_1,\mathbf{r}_2;\tau)}{\sqrt{I(\mathbf{r}_1)I(\mathbf{r}_2)}}$	COMPLEX DEGREE OF COHERENCE

$$0 \le \left|\gamma(\mathbf{r}_1,\mathbf{r}_2;\tau)\right| \le 1$$

INCOHERENT — COHERENT

DOMAIN $\mathcal{D}$

$$\Gamma(\mathbf{r}_1,\mathbf{r}_2;\tau)=U^*(\mathbf{r}_1)U(\mathbf{r}_2)e^{-i\omega\tau}$$

STRICTLY MONOCHROMATIC

$$(\nabla^2+k^2)U(\mathbf{r})=0$$

YOUNG'S INTERFEROMETER

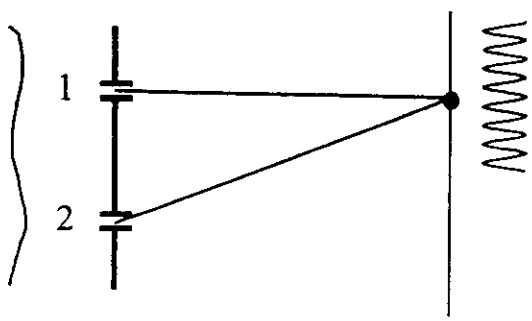

Delay τ

Visibility $\mathcal{V} \propto |\gamma_{12}(\tau)|$

Fringe location $\propto$ phase of γ

COHERENCE PARAMETERS

Michelson

$\Delta t \Delta \omega \lesssim 1$

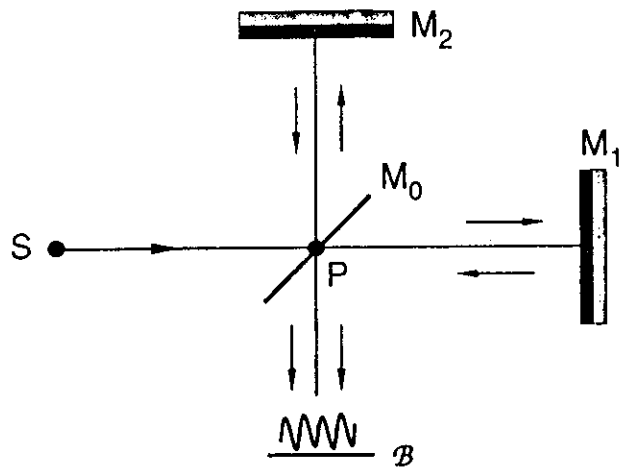

- Coherence time $\Delta t \sim \frac{1}{\Delta \omega}$
- Coherence length $l \sim c \Delta t$

$\Delta x \Delta \theta \lesssim \lambda$

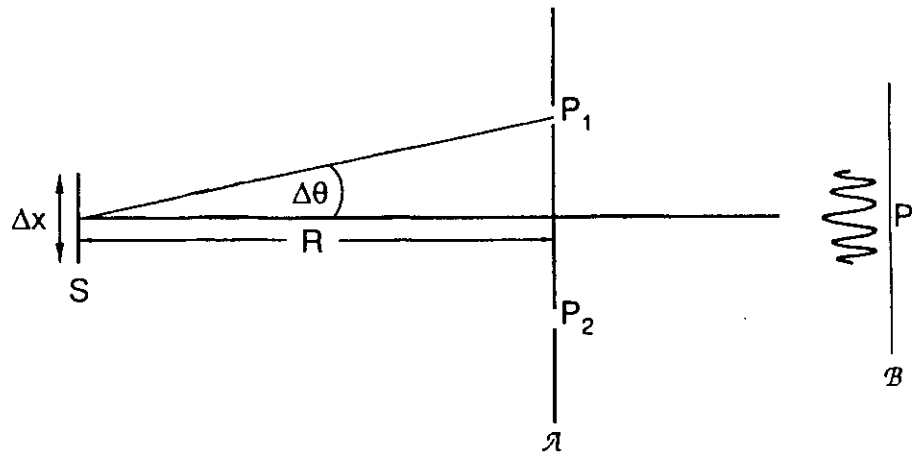

- coherence area $\Delta A \sim (R \Delta \theta)^2 \sim R^2 \left(\frac{\lambda}{\Delta x}\right)^2$
- coherence solid angle $\Delta \Omega \sim (\Delta \theta)^2$

- Degeneracy δ

SPACE-FREQUENCY COHERENCE

$$\begin{cases} \Gamma(\mathbf{r}_1,\mathbf{r}_2;\tau) = \int_0^\infty W(\mathbf{r}_1,\mathbf{r}_2;\omega)e^{-i\omega\tau}d\omega \\ \left\langle \tilde{V}^*(\mathbf{r}_1,\omega)\tilde{V}(\mathbf{r}_2,\omega')\right\rangle = W(\mathbf{r}_1,\mathbf{r}_2;\omega)\delta(\omega-\omega') \end{cases}$$

WIENER-KHINTCHINE THEOREM

CROSS-SPECTRAL DENSITY

$S(\mathbf{r},\omega) = W(\mathbf{r},\mathbf{r};\omega)$ SPECTRUM (SPECTRAL INTENSITY)

$$\mu(\mathbf{r}_1,\mathbf{r}_2;\omega) = \frac{W(\mathbf{r}_1,\mathbf{r}_2;\omega)}{\sqrt{S(\mathbf{r}_2,\omega)S(\mathbf{r}_1,\omega)}}$$

COMPLEX DEGREE OF SPECTRAL (SPATIAL) COHERENCE

$$0 \le \left|\mu(\mathbf{r}_1,\mathbf{r}_2;\omega)\right| \le 1$$

INCOHERENT COHERENT

DOMAIN $\mathcal{D}$

$$W(\mathbf{r}_1,\mathbf{r}_2;\omega) = U^*(\mathbf{r}_1,\omega)U(\mathbf{r}_2,\omega)$$

FACTORIZATION

⇒ stationary field may be partially coherent at single frequencies !

YOUNG + SPECTRAL FILTERS

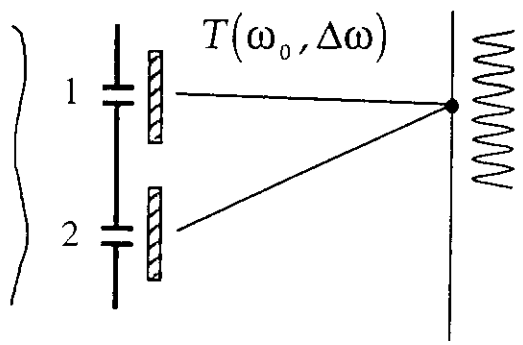

As $\Delta\omega \to 0$

$\gamma(\mathbf{r}_1,r_2;\tau) = \mu(\mathbf{r}_1,r_2;\omega_0)\theta(\tau)$

$\theta(\tau) \sim T(\omega)$

$\theta(0) = 1$

A.T. Friberg & E. Wolf, Opt. Lett. 20, 623-625 (1995)

γ versus μ

space-time degree

space-frequency degree

relation ?

INTENSITY

$$I(\mathbf{r}) = \int_0^\infty S(\mathbf{r},\omega)\,d\omega$$

NORMALIZED SPECTRUM

$$\delta(\mathbf{r},\omega) = \frac{S(\mathbf{r},\omega)}{\int_0^\infty S(\mathbf{r},\omega)\,d\omega}$$

$$\gamma(\mathbf{r}_1,\mathbf{r}_2;\tau) = \int_0^\infty \sqrt{\delta(\mathbf{r}_1,\omega)\delta(\mathbf{r}_2,\omega)}\,\mu(\mathbf{r}_1,\mathbf{r}_2;\omega)\,e^{-i\omega\tau}\,d\omega$$

FT-pair

EXAMPLE: Black-body

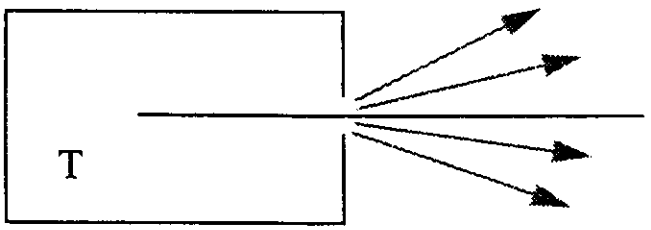

Lambertian

$$\mu(\mathbf{r}_1,\mathbf{r}_2;\omega) = \frac{\sin k|\mathbf{r}_1-\mathbf{r}_2|}{k|\mathbf{r}_1-\mathbf{r}_2|}$$

$\delta(\omega)$ ~ Planck's law

homogeneous, isotropic

E, **H** vectors

$W = \mathrm{Tr}\left\{W_{ij}^{(E)}\right\}$

$$\alpha = \frac{\hbar}{KT}$$

$$\Delta\tau \approx \frac{2\pi}{\omega_{\max}} = \frac{2\pi}{2.82}\left(\frac{\hbar}{KT}\right) = 2.23\alpha$$

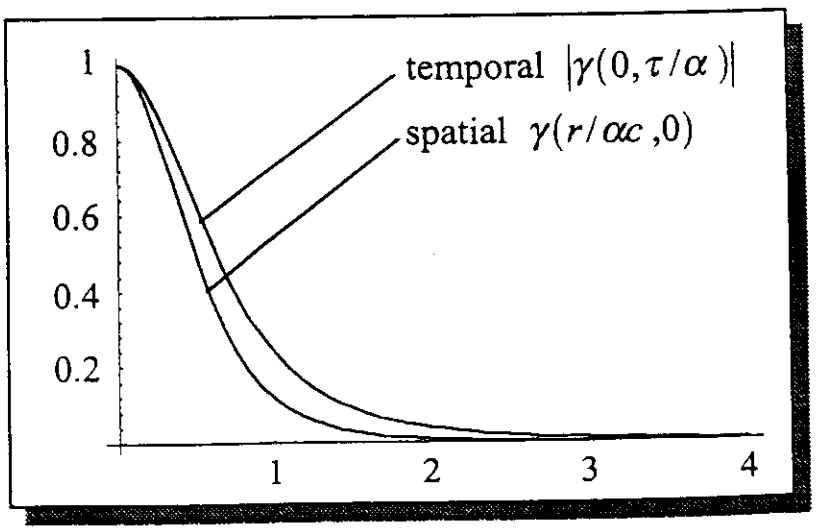

PROPAGATION

- ✧ Wave equations for $\Gamma(\mathbf{r}_1,\mathbf{r}_2;\tau)$
- ✧ Sudarshan's equations
- ✧ Helmholtz equations for $W(\mathbf{r}_1,\mathbf{r}_2;\omega)$

$$\left(\nabla_j^2 + k^2\right)W(\mathbf{r}_1,\mathbf{r}_2;\omega) = 0 \qquad (k = \omega/c)$$

- ✧ Solutions:
  - Angular spectrum representation (exact)
  - 1st and 2nd Rayleigh Integrals (exact)
  - Extended Fresnel diffraction (beams)

$$\begin{pmatrix}\rho\\ \rho'\end{pmatrix}_{out} = \begin{pmatrix}A & B\\ C & D\end{pmatrix}\begin{pmatrix}\rho\\ \rho'\end{pmatrix}_{in} = M\begin{pmatrix}\rho\\ \rho'\end{pmatrix}_{in}$$

  - symmetric lens systems (2 x 2 ABCD matrices)
  - non-symmetric systems (4 x 4 matrices)
  - tilt & decenter (5 x 5 matrices)

$$U(\rho,z_{out}) = \frac{-ik}{2\pi}e^{ikL}(\det B)^{-1}\iint U(\rho_0,z_{in}) \times \exp\left[ik\left(\rho^{\mathrm{T}}DB^{-1}\rho - 2\rho_0^{\mathrm{T}}B^{-1}\rho + \rho_0^{\mathrm{T}}B^{-1}A\rho_0\right)/2\right]d^2\rho_0$$

EXTENSIONS

- ✧ Non-stationary fields (pulses)
- ✧ Electromagnetic coherence tensors
  - correlation functions
  - Maxwell's equations
- ✧ Partial polarization
  - Blackbody radiation unpolarized
- ✧ Higher-order correlations

INCREASE OF COHERENCE

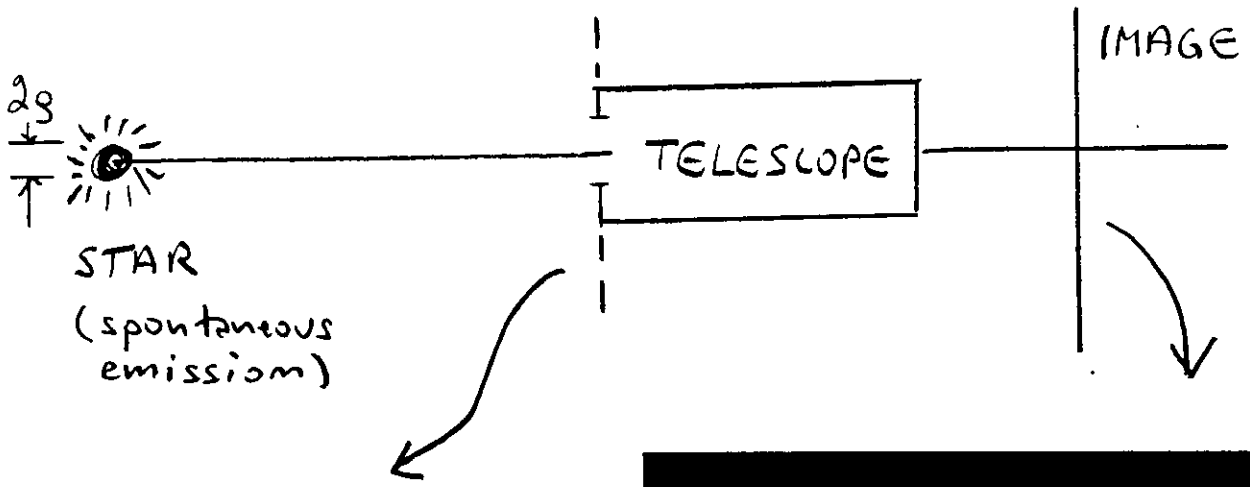

$$\gamma_{12}(0) = \frac{2J_1(v)}{v}$$

$$v = k\varrho \sin\Theta$$

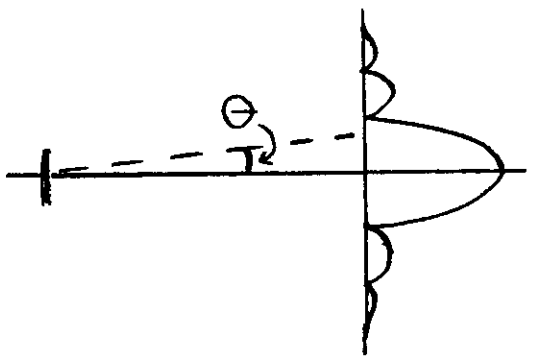

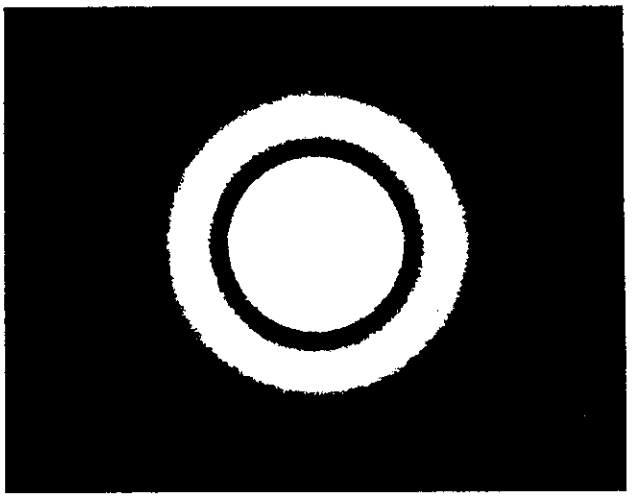

FIG. 6. The diffraction image of a star formed by a well-corrected telescope (courtesy of B. J. Thompson).

Airy Pattern

$$\left| \frac{2J_1(x)}{x} \right|^2$$

1. zero $\sin\Theta \sim 0.16 \frac{\lambda}{\varrho}$

- VAN CITTERT - ZERNIKE THEOREM

$$\mathcal{F}\{S(\varrho,\omega)\} \propto \mu^{(\infty)}(\Delta\varrho,\omega)$$

- For decrease of coherence in free space, see A. J. Devaney et al. Opt. Lett. 22, 1672-1673 (1997)

FIXED-BASELINE SOURCE RECONSTRUCTION

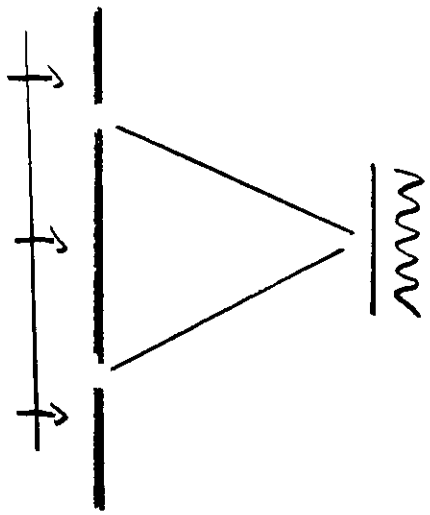

At frequency ω

$$S(\omega) = S_1(\omega) + S_2(\omega)$$

$$+ 2\sqrt{S_1(\omega) S_2(\omega)}\,|\mu_{12}(\omega)| \cos\beta_{12}(\omega)$$

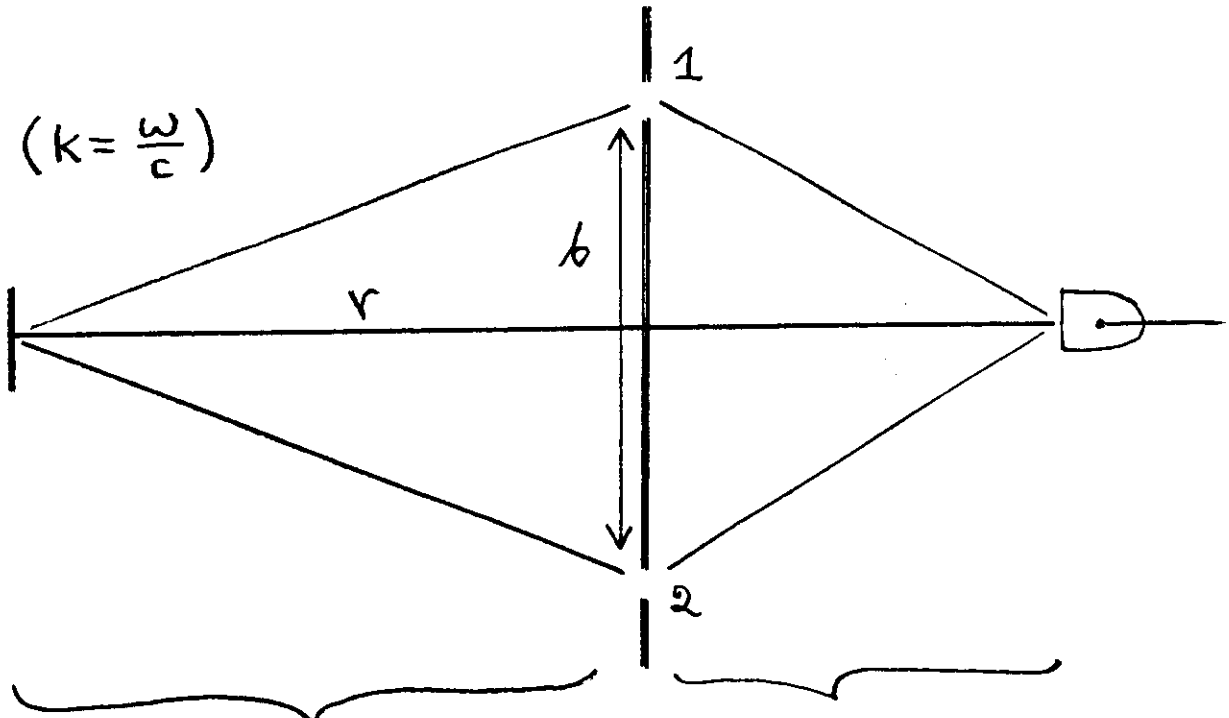

$$\tilde{S}\left(\frac{kb}{r}\right) \propto \mu_{12}(\omega) \qquad \mathrm{Re}\{\mu_{12}(\omega)\} = \frac{S(\omega)}{2S_1(\omega)} - 1$$

- Measurement of spectrum at single point yield spatial source profile
- Needs broad-band radiation

MICHELSON'S STELLAR INTERFEROMETER

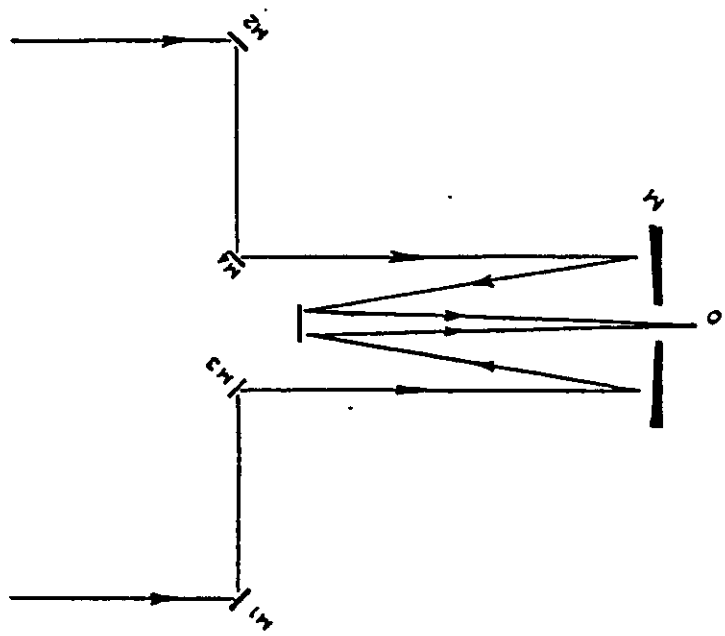

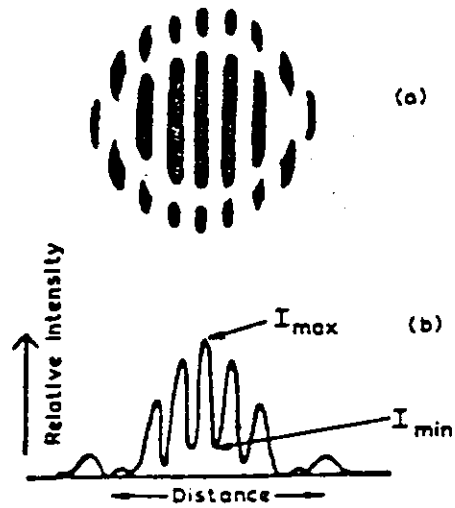

Fringes formed in a Michelson interferometer.

angular resolution $\alpha \sim 0.02''$
(limited by atmospheric turbulence)

COHERENCY MATRICES

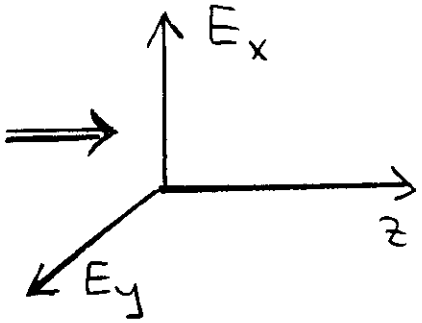

$$\mathcal{E} = \begin{bmatrix} \langle E_x E_x^* \rangle & \langle E_x E_y^* \rangle \\ \langle E_y E_x^* \rangle & \langle E_y E_y^* \rangle \end{bmatrix}$$

$$\mu_{xy} = \frac{\langle E_x E_y^* \rangle}{\sqrt{\langle E_x E_x^* \rangle \langle E_y E_y^* \rangle}} \qquad 0 \le |\mu_{xy}| \le 1$$

$$\underset{(\theta)}{\text{Max}}\, |\mu_{xy}| = P = \sqrt{1 - \frac{4 \det \mathcal{E}}{(\text{Tr}\, \mathcal{E})^2}}$$ degree of polarization

EM

Coherence tensors

$$\mathcal{E}_{jk}(\mathbf{r}_1,\mathbf{r}_2,\tau) = \left\langle E_j(\mathbf{r}_1, t+\tau) E_k^*(\mathbf{r}_2, t) \right\rangle$$

$$\mathcal{H}_{jk}(\mathbf{r}_1,\mathbf{r}_2,\tau) = \left\langle H_j(\mathbf{r}_1, t+\tau) H_k^*(\mathbf{r}_2, t) \right\rangle$$

$$\mathcal{M}_{jk}(\mathbf{r}_1,\mathbf{r}_2,\tau) = \left\langle E_j(\mathbf{r}_1, t+\tau) H_k^*(\mathbf{r}_2, t) \right\rangle$$

$$\mathcal{N}_{jk}(\mathbf{r}_1,\mathbf{r}_2,\tau) = \left\langle H_j(\mathbf{r}_1, t+\tau) E_k^*(\mathbf{r}_2, t) \right\rangle$$

$(j,k = x,y,z)$

Field equations

$$\varepsilon_{jkl}\, \partial_k^1\, \mathcal{E}_{lm} + \frac{1}{c} \frac{\partial}{\partial \tau}\, \mathcal{N}_{jm} = 0$$

$$\varepsilon_{jkl}\, \partial_k^1\, \mathcal{M}_{lm} + \frac{1}{c} \frac{\partial}{\partial \tau}\, \mathcal{H}_{jm} = 0$$

$$\varepsilon_{jkl}\, \partial_k^1\, \mathcal{N}_{lm} - \frac{1}{c} \frac{\partial}{\partial \tau}\, \mathcal{E}_{jm} = 0$$

$$\varepsilon_{jkl}\, \partial_k^1\, \mathcal{H}_{lm} - \frac{1}{c} \frac{\partial}{\partial \tau}\, \mathcal{M}_{jm} = 0$$

$$\partial_j^1\, \mathcal{E}_{jk} = \partial_j^1\, \mathcal{H}_{jk} = \partial_j^1 \mathcal{M}_{jk} = \partial_j^1 \mathcal{N}_{jk} = 0$$

$$\varepsilon_{jkl} = \begin{cases} +1 \text{ if j, k, } l\text{, } \textit{even} \text{ permutations of 1, 2, 3} \\ -1 \text{ if j, k, } l \textit{ odd} \text{ permutations of 1, 2, 3} \\ 0 \text{ if two indices equal} \end{cases}$$

$$\partial_k^1 = \frac{\partial}{\partial x_1^k}, \qquad (k = 1, 2, 3)$$

QUANTUM COHERENCE

Classical $$\underline{E}^{(r)}(\underline{r},t) = \underbrace{\underline{E}(\underline{r},t)}_{\text{complex analytic signal}} + \underline{E}^{*}(\underline{r},t)$$

Quantum $$\hat{\underline{E}}(\underline{r},t) = \hat{\underline{E}}^{(+)}(\underline{r},t) + \hat{\underline{E}}^{(-)}(\underline{r},t)$$

$$\begin{cases} \hat{\underline{E}}^{(+)}(\underline{r},t) = \int_0^\infty \hat{\underline{e}}(\underline{r},\omega)\, e^{-i\omega t}\, d\omega & \text{(annihilation)} \\ \hat{\underline{E}}^{(-)}(\underline{r},t) = \int_{-\infty}^0 \hat{\underline{e}}(\underline{r},\omega)\, e^{-i\omega t}\, d\omega & \text{(creation)} \end{cases}$$

$$G^{(m,n)}_{j_1 j_2 \cdots j_{m+n}}(x_1, x_2, \cdots, x_{m+n})$$

$$= Tr\left\{\hat{\rho}\, \underbrace{\hat{E}^{(-)}_{j_1}(x_1) \cdots \hat{E}^{(-)}_{j_m}(x_m)}_{m}\, \underbrace{\hat{E}^{(+)}_{j_{m+1}}(x_{j_{m+1}}) \cdots \hat{E}^{(+)}_{j_{m+n}}(x_{m+n})}_{n}\right\}$$

$\hat{\rho}$ = density operator $\qquad x_j = (\underline{r}_j, t_j)$

- order of non-commuting operators
- normal order (photodetection)

INTENSITY INTERFEROMETRY

(Hanbury-Brown & Twiss, 1956)

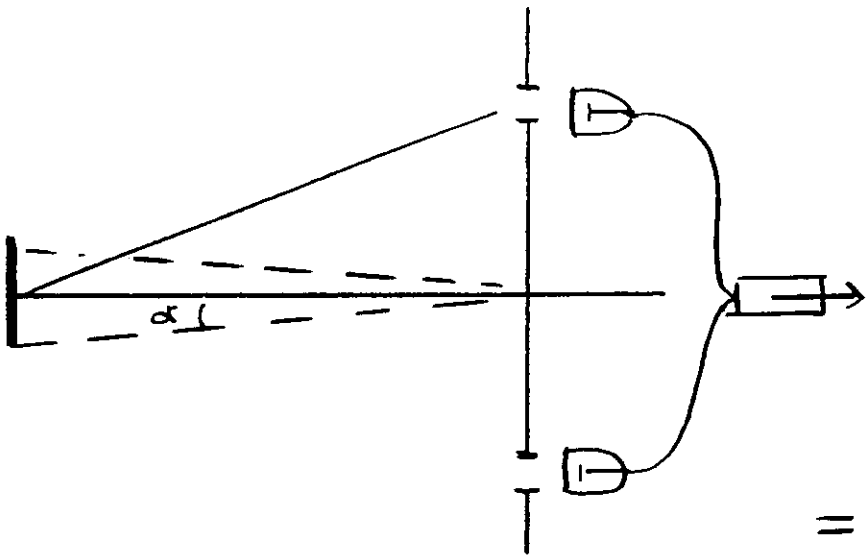

$\alpha \sim 0.0005''$

$$T^{(2,2)} \sim$$

$$\langle I_1(t) I_2(t+\tau) \rangle$$

$$= I_1 I_2 \left[1 + |\gamma_{12}(\tau)|\right]$$

(Gaussian moment theorem)

PHOTODETECTION

$p_c(\tau)$ = probability of photodection after τ from the previous one

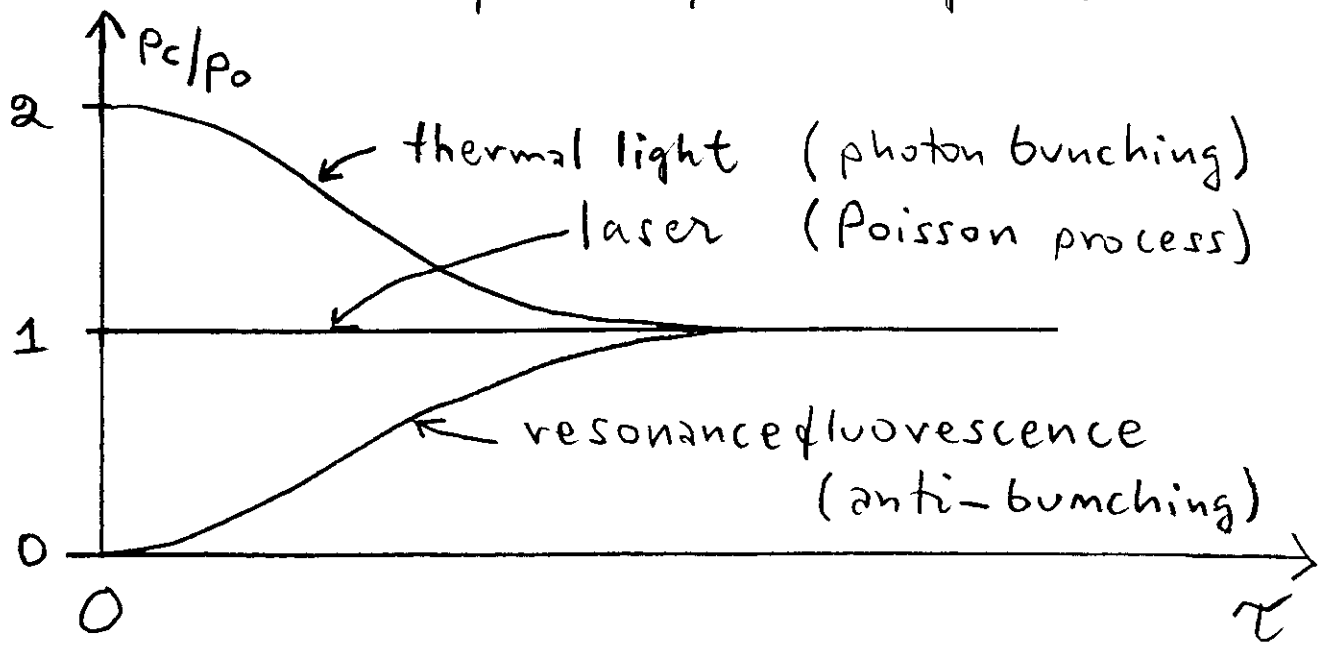

$W(\mathbf{r}_1,\mathbf{r}_2;\omega)$ continuous in ω

a) $\iint \left|W(\mathbf{r}_1,\mathbf{r}_2;\omega)\right|^2 d^3r_1 d^3r_2 < \infty$ (Finite energy, Hilbert-Schmidt)

b) $W(\mathbf{r}_2,\mathbf{r}_1;\omega) = W^*(\mathbf{r}_1,\mathbf{r}_2;\omega)$ (Hermitian)

c) $\iint W(\mathbf{r}_1,\mathbf{r}_2;\omega) f^*(\mathbf{r}_1) f(\mathbf{r}_2)\, d^3r_1 d^3r_2 \geq 0$ (Non-negative definite)

$\left[\text{any function } f, \text{ eg. } f(\mathbf{r}) \propto e^{ik\mathbf{s}\cdot\mathbf{r}} \text{ far - field}\right]$

$\Rightarrow$ (Mercer's theorem)

$$W(\mathbf{r}_1,\mathbf{r}_2;\omega) = \sum_n \lambda_n(\omega)\psi_n^*(\mathbf{r}_1,\omega)\psi_n(\mathbf{r}_2,\omega) \qquad (\lambda_n \geq 0)$$

$$\int W(\mathbf{r}_1,\mathbf{r}_2;\omega)\psi_n(\mathbf{r}_1,\omega) d^3\mathbf{r}_1 = \lambda_n(\omega)\psi_n(\mathbf{r}_2,\omega) \qquad \left(\int \psi_n^*\psi_m = \delta_{nm}\right)$$

(Fredholm integral equation)

☞ ✧ Factorization $\rightarrow$ each term spatially coherent
Helmholtz eq. $\rightarrow$ **coherent (natural) modes**

☞ ✧ Let $U(\mathbf{r}) = \sum a_n(\omega)\psi_n(\mathbf{r},\omega)$

$$\left\langle a_n^*(\omega) a_m(\omega)\right\rangle = \lambda_n(\omega)\delta_{nm}$$

$\Rightarrow$ $W(\mathbf{r}_1,\mathbf{r}_2;\omega) = \left\langle U^*(\mathbf{r}_1,\omega) U(\mathbf{r}_2,\omega)\right\rangle$

(correlation of ordinary functions !)

Space-time domain

$\{Q(\mathbf{r}, t)\}$ ---------- $\{\hat{Q}(\mathbf{r}, \omega)\}$
(forbidden)

$\Gamma_Q(\mathbf{r}_1, \mathbf{r}_2, \tau) \xrightarrow{\text{FT}} W_Q(\mathbf{r}_1, \mathbf{r}_2, \omega)$

$$\Gamma_Q(\mathbf{r}_1, \mathbf{r}_2, \tau) = \left\langle Q^*(\mathbf{r}_1, t)\, Q(\mathbf{r}_2, t+\tau) \right\rangle_t$$

Space-frequency domain

$\{Q(\mathbf{r}, t)\}$ ---------- $\{U_Q(\mathbf{r}, \omega)\}$
(forbidden)

$\Gamma_Q(\mathbf{r}_1, \mathbf{r}_2, \tau) \xleftarrow{\text{FT}} W_Q(\mathbf{r}_1, \mathbf{r}_2, \omega)$

$$W_Q(\mathbf{r}_1, \mathbf{r}_2, \omega) = \left\langle U_Q^*(\mathbf{r}_1, \omega)\; U_Q(\mathbf{r}_2, \omega) \right\rangle_\omega$$

$$W_V(\underline{r}_1, \underline{r}_2, \omega) = \sum_n \lambda_n(\omega)\, \psi_n^*(\underline{r}_1, \omega)\, \psi_m(\underline{r}_2, \omega)$$

Mode representation of a radiated field.

QUASI-HOMOGENEITY

$$\mu(\underline{r}_1, \underline{r}_2, \omega) = g(\underline{r}_1 - \underline{r}_2, \omega)$$

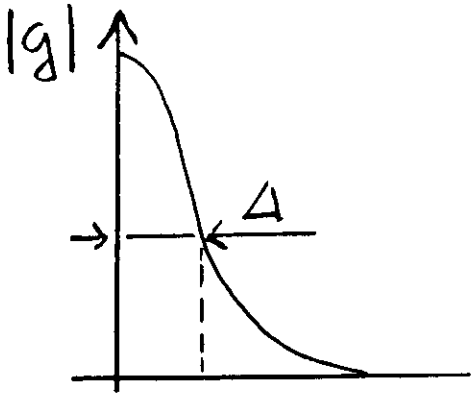

degree of coherence (fast)

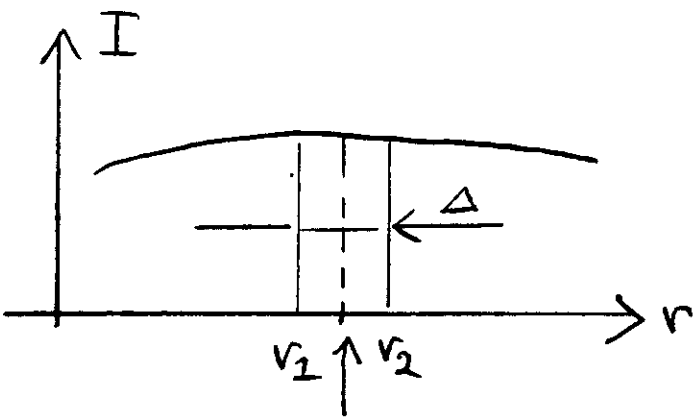

$\frac{1}{2}(\underline{r}_1 + \underline{r}_2)$

intensity (slow)

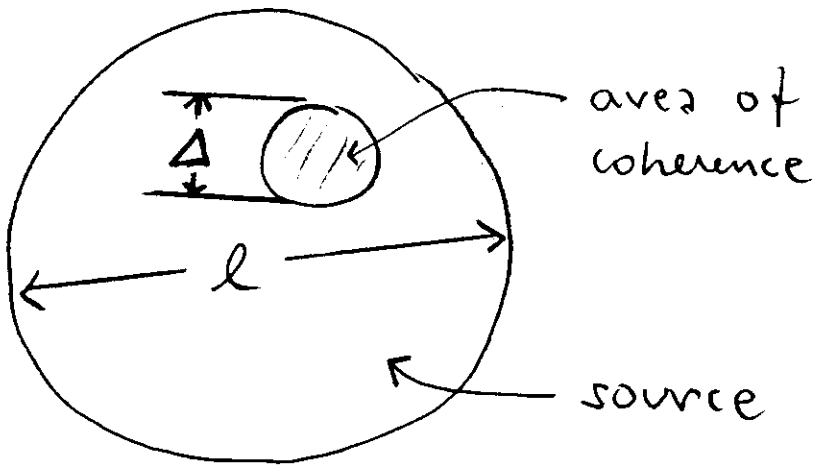

- globally incoherent $\Delta \ll \ell$

{ locally incoherent if $\Delta \approx \lambda$
{ locally coherent if $\Delta \gg \lambda$

EXAMPLE: GAUSSIAN SCHELL-MODEL SOURCES

SCHELL-MODEL: $\mu(\mathbf{r}_1, \mathbf{r}_2; \omega) = g(\mathbf{r}_2 - \mathbf{r}_1; \omega)$

$$\begin{cases} W(\mathbf{r}_1, \mathbf{r}_2; \omega) = \sqrt{S(\mathbf{r}_1, \omega) S(\mathbf{r}_2, \omega)}\, g(\mathbf{r}_2 - \mathbf{r}_1; \omega) \\ S(\mathbf{r}, \omega) = S(\omega)\, e^{-r^2/2\sigma_S^2} \\ g(\mathbf{r}'; \omega) = e^{-r'^2/2\sigma_g^2} \end{cases}$$

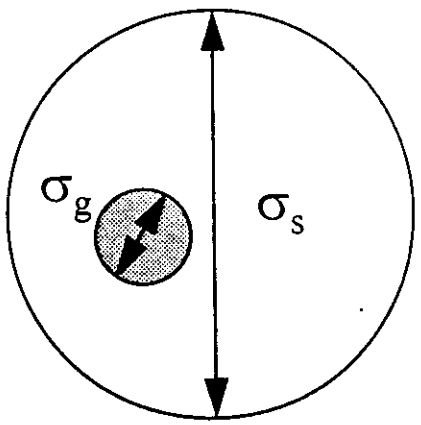

✧ $\sigma_S >> \sigma_g$ → globally incoherent (quasihomogeneous)
$\sigma_g >> \lambda$ → locally coherent
$\sigma_g \sim \lambda$ → locally incoherent

Coherent modes (Hermite-Gaussian functions)

$$\psi_n(x, \omega) = \left(\frac{2}{\pi w_S^2 \beta}\right)^{1/4} \frac{1}{\sqrt{2^n n!}} H_n\left(\frac{\sqrt{2}x}{w_S\sqrt{\beta}}\right) e^{-x^2/w_S^2\beta}$$

$$\lambda_n(\omega) = S(\omega)\sqrt{2\pi}\, w_S \frac{\beta}{1+\beta}\left(\frac{1-\beta}{1+\beta}\right)^n$$

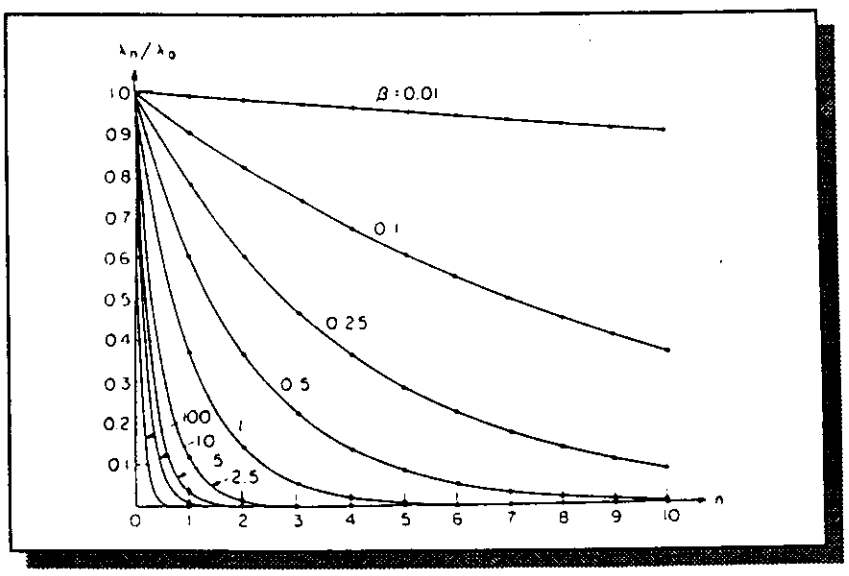

$w_S = 2\sigma_S$

$\alpha = \dfrac{\sigma_g}{w_S}$ global degree of coherence

$\beta = \dfrac{1}{\sqrt{1+\alpha^{-2}}}$ $(0 \le \beta \le 1)$

✧ Bessel J_0-correlated sources
✧ Short-correlation limit

TRANSVERSE STRUCTURE DETERMINATION

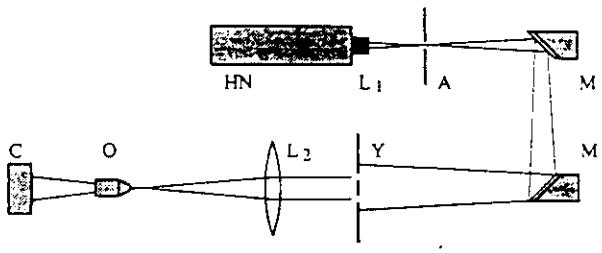

Fig. 1. Experimental setup to determine the modal weights of a multimode laser. HN = He–Ne laser, L_1 = positive lens, A = aperture to block off undesired reflections from the laser optics, M = mirror, Y = Young's interferometer, L_2 = Fourier-transforming lens, O = microscope objective for enlarging the interference pattern, and C = CCD line element

- ✧ Needs spatial coherence data
- ✧ Different modes $\psi_n(\mathbf{r},\omega)$ have slightly different frequencies $\rightarrow$ mutual intensity
- ✧ Spot size and curvature same
- ✧ Let $\psi_n(\rho,z) = \phi_n(\rho,z)\, e^{i\alpha_n(\rho,z)}$

$$W_R(\rho_1,\rho_2;z) = \sum \lambda_n \phi_n(\rho_1,z)\phi_n(\rho_2,z)$$

$$\int W_R(\rho_1,\rho_2;z)\phi_n(\rho_1,z)d^2\rho_1 = \lambda_n \phi_n(\rho_2,z)$$

Spot-size w in $\phi_n(\rho,z)$ not known !

PROCEDURE:

- ✧ Measure $W_R(\rho_1,\rho_2)$ with respect to **two** fixed points (zero crossings are observed from interference phase shifts)
- ✧ Solve spot size w numerically
- ✧ Compute modal weights λ_n

☝ NUMERICALLY AND EXPERIMENTALLY STABLE !

(20 by 20 grid) (Siemens 7621 MM HeNe)

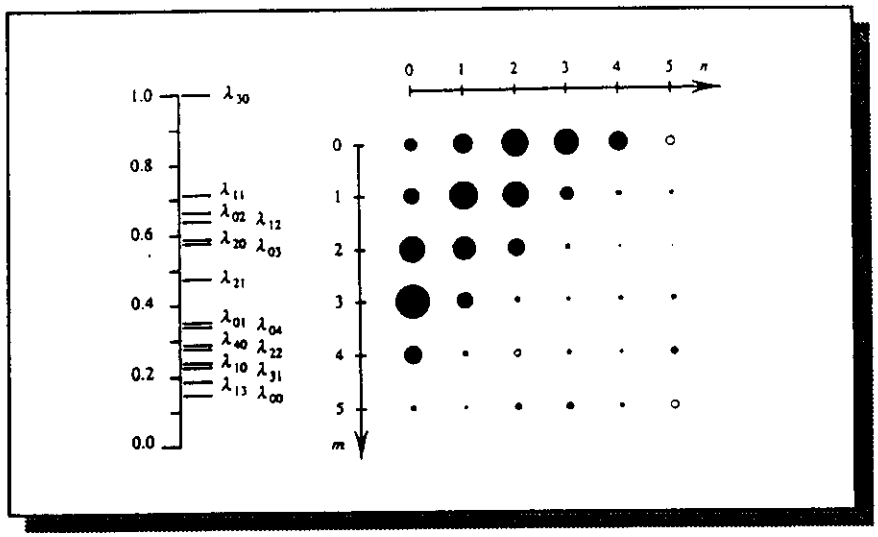

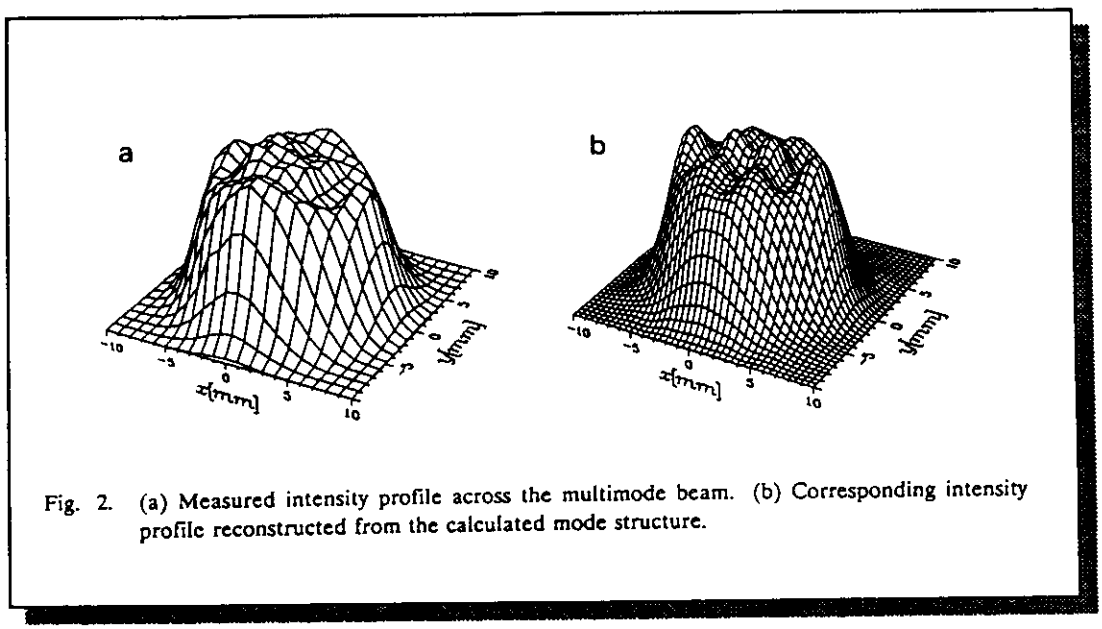

Fig. 2. (a) Measured intensity profile across the multimode beam. (b) Corresponding intensity profile reconstructed from the calculated mode structure.

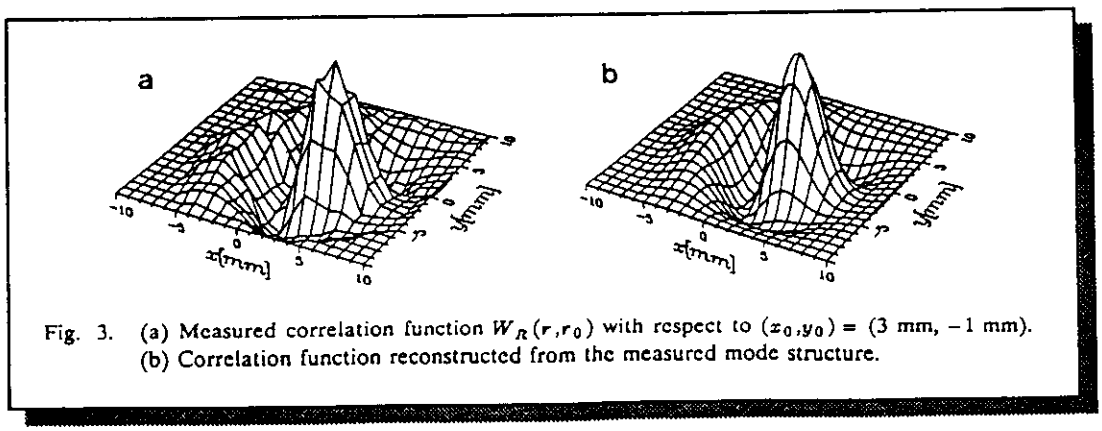

Fig. 3. (a) Measured correlation function $W_R(r,r_0)$ with respect to $(x_0,y_0) = (3\text{ mm}, -1\text{ mm})$. (b) Correlation function reconstructed from the measured mode structure.

SOME METHODS FOR PRODUCING SOURCES OF CONTROLLED COHERENCE PROPERTIES

ROTATING ROUGH SURFACES:

W. Martienssen and E. Spiller, *Am. J. Phys.* **32**, 919 (1964)

P. de Santes, F. Gori, G. Guattari and C. Palma, *Opt. Commun.* **29**, 256 (1979)

J. D. Farina, L. M. Narducci and E. Collett, *Opt. Commun.* **32**, 203 (1980)

LIQUID CRYSTALS:

F. Scudieri, M. Bertolotti and R. Bartolini, *Appl. Opt.* **13**, 181 (1974)

M. Bertolotti, F. Scudieri and S. Verginelli, *Appl. Opt.* **15**, 1842 (1976)

HOLOGRAPHIC FILTERS:

D. Courjon, J. Bulabois and W. H. Carter, *J. Opt. Soc. Amer.* **71**, 469 (1981)

ULTRASONIC WAVES:

Y. Ohtsuka, *Opt. Commun.* **17**, 234 (1976)

Y. Ohtsuka, *J. Opt. Soc. Amer.* **A3**, 1247 (1986)

SYNTHETIC ACOUSTO-OPTIC HOLOGRAMS:

J. Turunen, E. Tervonen and A. T. Friberg, *J. Appl. Phys.* **67**, 49 (1990)

E. Tervonen, A. T. Friberg and J. Turunen, *J. Opt. Soc. Amer.* **9**, 796 (1992)

LENSLESS FEEDBACK SYSTEMS:

J. Deschamps, D. Courjon and J. Bulabois, *J. Opt. Soc. Amer.* **73**, 256 (1983)

ACHROMATIC FOURIER TRANSFORM LENSES:

G. M. Morris and D. Faklis, *Opt. Commun.* **62**, 5 (1987)

D. Faklis and G. M. Morris, *Opt. Lett.* **13**, 4 (1988)

PUPIL MASKS IN DISPERSIVE SYSTEMS:

G. Indebetouw, *J. Mod. Phys.* **36**, 251 (1989)

D. Faklis and G. M. Morris, *J. Mod. Opt.* **39**, 941 (1992)

SOURCE FILTERS:

T. Shirai and T. Asakura, *Optik* **94**, 1 (1993)

(From EW's notes)

✧ Apertures + propagation

✧ Laser + diffuser

- Liquid crystals
- Holographic transparencies
- Sprayed mist (Krylon)
- Ultrasound
- ASE (Amplified Spontaneous Emission)

✧ Systems

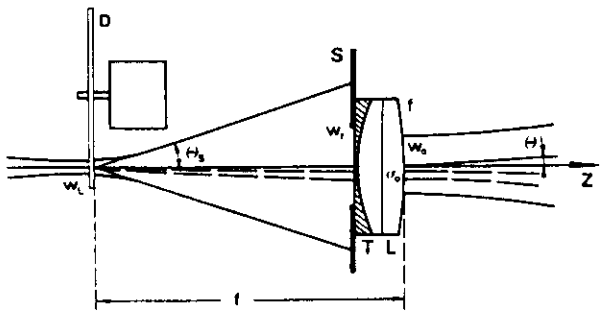

Fig. 1. The optical configuration used to create a variable-coherence gaussian Schell-model source. D=rotating diffuser, S=aperture stop, T=gaussian transmission filter, and L=collimating lens.

GSM source:

$$w_0 = w_f$$

$$\sigma_0 = \frac{\lambda f}{\pi w_L}$$

$$R = \infty$$

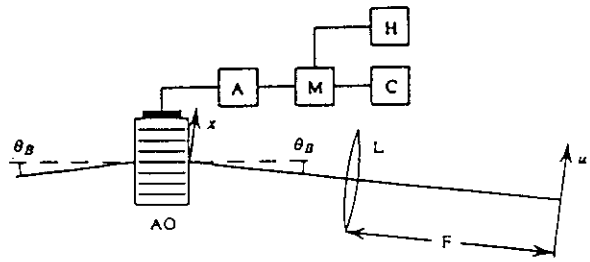

Figure 1. The experimental set-up. AO = acousto-optic deflector, θ_B = Bragg angle, A = amplifier, M = mixer, C = driver, H = infromation source, L = positive lens.

Synthetic acousto-optic coherence-control technique

✧ Independent *parallel* beams

- directionality

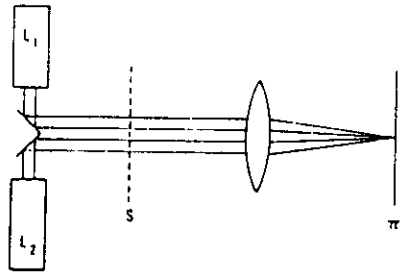

Fig. 1. The beams from two independent identical lasers L_1 and L_2 are made parallel to each other and brought to a focus (focal plane π) of a converging lens. Plane S, intersecting the beams, is the equivalent source.

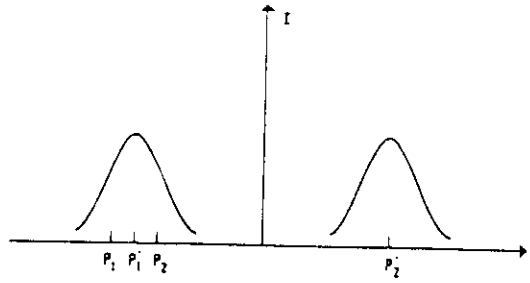

Fig. 2. The field amplitude distribution produced by the laser beams on the plane S of fig. 1, versus an abscissa taken along a line joining the centers of the beams.

✧ Independent *inclined* beams

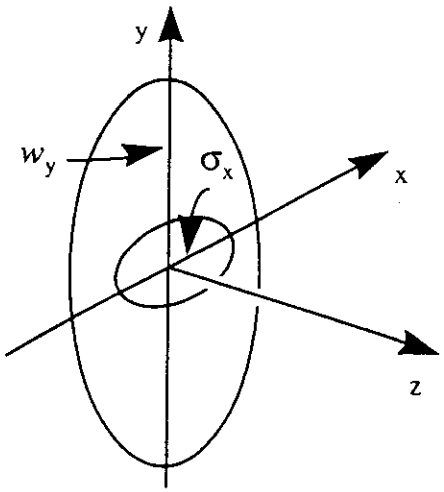

elliptic GSM

- w_x , σ_x
- w_y , σ_y

$$W(\rho_1,\rho_2)=\iint P(\theta_x,\theta_y)U^*(\rho_1;\theta_x,\theta_y)U(\rho_2;\theta_x,\theta_y)d\theta_x d\theta_y$$

$$U(\rho;\theta_x,\theta_y)=\sqrt{S(\omega)}\,e^{-\frac{x^2}{w_x^2}}e^{-\frac{y^2}{w_y^2}}e^{ik\theta_x x}e^{ik\theta_y y}$$

$$P(\theta_x,\theta_y)=\frac{k^2\sigma_x\sigma_y}{2\pi}e^{-\frac{1}{2}(k\sigma_x)^2\theta_x^2}e^{-\frac{1}{2}(k\sigma_y)^2\theta_y^2}$$

✧ Twists

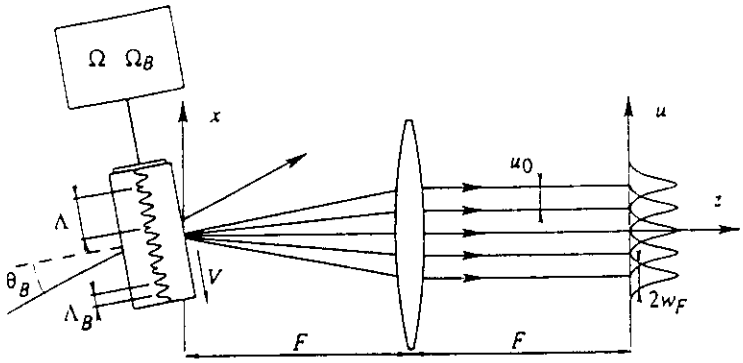

The experimental set-up for reconstructing computer-optimized acousto-optic holograms. The angles and dimensions are not drawn to scale.

$$u_0 = F\lambda/\Lambda$$

$$w_F = F\lambda/\pi w_0$$

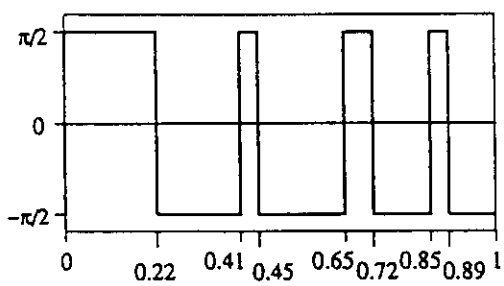

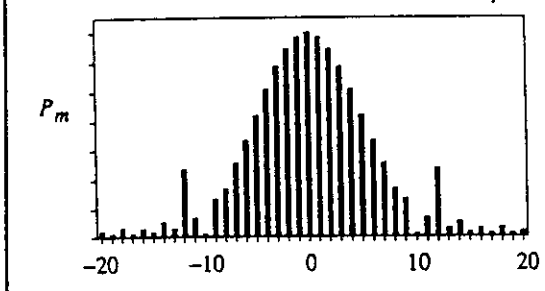

✧ Coherence-control
$(u_0 << w_F)$

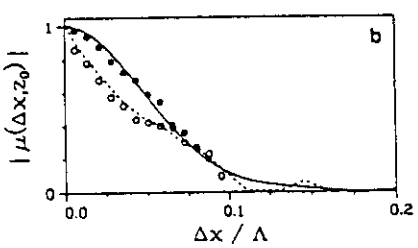

b, Unfiltered (open circles) and filtered (filled circles) spatial coherence profiles across the secondary source.

✧ Beam shaping
$(u_0 \sim w_F)$

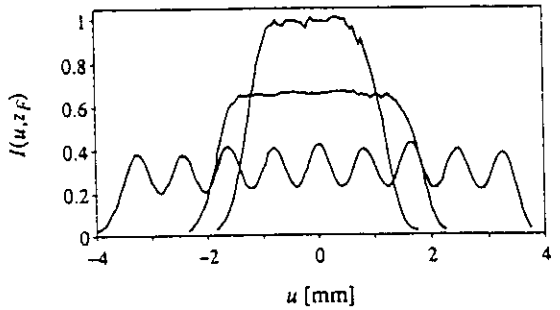

✧ Beam splitting
$(u_0 >> w_F)$

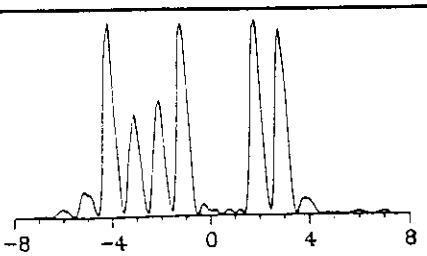

Fig. 5. Experimental result: three-level interconnection pattern with goal distribution $\{I_n\} = \{1, 0.5, 0.5, 1, 0, 0, 1, 1\}$ for diffraction orders $n = -4, \ldots, +3$.

GSM BEAMS

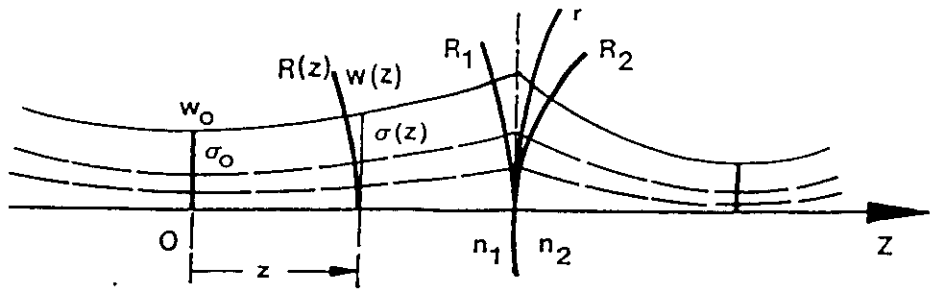

Illustration of the propagation and refraction of a gaussian Schell-model beam.

$$W(\rho_1,\rho_2,z)=\frac{S_0}{w^2(z)}\,e^{-\frac{\rho_1^2+\rho_2^2}{w^2(z)}}\,e^{-\frac{(\rho_1-\rho_2)^2}{2\sigma^2(z)}}\,e^{-\frac{ik\left(\rho_1^2-\rho_2^2\right)}{2R(z)}}$$

$w(z)$ = "spot size"
$R(z)$ = radius of wavefront curvature
$\sigma(z)$ = transverse coherence length

Define:

$$\alpha=\frac{\sigma(z)}{w(z)}=\text{constant}$$ "global degree of coherence"

$$\beta=\left(\sqrt{1+\frac{1}{\alpha^2}}\right)^{-1/2}$$ $0\le\beta\le 1$

$$b(z)=\frac{\pi n w^2(z)\beta}{\lambda}$$ "beam parameter"

$$b(z)=b_0\left[1+\left(\frac{z}{b_0}\right)^2\right] \qquad R(z)=z\left[1+\left(\frac{b_0}{z}\right)^2\right]$$

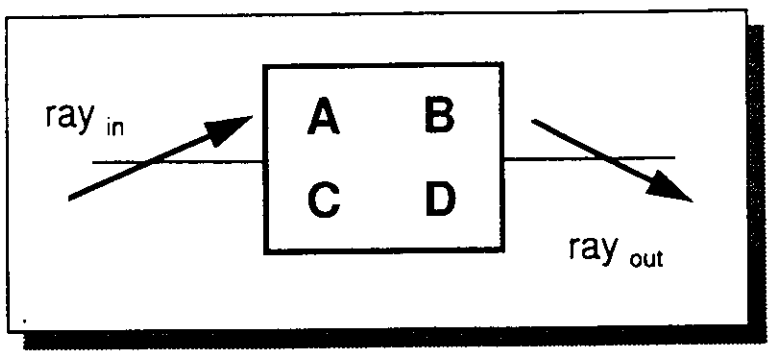

GSM in
⇒
GSM out

GSM beam:

$$\frac{1}{q} = \frac{1}{R} - \frac{i}{b}$$

"complex ray"

Any ABCD system:

$$q_{\text{out}} = \frac{Aq_{\text{in}} + B}{Cq_{\text{in}} + D}$$

Generalized Kogelnik's ABCD-law

Proof:
- by symmetry considerations
- using Wigner distribution function
- by induction
- using extended Fresnel diffraction

Use:

Separate	real & imaginary parts
and solve for	b_{out} & R_{out}
in terms of	b_{in} & R_{in}

$$\Rightarrow \; b_{\text{out}} \;\&\; R_{\text{out}}$$

IMAGING EQUATIONS

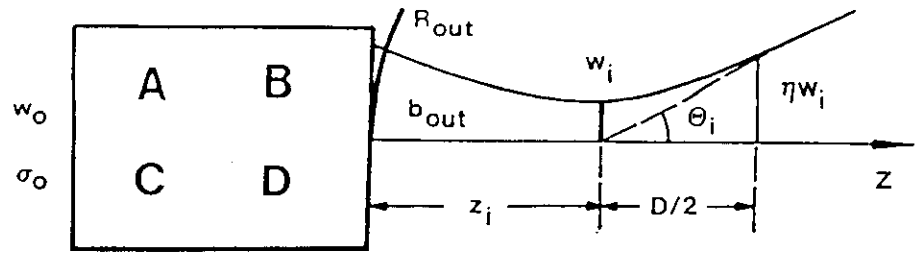

Observable quantities of interest associated with a gaussian Schell-model beam emerging from an arbitrary optical system.

✧ Start ABCD system from input GSM waist

- no loss of generality
- considerable simplification

$$\left.\begin{aligned} b_{out} &= b_0\left[A^2 + B^2 b_0^{-2}\right] \\ R_{out} &= \frac{A^2 + B^2 b_0^{-2}}{AC + BDb_0^{-2}} \end{aligned}\right\} \rightarrow \begin{cases} z_i = -R_{out}\left[1 + R_{out}^2 b_{out}^{-2}\right]^{-1} \\ b_i = b_{out}\left[1 + b_{out}^2 R_{out}^{-2}\right]^{-1} \end{cases}$$

➡

$$z_i = -\frac{A^2 + B^2 b_o^{-2}}{AC + BDb_o^{-2} + \left(ACb_o^2 + BD\right)^{-1}}$$ "image" distance

$$m^2 = \frac{A^2 + B^2 b_o^{-2}}{1 + \left(ACb_o + BDb_o^{-1}\right)^2} \qquad m = \frac{w_i}{w_o}$$ magnification

$$\sigma_i = m\sigma_o$$ transverse coherence

$$D = 2m^2 b_o \sqrt{\eta^2 - 1}$$ depth of focus

$$\Theta_i = \arctan\frac{\lambda}{\pi n m \omega_o \beta} \qquad \Theta_i = \arctan \lim_{z\to\infty} \frac{w(z)}{z}$$

CONSEQUENCES

✧ **coherent limit** $(\alpha \to \infty\ ,\ \beta \to 1)$

- $b_o = \dfrac{\pi n w_o^2 \beta}{\lambda} \to \dfrac{\pi n w_o^2}{\lambda}$ GAUSSIAN LASER

✧ **equivalence relations**

- z_i, m, D } depend only on $\boxed{b_o \sim \dfrac{w_o^2 \beta}{\lambda}}$
- w_i, σ_i, Θ_i } depend also on w_o & σ_o
- in non-dispersive (color-corrected) systems, scale *e.g.* $\lambda_{laser} = \lambda/\beta$

✧ **incoherent limit** $(\alpha \to 0\ ,\ \beta \to 0\ \Rightarrow\ \boxed{b_o \to 0}\ )$

- $\boxed{\begin{aligned} z_i &\to -B/D \\ |m| &\to 1/D \end{aligned}}$ GEOMETRICAL OPTICS (transition region $\alpha \approx 1$)

$\Rightarrow$ when $\alpha \to 0$ (λ = fixed), the GSM source reduces to a Gaussian ensemble of independently radiating points

✧ **limit** $\lambda \to 0$ (α, β fixed $\Rightarrow$ $\boxed{b_o \to \infty}$)

- $\boxed{\begin{aligned} z_i &\to -A/C \\ |m| &\to 0 \end{aligned}}$ ASYMPTOTIC LIMIT (point image in the backfocal plane)

$\Rightarrow$ when $\lambda \to 0$ (α = finite), the GSM beam reduces to an infinite plane wave

THIN LENS

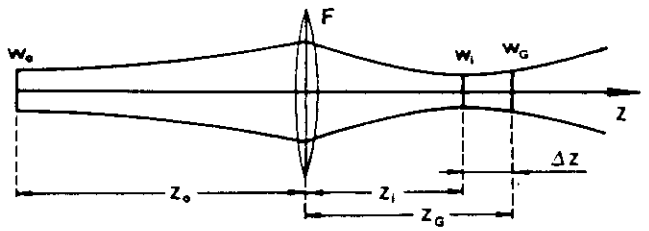

Fig. 2. Focusing of a Gaussian Schell-model beam by a thin lens: w_0, w_i, and w_G and z_0, z_i, and z_G are the sizes and distances, respectively, of the object, the image, and the Gaussian (geometrical-optics) image.

$$\mathcal{F} = \begin{bmatrix} 1 & 0 \\ -\dfrac{1}{F} & 1 \end{bmatrix}$$

$$\mathcal{M} = \begin{bmatrix} 1 & z_0 \\ -\dfrac{1}{F} & 1-\dfrac{z_0}{F} \end{bmatrix}$$

$$\frac{1}{z_i} = \frac{1}{F} - \frac{1}{z_0 + b_0^2 / (z_0 - F)}$$

$$m = \left[\left(1 - \frac{z_0}{F}\right)^2 + \left(\frac{b_0}{F}\right)^2 \right]^{-1/2}$$

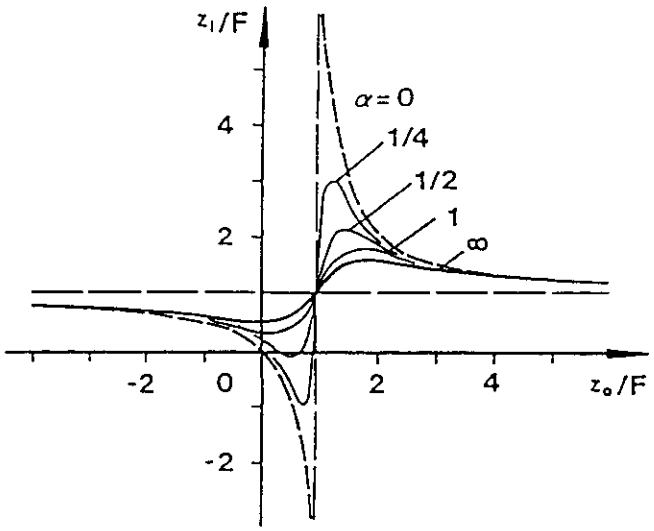

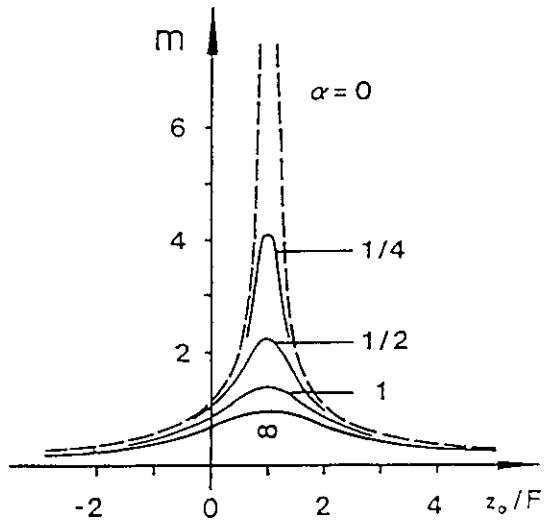

✧ when $b_o \to 0$, $\quad \dfrac{1}{z_o} + \dfrac{1}{z_i} = \dfrac{1}{F}$, $\quad |m| = \left|\dfrac{z_i}{z_o}\right|$

✧ $\Delta z = z_i - z_G$ "focus shift" (low *f*#-systems)

EXPERIMENTAL VERIFICATION

- wavefront-folding interferometer

✧ propagation

$$w(z) = w_0\left[1+\left(\frac{z}{b_0}\right)^2\right]^{1/2}$$

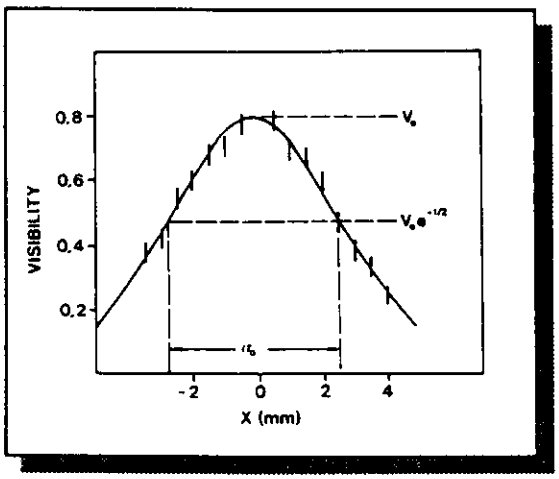

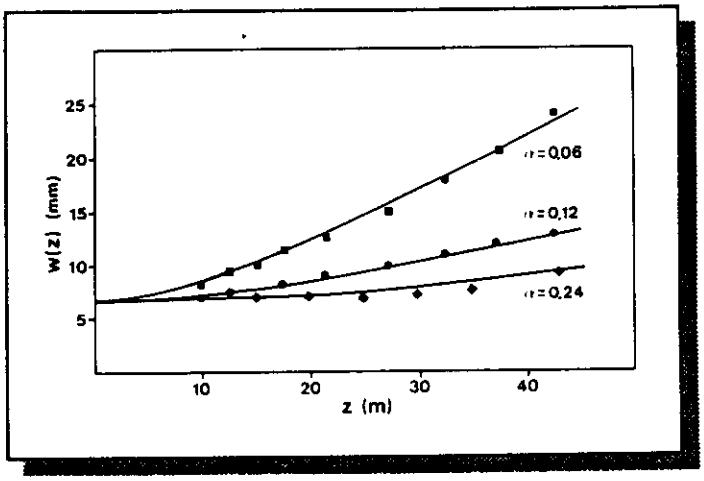

✧ focusing

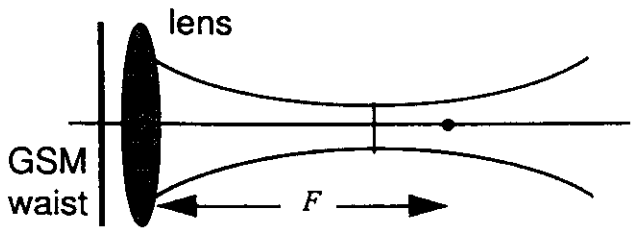

$$w_i = w_0\left[1+\left(\frac{b_0}{F}\right)^2\right]^{-1/2}$$

$$z_i = F\left[1+\left(\frac{F}{b_0}\right)^2\right]^{-1}$$

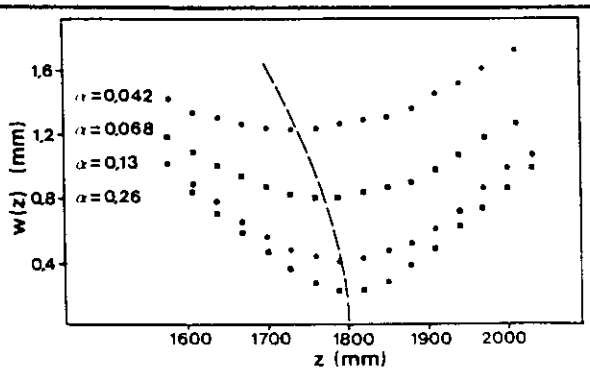

Fig. 6. Beam profiles in the vicinity of the focused beam waist, with several different values of α. The dashed line is the theoretical dependence of focal shift on focused beam waist size for this particular arrangement. This curve (obtained from eqs. (2) and (3)) should cross the measured profiles in the beam waist planes.

F = 1800 mm

w_0 = 6.8 mm

$z_i - F$ = "focal shift"

TWISTED GSM BEAMS

$$W(\rho_1,\rho_2,z)=\frac{S_0}{w^2(z)}\,e^{-\frac{\rho_1^2+\rho_2^2}{w^2(z)}}\,e^{-\frac{(\rho_1-\rho_2)^2}{2\sigma^2(z)}}\,e^{-\frac{ik\left(\rho_1^2-\rho_2^2\right)}{2R(z)}}$$

$$\times\ \underbrace{e^{-ik\,u(z)\,\rho_1\varepsilon\rho_2}}_{\text{"twist phase"}}$$

$$\rho_1\varepsilon\rho_2=\begin{pmatrix}x_1 & y_1\end{pmatrix}\begin{pmatrix}0 & 1\\ -1 & 0\end{pmatrix}\begin{pmatrix}x_2\\ y_2\end{pmatrix}=x_1y_2-y_1x_2$$

✧ four parameters $w(z)$, $\sigma(z)$, $R(z)$ & $u(z)$

✧ $|u(z)|\le 1/k\sigma^2(z)$

$\Rightarrow$ *twist phase disappears in the limit of full coherence*

✧ twist phase rotates the beam

✧ twist parameter alters the propagation laws;
it increases the "effective" degree of incoherence

$\Rightarrow$

$$\Theta_D=\left[kw_0\beta/2\right]^{-1}\left[1+\eta^2\left(1-\beta^2\right)^2/4\beta^2\right]^{1/2}$$

$$\left(\beta=\left[1+\frac{1}{\alpha^2}\right]^{-1/2}\quad\&\quad\eta=k\sigma_0^2u_0\right)$$

✧ useful limits:

$\eta = 0 \leftrightarrow$ ordinary GSM beam
$\beta = 1 \leftrightarrow$ laser beam

RESULTS

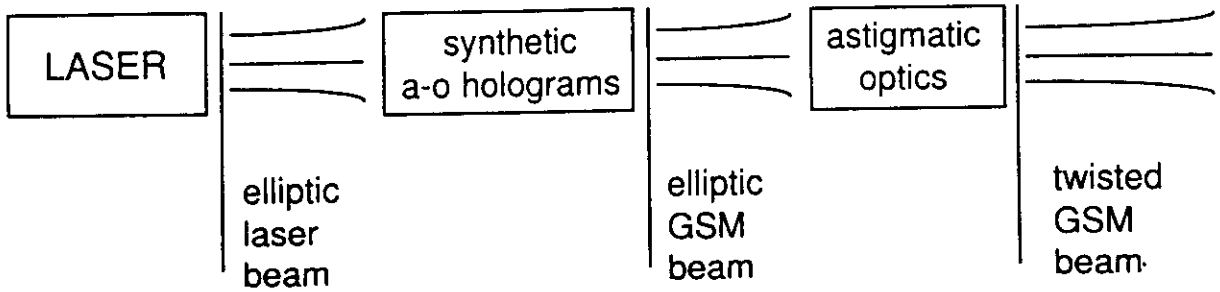

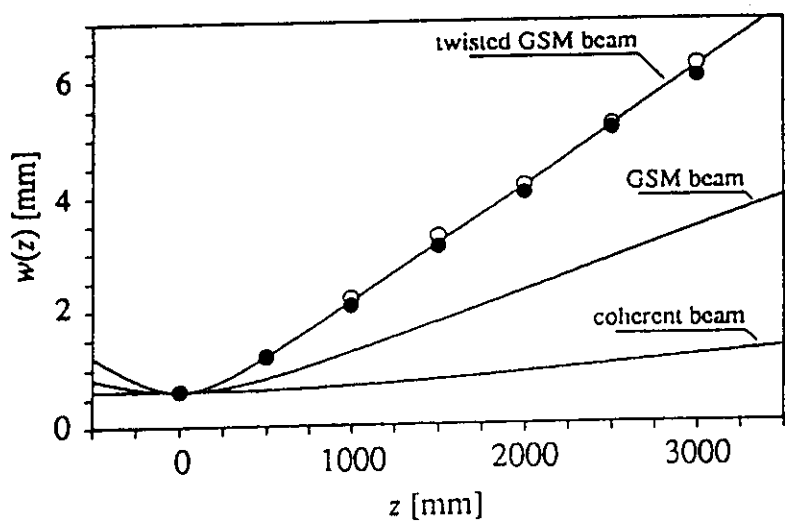

measured beam radius of twisted GSM beam

● in x-direction ○ in y-direction

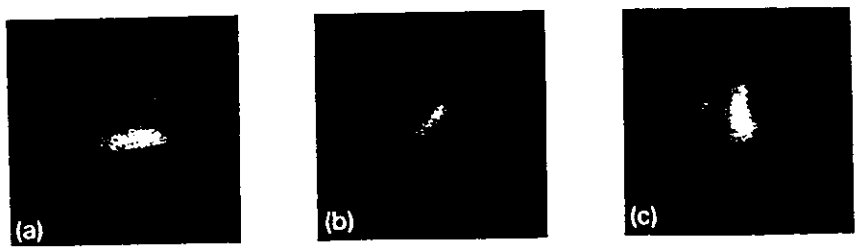

Fig. 5. Illustration of beam rotation in the focusing geometry of fig. 1. Three discrete spatial frequency components are generated by the acousto-optic deflector to simulate the situation illustrated in fig. 2. (a) The intensity profiles in the source plane, (b) in the plane of best focus, i.e., $z = f/2 = 150$ mm in fig. 4, and (c) in the plane $z = f = 300$ mm.

PROPAGATION-INVARIANT BEAMS

$$S(\rho,z) = S(\rho,0)$$

- Bessel beams $J_0^2(\alpha\rho)$
- Axicon line images
- Conical fields
- Interference pattern

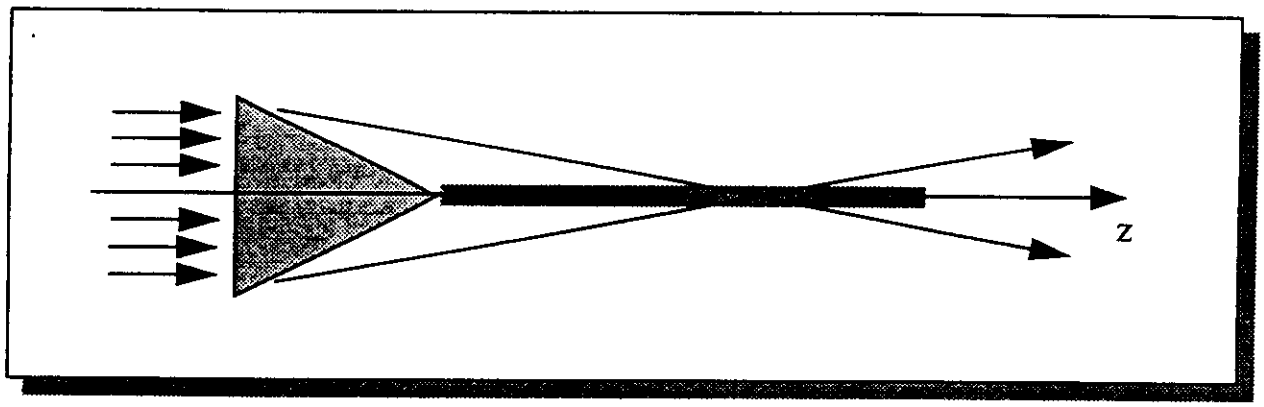

$$U(\rho,z) = e^{i\beta z}\int_0^{2\pi} F(\theta)e^{i\alpha(x\cos\theta+y\sin\theta)}d\theta$$

$$\alpha^2+\beta^2 = k^2$$

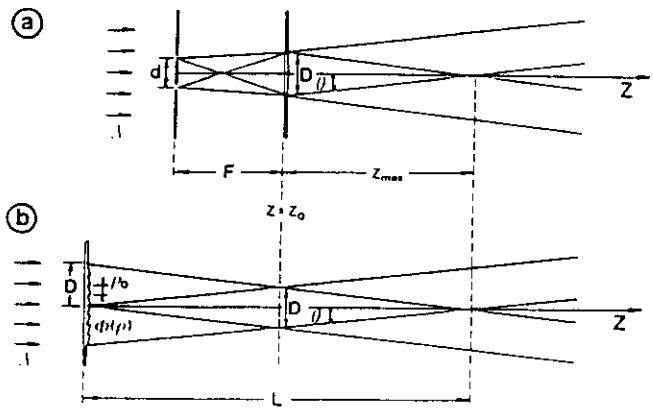

Fig. 1. (a) Original experimental arrangement for the generation of an approximate Bessel beam; (b) the modified system based on a holographic optical element (HOE).

Computer holograms generate any diffraction-free field

$$\rho_{HW} \sim \frac{1}{\alpha}$$

$$L \approx 2\pi D\rho_{HW} / \lambda$$

PARTIALLY COHERENT INVARIANT BEAMS

$$W(\rho_1,\rho_2;z) = W(\rho_1,\rho_2;0)$$

- invariant spectral intensity
- invariant coherence

CONICAL PLANE WAVES ARE UNCORRELATED IN RADIAL DIRECTION !

$$W(\mathbf{r}_1,\mathbf{r}_2) = \int_0^{k/2\pi} \int_0^{2\pi} f^2 S(f,\theta_1,\theta_2) e^{i(z_2-z_1)\sqrt{k^2-(2\pi f)^2}} \times e^{i2\pi f\left(x_2\cos\theta_2 - x_1\cos\theta_1 + y_2\sin\theta_2 - y_1\sin\theta_1\right)} df d\theta_1 d\theta_2$$

EXAMPLE: Bessel J_0-correlated beam

$$W(\mathbf{r}_1,\mathbf{r}_2) = S_0 e^{i\beta\left(z_2-z_1\right)} J_0\left(\alpha|\rho_1-\rho_2|\right)$$

- ✧ Generation by computer holography
- ✧ Fabry-Perot modes (self-imaging)
- ✧ Satisfy (planar) paraxial equation !
- ✧ Shape-invariant in *ABCD* systems

FOCUSING

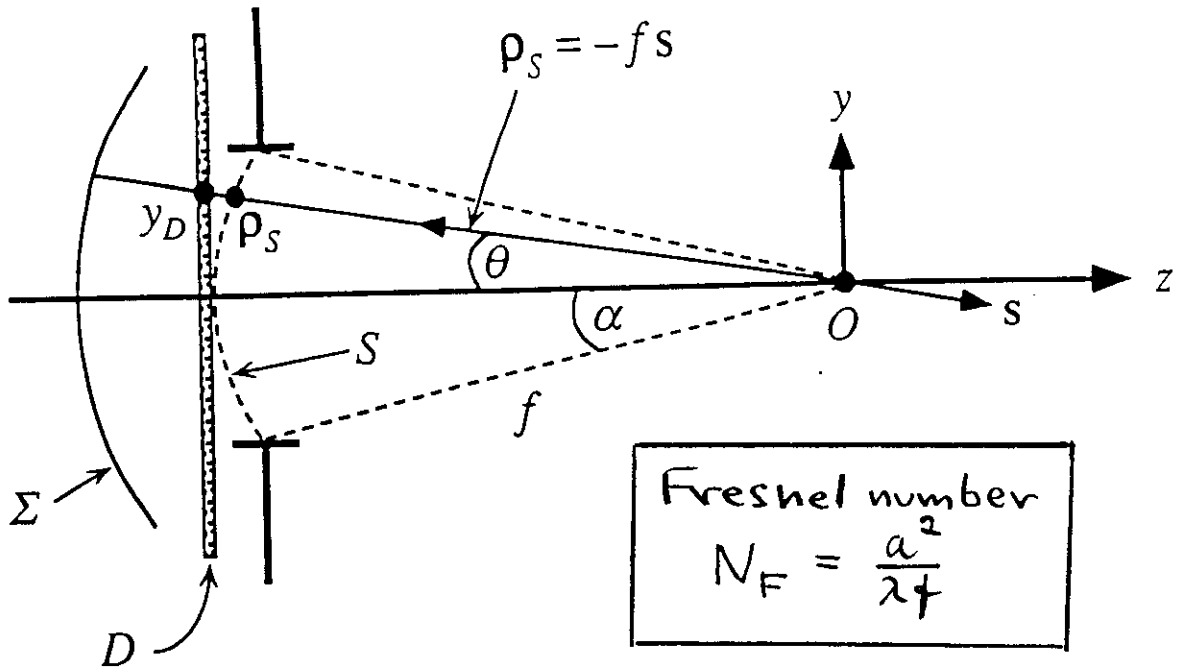

Fresnel number

$$N_F = \frac{a^2}{\lambda f}$$

$N_F \gg 1$ ~ DEBYE THEORY

$N_F \lesssim 1$ ~ FOCUS SHIFT

- SPOT SIZE
- FOCAL DEPTH
- 3D-PROFILE

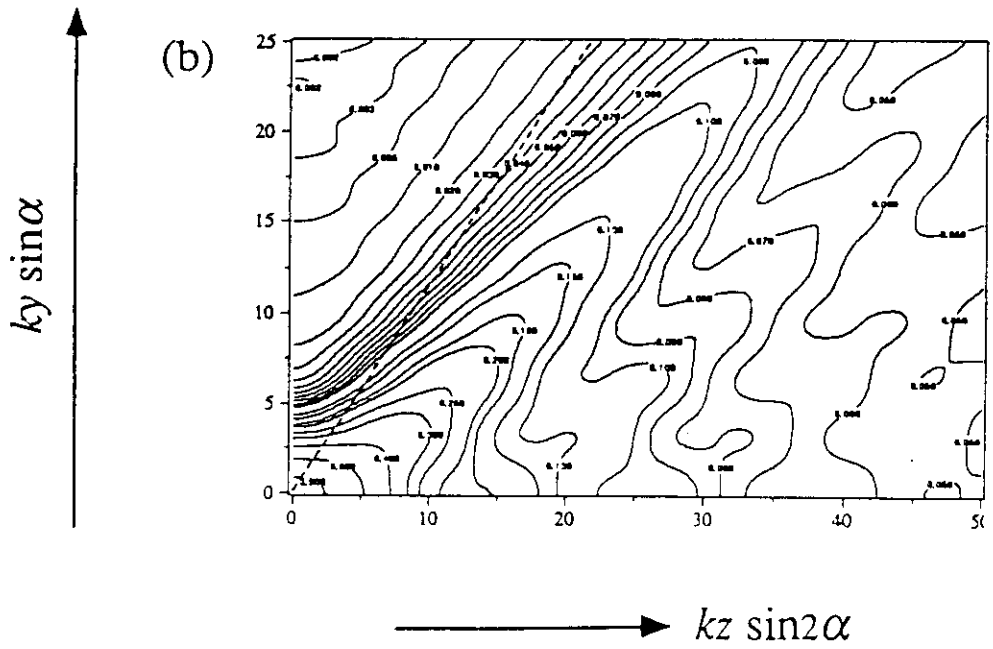

WAVE MODEL

AXICON LINE IMAGE

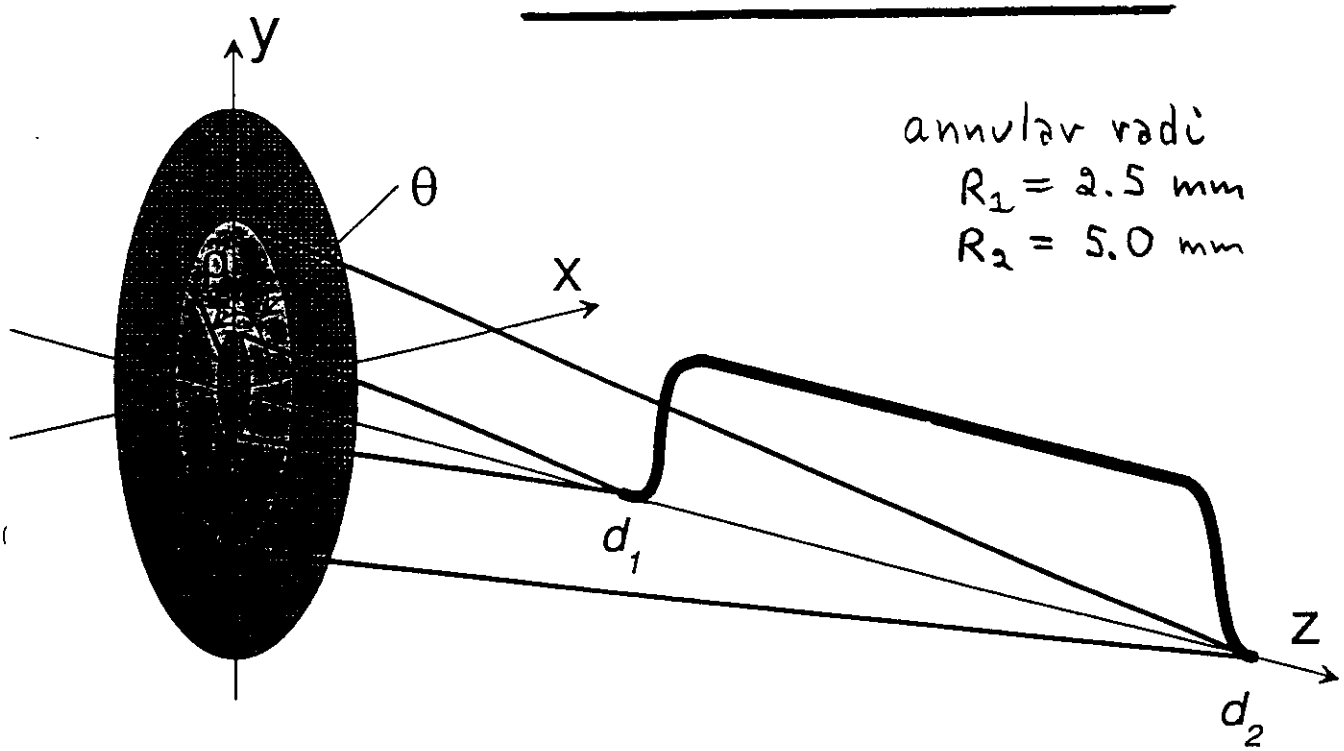

$$U(\vec{\rho},z) = -\frac{i}{\lambda z} e^{ikz} \iint U_0 \, e^{i\frac{k}{2z}(\vec{\rho}-\vec{\rho}')^2} d^2\vec{\rho}'$$

$$U_0 = e^{ik\varphi(\rho)} \qquad \varphi(\rho) = -1/2 \ln\left[d_1 + a(\rho^2 - r^2)\right]$$

⇨

$$I(\rho,z) = \left(\frac{k}{2\pi z}\right)^2 \iint \left[I_a(\rho_1) I_a(\rho_2)\right]^{1/2} C(\rho_1,\rho_2;\rho,z;\sigma_g) e^{-\frac{(\rho_1^2+\rho_2^2)}{2\sigma_g^2}}$$

$$\times e^{-ik\frac{(\rho_1^2-\rho_2^2)}{2z}} e^{-ik\left[\varphi(\rho_1)-\varphi(\rho_2)\right]} \rho_1\rho_2 d\rho_1 d\rho_2$$

where

$$C(\rho_1,\rho_2;\rho,z;\sigma_g) = \iint e^{\frac{(\rho_1\rho_2\cos(\theta_1-\theta_2))}{\sigma_g^2}} e^{-ik\rho\frac{(\rho_1\cos\theta_1-\rho_2\cos\theta_2)}{z}} d\theta_1 d\theta_2$$

RIGOROUS WAVE THEORY

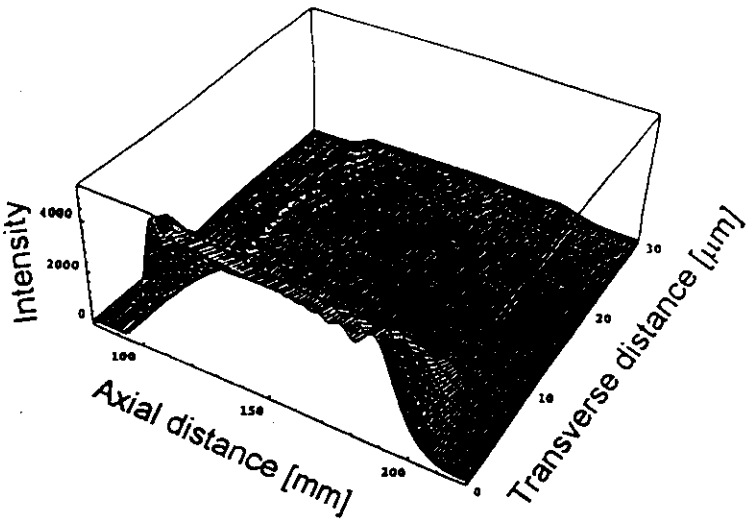

$\sigma = 7.5$ mm

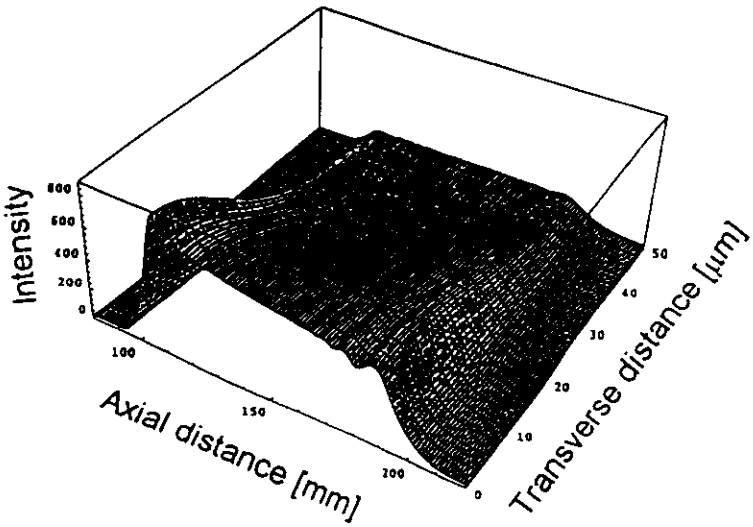

$\sigma = 1.0$ mm

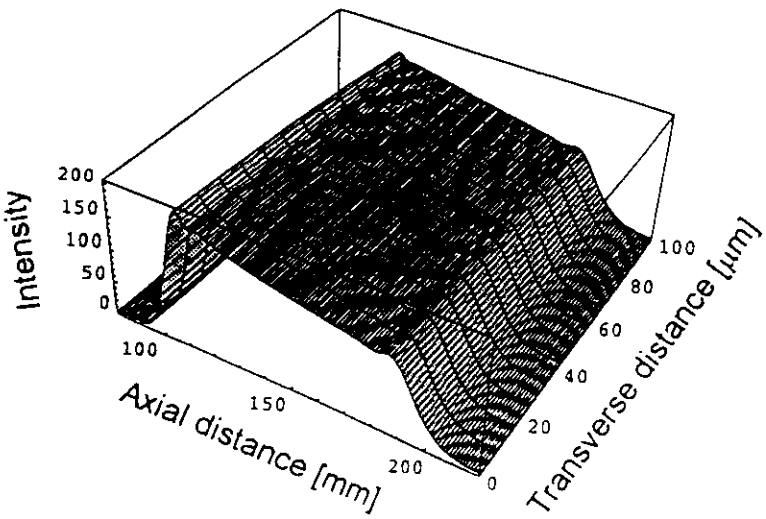

$\sigma = 0.25$ mm

PROPAGATION

Coherent fields (eg. modes) in half-space

A) ANGULAR SPECTRUM

$$E(\underline{\rho},z) = \iint_{-\infty}^{\infty} a(\underline{q}) e^{ik(\underline{q}\cdot\underline{\rho} + mz)} d^2\underline{q}$$

$$m = \sqrt{1-q^2}\ , \quad \text{if } |\underline{q}| \le 1$$

$$= i\sqrt{q^2-1}\ , \quad \text{if } |\underline{q}| > 1$$

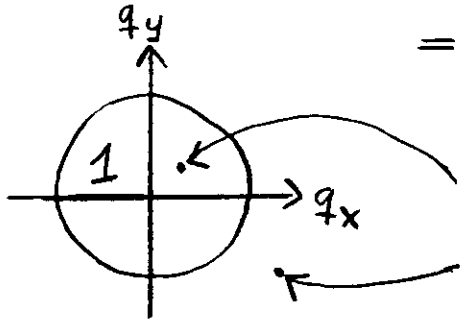

propagating wave

evanescent wave

B) GREEN FUNCTION

$$E(\rho,z) = -\frac{1}{2\pi}\int_{-\infty}^{\infty}\int_{-\infty}^{\infty} E(\rho',0)\frac{\partial}{\partial z}\left(\frac{e^{ikr'}}{r'}\right)d^2\rho', \qquad \text{(exact)}$$

$$E(\rho,z) = -\frac{ik}{2\pi}\int_{-\infty}^{\infty}\int_{-\infty}^{\infty} E(\rho',0)\cos\theta'\frac{e^{ikr'}}{r'}d^2\rho', \qquad \text{(nearly exact)}\ (kr \gg 1)$$

$$E_\infty(\rho,z) = -i2\pi k\cos\theta\tilde{E}_0(ks_t)\frac{e^{ikr}}{r}, \qquad \text{(asymptotic)}$$

$$\left(r' = \left[(\rho-\rho')^2 + z^2\right]^{1/2}, \quad \cos\theta' = z/r' \right)$$

FAR-ZONE BEHAVIOR

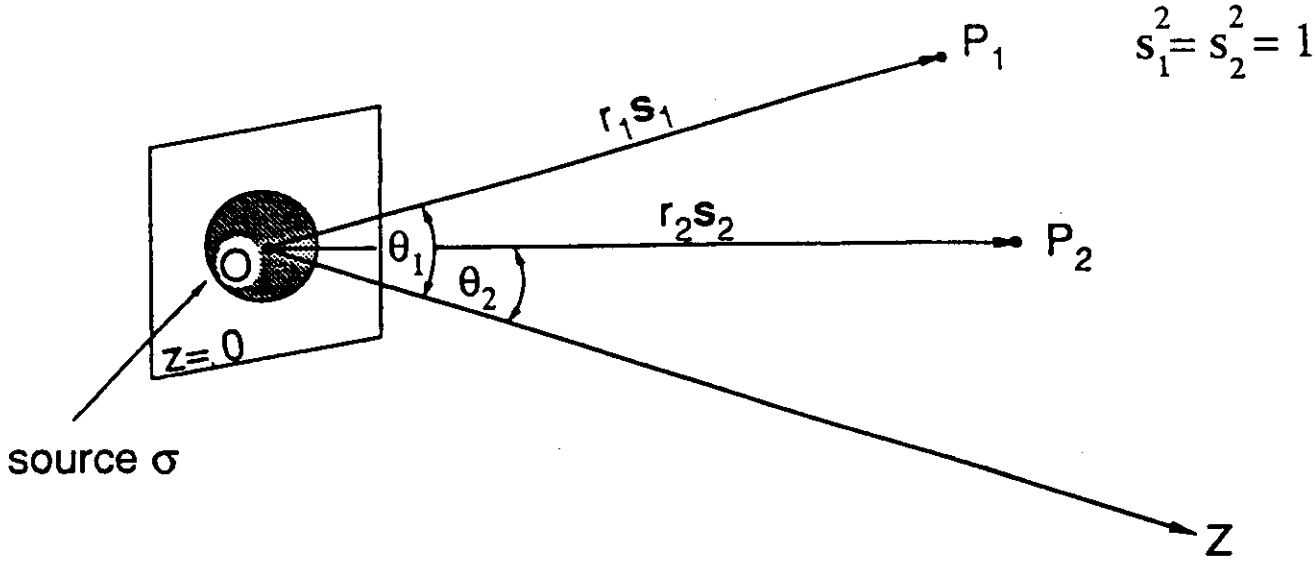

$$W^{(\infty)}(r_1 s_1, r_2 s_2, \omega) = (2\pi k)^2 \tilde{W}^{(0)}(k s_{1\perp}, -k s_{2\perp}, \omega) \frac{e^{ik(r_1 - r_2)}}{r_1 r_2} \cos\theta_1 \cos\theta_2$$

$$(k r_1 \to \infty, \quad k r_2 \to \infty)$$

$\tilde{W}$ ~ 2D spatial Fourier transform

- ANGULAR CORRELATION FUNCTION

$$A(s_{1\perp}, s_{2\perp}; \omega) = k^4 \tilde{W}^{(0)}(k s_{1\perp} - k s_{2\perp}, \omega)$$

— characterizes correlations between plane waves

[E.W. Marchand & E. Wolf, JOSA 62, 379 (1972)]

RADIANT INTENSITY

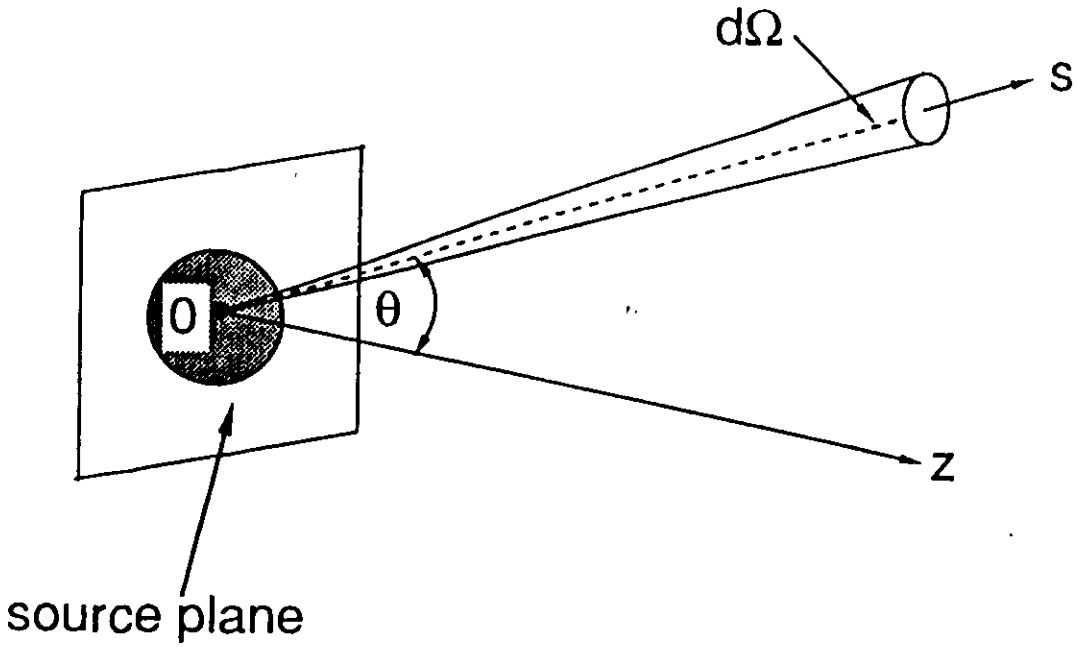

$$J(\underline{s}) = (2\pi k)^2 \tilde{W}^{(0)}(k\underline{s}_\perp, -k\underline{s}_\perp)\cos^2\Theta$$

- depends only on the anti-diagonal elements of $\tilde{W}^{(0)}$

$\Rightarrow$ EQUIVALENCE RELATIONS

(i.e., many sources with different spatial coherence properties may generate identical radiant intensity)

• RECIPROCITY FOR QUASI-HOMOGENEOUS SOURCES

$$J(\underline{s}) = (2\pi k)^2 C\, \tilde{q}^{(0)}(k s_1) \cos^2\Theta$$

$$\mu^{(\infty)}(r\underline{s}_1, r\underline{s}_2) = \frac{1}{C}\, \tilde{I}^{(0)}[k(\underline{s}_{21} - \underline{s}_{21})]$$

$$C = \tilde{I}^{(0)}(0) = \frac{1}{(2\pi)^2} \iint I^{(0)}(\underline{s})\, d^2\rho$$

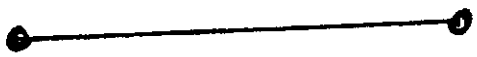

SOURCE PLANE FAR ZONE

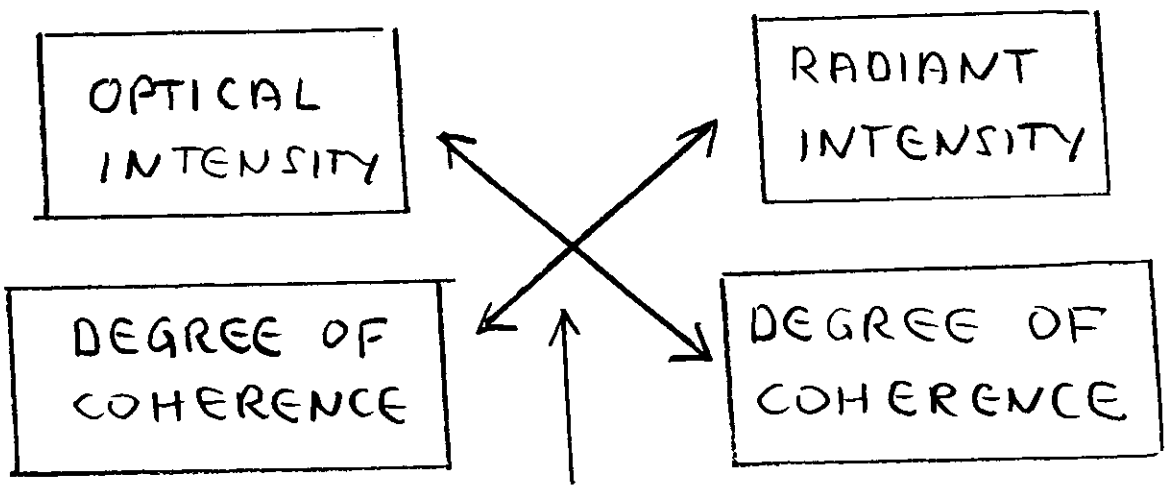

Spatial Fourier transforms

EQUIVALENT GAUSSIAN MODEL SOURCES

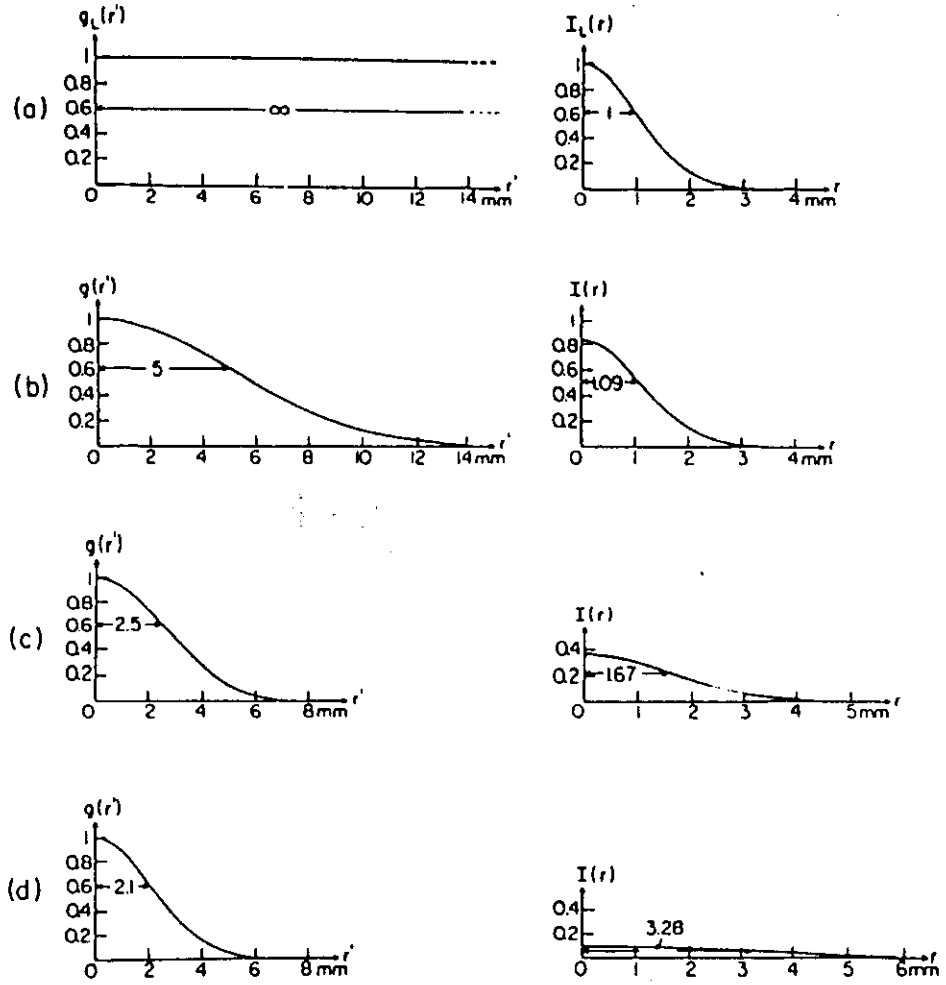

Illustrating the coherence and the intensity distributions across three partially coherent sources [(b), (c), (d)] which produce fields whose far-zone intensity distributions are the same as that generated by a coherent laser source [(a)]. The parameters characterizing the four sources are:

(a) $\sigma_g = \infty$, $\sigma_I = \delta_L = 1$ mm, $A = 1$ (arbitrary units) (b) $\sigma_g = 5$ mm, $\sigma_I = 1.09$ mm, $A = 0.84$

(c) $\sigma_g = 2.5$ mm, $\sigma_I = 1.67$ mm, $A = 0.36$ (d) $\sigma_g = 2.1$ mm, $\sigma_I = 3.28$ mm, $A = 0.09$.

The normalized radiant intensity generated by all these sources is $J(\theta)/J(0) = \cos^2\theta \exp\{-2(k\delta_L)^2 \sin^2\theta\}$, ($\delta_L = 1$ mm).

[After E. Wolf and E. Collett, Opt. Commun., 25, 293, 1978)]

- all produce the same radiant intensity as the laser
- "trade-off"

PLANAR RADIOMETRY

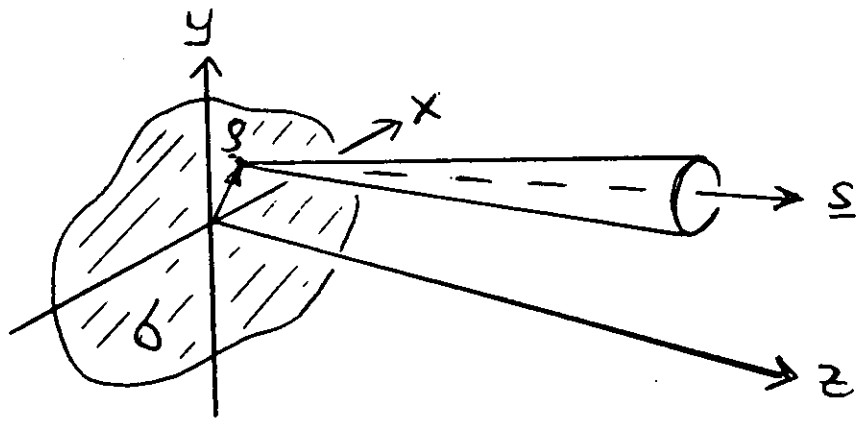

* **RADIANT INTENSITY** $J(s)$

  - EXACT FAR-FIELD PROPAGATION
  - PHYSICAL -OPTICS DEFINITION
  - MAIN OBSERVABLE QUANTITY
  - ANGULAR DISTRIBUTION
  - RADIATION EFFICIENCY

* **RADIANCE (BRIGHTNESS)** $B(\rho, s)$

  - MAIN RADIOMETRIC QUANTITY
  - AMBIGUOUS
    (SEVERAL DEFINITIONS IN USE)

* **RADIANT EMITTANCE** $E(\rho)$

  - IRRADIANCE

$$J(s) = \left(\frac{k}{2\pi}\right)^2 \cos^2\theta \iint W(\rho_1, \rho_2; 0) e^{-iks\bullet(\rho_2-\rho_1)} d^2\rho_1 d^2\rho_2$$

$$= \cos\theta \int B(\rho, s; 0) d^2\rho$$

TABLE I. Radiation from Partially Coherent Model Sources.

MODEL	QUASIHOMOGENEOUS			SCHELL
INTENSITY	NOT RELEVANT			GAUSSIAN
COHERENCE	GAUSSIAN	EXPONENTIAL	BESSEL	GAUSSIAN
COEFFICIENT OF DIRECTIONALITY	$e^{-\underline{r}'^2/2\sigma_\mu^2}$	$e^{-\lvert\underline{r}'\rvert/D}$	$\frac{2}{\sqrt{\pi}}\,\Gamma(\nu+\frac{3}{2})\frac{j_\nu(k\lvert\underline{r}'\rvert)}{(\frac{1}{2}k\lvert\underline{r}'\rvert)^\nu}$	$e^{-\underline{r}'^2/2\Delta^2}$ $\frac{1}{\Delta^2}=\frac{1}{\sigma_\mu^2}+\frac{1}{(2\sigma_I)^2}$
RADIANT INTENSITY	$J_{\omega,o}\cos^2\theta e^{-\frac{1}{2}(k\sigma_\mu)^2\sin^2\theta}$ $J_{\omega,o}=\frac{(k\sigma_\mu)^2}{2\pi}\int I^{(0)}(\underline{r},\omega)d^2r$	$J_{\omega,o}\cos^2\theta[1+(kD)^2\sin^2\theta]^{-\frac{3}{2}}$ $J_{\omega,o}=\frac{(kD)^2}{2\pi}\int I^{(0)}(\underline{r},\omega)d^2r$	$J_{\omega,o}\cos^{2\nu+1}\theta$ $J_{\omega,o}=\frac{1}{\pi}(\nu+\frac{1}{2})\int I^{(0)}(\underline{r},\omega)d^2r$	$J_{\omega,o}\cos^2\theta e^{-\frac{1}{2}(k\Delta)^2\sin^2\theta}$ $J_{\omega,o}=(k\Delta\sigma_I)^2 I_o$
RADIATION EFFICIENCY	$1-\frac{F(k\sigma_\mu/\sqrt{2})}{k\sigma_\mu/\sqrt{2}}$ $F(a)=e^{-a^2}\int_o^a e^{u^2}du$	$1-\frac{1}{(kD)}\sin^{-1}\left(\frac{kD}{\sqrt{1+(kD)^2}}\right)$	$\frac{2\nu+1}{2\nu+2}$	$1-\frac{F(k\Delta/\sqrt{2})}{k\Delta/\sqrt{2}}$ $F(a)=e^{-a^2}\int_o^a e^{u^2}du$

ANGULAR DISTRIBUTION

$$\frac{J(\theta)}{J(0)}$$

(exact)

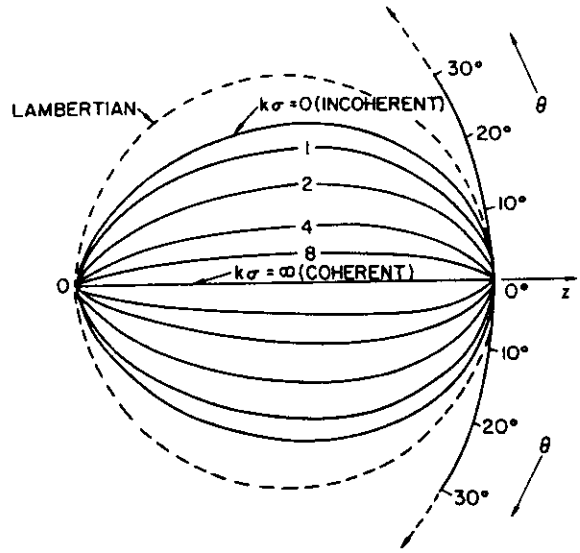

RADIATIVE TRANSFER

$$(\underline{s}\cdot\nabla)I(\underline{r},\underline{s}) = -\alpha(\underline{r},\underline{s})I(\underline{r},\underline{s}) + \int\beta(\underline{r},\underline{s},\underline{s}')I(\underline{r},\underline{s}')d\Omega' + D(\underline{r},\underline{s})$$

	$\underline{r}$	$\underline{s}$
CONV.	Yes	Yes
WAVE	Yes	No
QM	No	No

ASYMPTOTIC RADIOMETRY & COHERENCE TRANSPORT

- $B(\underline{r}, \underline{s}) = k^2 s_z \, I^{(0)}(\underline{\rho}_0, \omega) \, \tilde{g}(k\underline{s}_\perp, \omega)$

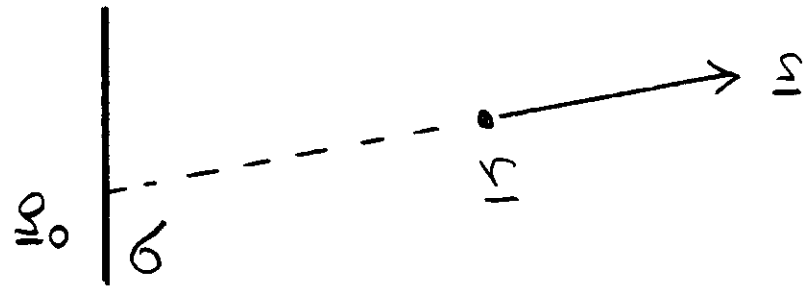

- $B(\underline{r}, \underline{s})$ = constant along straight lines

- $W(\underline{r}_1, \underline{r}_2) = \int_{(2\pi)} B\left(\frac{\underline{r}_2 + \underline{r}_2}{2}, \underline{s}\right) \cdot e^{ik\underline{s}\cdot(\underline{r}_2 - \underline{r}_1)} \, d\Omega$

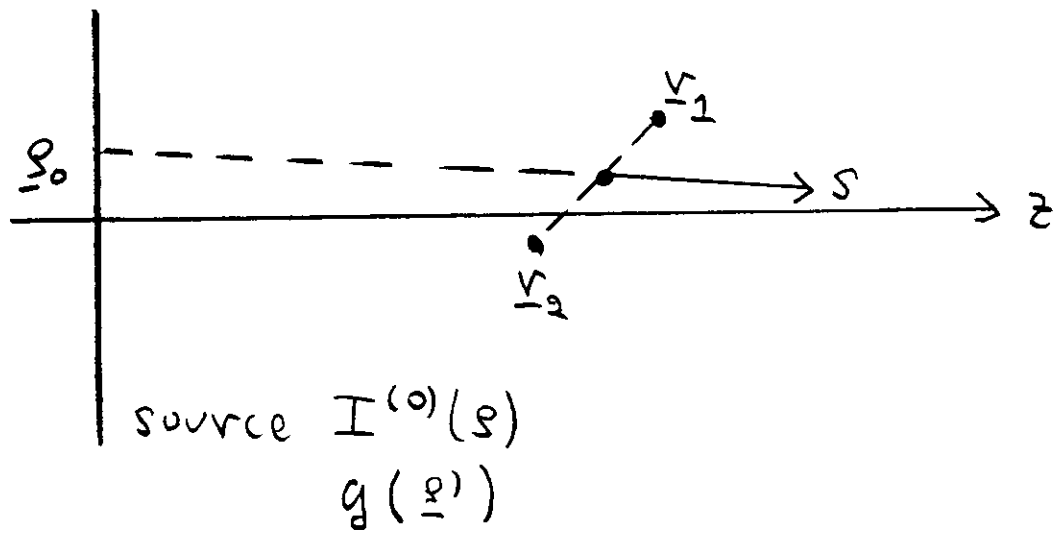

AXICON LINE IMAGE
Spatial Coherence

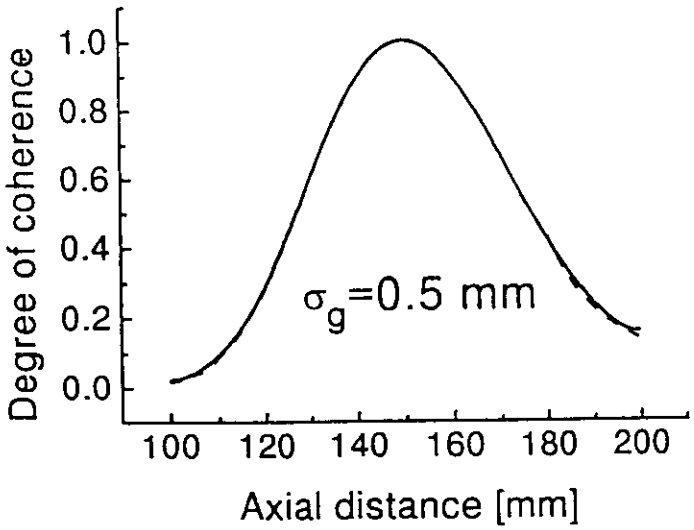

Complex Degree of Spectral Coherence

$$\mu(r_1, r_2) = \frac{W(r_1, r_2)}{[S(r_1)S(r_2)]^{1/2}}$$

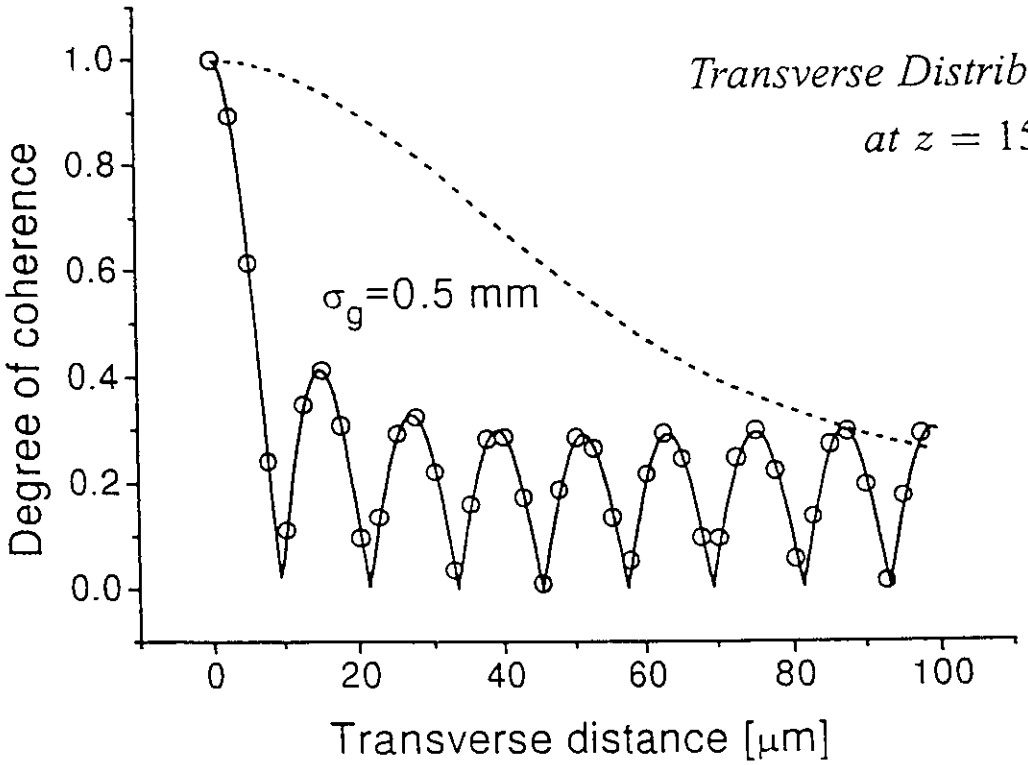

Transverse Distributions
at $z = 150\ mm$

* Radiometric and wave-theoretic results are indistinguishable!

TWISTED GAUSSIAN SCHELL-MODEL BEAM

$$W(\rho_1,\rho_2,z)=\left(\frac{S_0}{w^2(z)}\right)e^{-(\rho_1^2+\rho_2^2)/w^2(z)}$$

$$\cdot e^{-(\rho_1-\rho_2)^2/2\sigma^2(z)}e^{-ik(\rho_1^2-\rho_2^2)/2R(z)}\;e^{-ik\rho_1\cdot\varepsilon\rho_2 u(z)}$$

where

$w(z)=w(0)[1+(z/z_R)^2]^{1/2}$ (beam radius)

$\sigma(z)=\sigma(0)[1+(z/z_R)^2]^{1/2}$ (transverse coherence)

$R(z)=z[1+(z_R/z)^2]$ (radius of curvature)

$u(z)=u(0)[1+(z/z_R)^2]^{-1}$ (twist parameter)

and

$z_R=\frac{\pi w^2(0)}{\lambda}\beta\left[1+\eta^2\left(\frac{1-\beta^2}{2\beta}\right)^2\right]^{-1/2}$ (Rayleigh range)

$\beta=\left\{1+[w(z)/\sigma(z)]^2\right\}^{-1/2}$ ('global' coherence)
$(0\le\beta\le 1)$

$\eta=k\sigma^2(z)u(z)$ (normalized twist parameter)
$(-1\le\eta\le 1)$

Comments:

* most general rotation-invariant Gaussian beam
* twist manifests itself e.g. in increased diffraction

$$\theta\approx\tan\theta=\lim_{z\to\infty}w(z)/z=w(0)/z_R$$

TWIST EFFECTS

* FAR-FIELd DIFFRACTION ANGLE

$$\theta = \frac{w(0)}{z_R} = \underbrace{\frac{\lambda}{\pi w(0)}}_{\text{LASER}} \quad \underbrace{\frac{1}{\beta}}_{\text{REDUCED COHERENCE}} \quad \underbrace{\sqrt{1+\eta^2\left(\frac{1-\beta^2}{2\beta}\right)^2}}_{\text{TWIST}}$$

* BEAM ROTATION

- IN FREE SPACE

  THE ROTATION ANGLE $\begin{cases} \phi = \pi/4 & \text{AT } z = z_R \\ \phi = \pi/2 & \text{AT } z \to \infty \end{cases}$

- IN QUADRATIC-INDEX (SELFOC) FIBERS

  THE BEAM ROTATES BY 2π
  IN EVERY SELF-IMAGING DISTANCE

➨ **BEAM ROTATION CAN BE SEEN BY DECOMPOSING THE TWISTED GSM BEAM INTO AN INCOHERENT SUPERPOSITION OF ELLIPTIC GAUSSIAN BEAMS**

⇒ **PRACTICAL GENERATION TECHNIQUE**

TWIST GENERATION

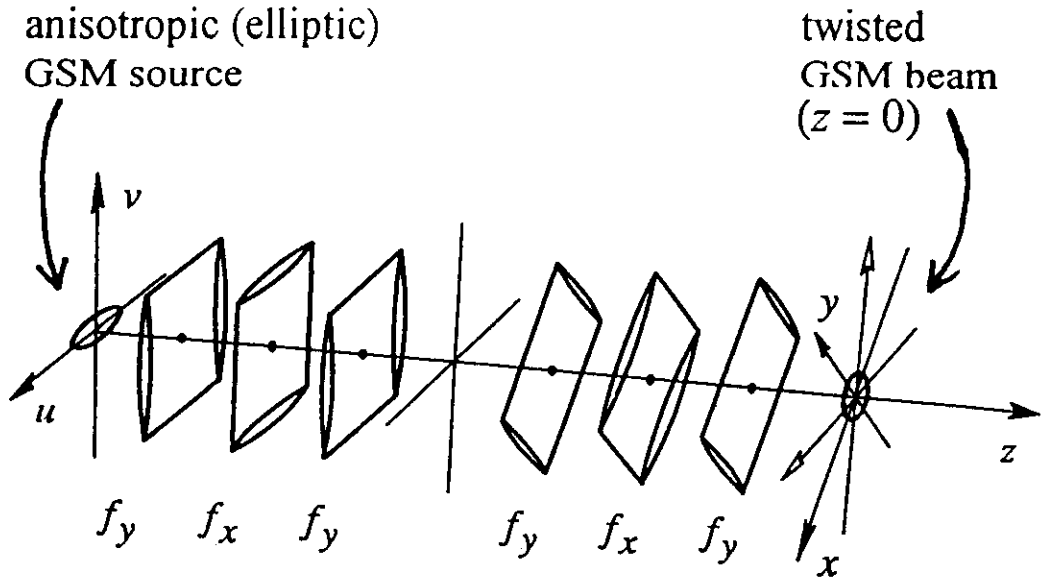

Astigmatic lens blocks

* $4f$ - imaging in one dimension
* $2f$ - Fourier transform in the other
* second block rotated by 45 degrees

First-order systems[(b)]

$$\begin{pmatrix} \rho \\ \rho' \end{pmatrix}_{\text{OUT}} = \begin{pmatrix} A & B \\ C & D \end{pmatrix} \begin{pmatrix} \rho \\ \rho' \end{pmatrix}_{\text{IN}}$$

A,B,C,D are 2x2 matrices

$$U(\rho, z_{out}) = \frac{-ik}{2\pi} e^{ikL} (\det B)^{-1} \int\int U(\rho_0, z_{in})$$

$$\cdot \exp\left[ik(\rho^{\mathrm{T}} D B^{-1} \rho - 2\rho_0^{\mathrm{T}} B^{-1} \rho + \rho_0^{\mathrm{T}} B^{-1} A \rho_0)/2 \right] d^2\rho_0$$

(*b*) A.E. Siegman, *Lasers* (1986), Section 15.6

DECOMPOSITIONS

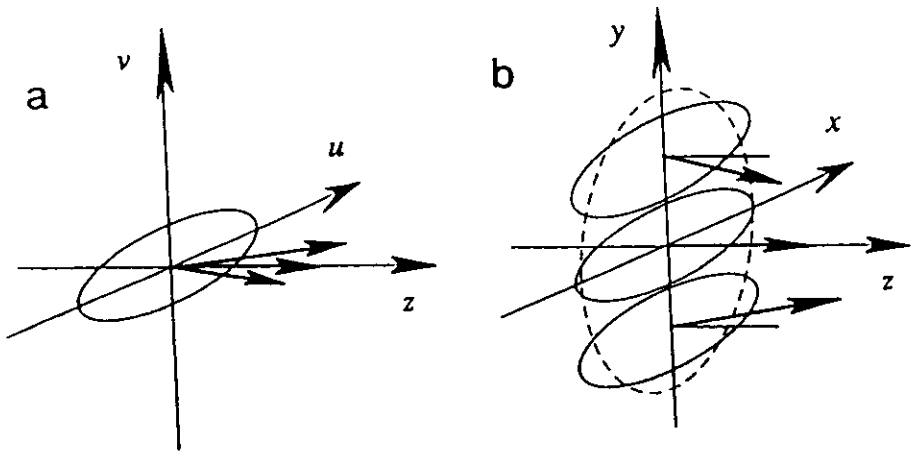

anisotropic GSM beam waist

twist beam waist

- INPUT

$$W(u_1, u_2, v_1, v_2) = \int P(\theta) U^*(u_1, v_1, \theta) U(u_2, v_2, \theta) d\theta$$

where

$$U(u, v, \theta) = \sqrt{I}\, \exp(-u^2/w_u^2)\exp(-v^2/w_v^2)\exp(ik\theta u)$$

$$P(\theta) = (2\pi)^{-1/2} k\sigma_u \exp\left[-\tfrac{1}{2}(k\sigma_u)^2\theta^2\right]$$

- OUTPUT
  - * weighted distribution of rotated ellipses
  - * displaced in y-direction by y_0
  - * propagate in xz-plane (increasing tilt phase)
  - * additional phase $const \cdot x(y - y_0)$

CONSTRAINTS

- INPUT: **Elliptic GSM source**
  - * characterized by $w_x, w_y, \sigma_x, \sigma_y$
  - * $\beta_{x,y} = \left\{1 + [w_{x,y}/\sigma_{x,y}]^2\right\}^{-1/2}$
  - * Rayleigh range $z_R = \pi w_x^2 \beta_x/\lambda = \pi w_y^2 \beta_y/\lambda$

    $= f_x = 2f_y =$ half of block length

- OUTPUT: **Twisted GSM source**

$$\begin{cases} \text{beam radius} & w = \sqrt{\frac{1}{2}(w_x^2 + w_y^2)} \\ \text{coherence} & \sigma = w\sqrt{\frac{\beta_x\beta_y}{1-\beta_x\beta_y}} \\ \text{curvature} & R = \infty \\ \text{twist phase} & u = \frac{1}{kw^2}\frac{\beta_x-\beta_y}{\beta_x\beta_y} \end{cases}$$

  - * $\beta = \sqrt{\beta_x\beta_y}$
  - * $\eta = \frac{\beta_x-\beta_y}{1-\beta_x\beta_y}$

○ IMPLICATIONS

- ○ symmetric input $\Rightarrow$ no twist ($\eta = 0$)
- ○ one $\beta = 1$ $\Rightarrow$ maximum twist ($|\eta| = 1$)
- ○ increased ellipticity $\Rightarrow$ $|\eta|$ increases

TWIST INTERPRETATION

($|\eta| = 1$)

twist
beam
waist

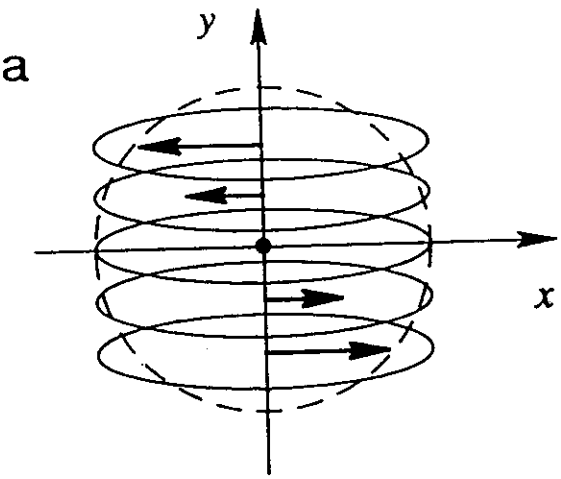

Rayleigh
range

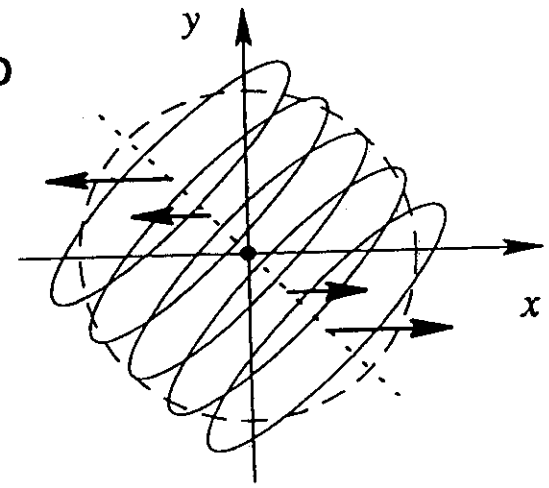

far-field

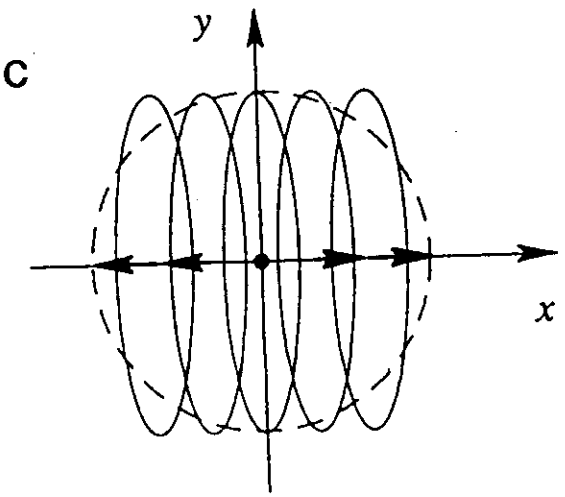

LASER TO ELLIPTIC GSM CONVERSION

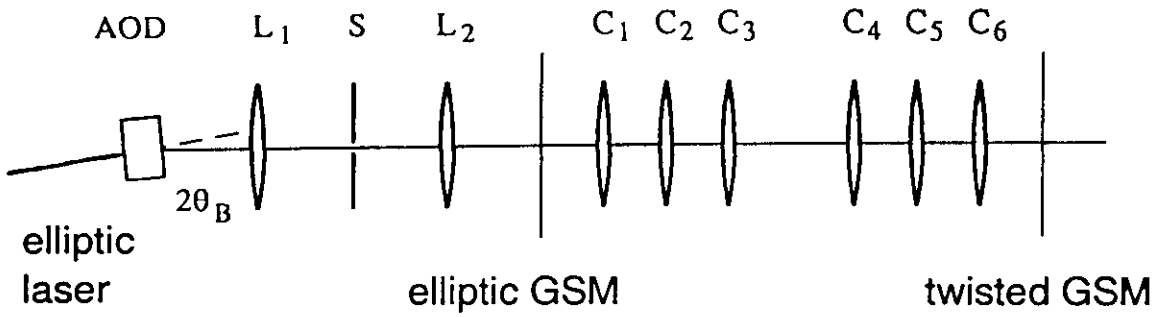

Synthetic Acousto-Optic Holograms[c]

* optimized, binary-phase modulated Bragg diffraction
* coherent, uncorrelated fields in different directions
* spatial filter removes unwanted orders

power spectrum (in x-direction)

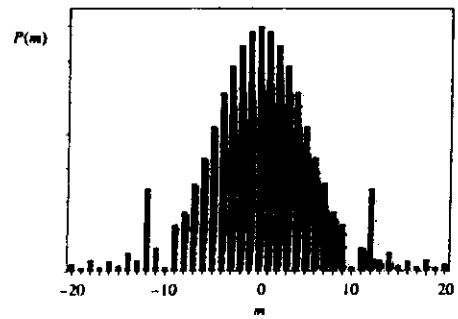

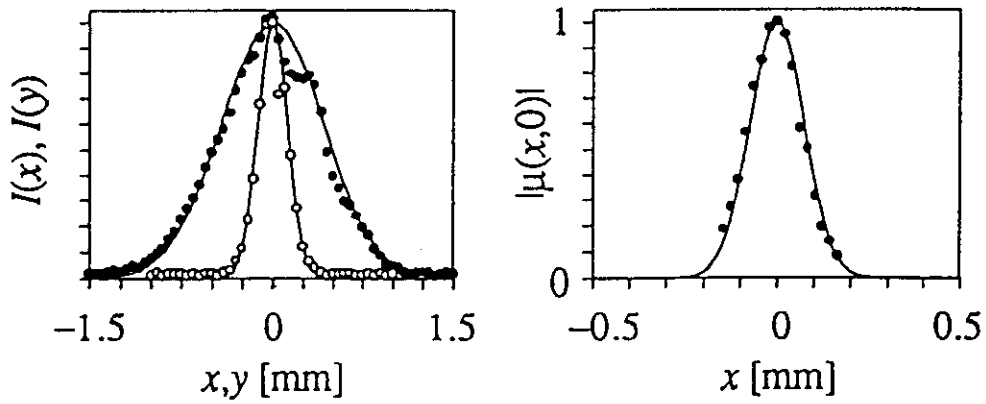

measured intensity and coherence across elliptic GSM source

• along x-direction ○ along y-direction

(c) J. Turunen, E. Tervonen, and A.T. Friberg, *J. Appl. Phys.* **67**, 49 (1990)

EXPERIMENTAL RESULTS

Twisted GSM waist:

$w = 0.616\ mm$
$\sigma = 0.190\ mm$
$\beta = 0.294$
$\eta = -1$

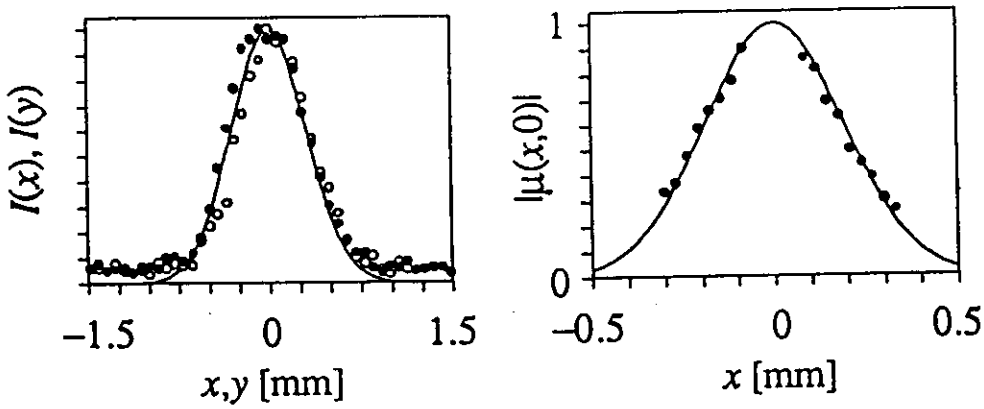

measured intensity and coherence across twisted GSM waist

- ● along x-direction
- ○ along y-direction

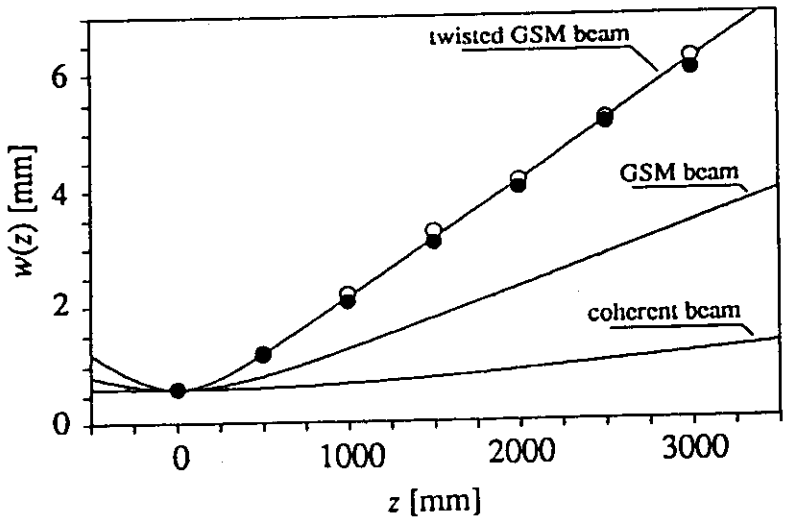

measured beam radius of twisted GSM beam

- ● in x-direction
- ○ in y-direction

FAR-FIELD DIFFRACTION ANGLE:

$\theta_{TGSM}/\theta_{GSM} = 1.85 \quad \theta_{TGSM}/\theta_{LASER} = 6.28$

RADIANT INTENSITY

* **ROTATIONALLY SYMMETRIC**

$$J(\theta) = J(0)\cos^2\theta e^{-\xi^2\sin^2\theta}$$

$$J(0) = S_0(2\sigma_S^2)\xi^2$$

$$\xi^2 = \left[\frac{1}{2(k\sigma_S)^2} + \frac{2}{(k\sigma_g)^2} + 2(\sigma_S u)^2\right]^{-1}$$

* **CONSEQUENCES**

  - EQUIVALENCE RELATIONS
  - TWIST u INCREASES $\Rightarrow \xi$ DECREASES
    $\Rightarrow$ RADIATION SPREADS MORE

PARAXIAL LIMIT:

$$\left(\cos\theta \approx 1,\ \sin\theta \approx \theta\right)$$

$$\theta_d = \sqrt{2}\,(1/\xi)$$

$$= \frac{\lambda}{\pi w(0)}\ \frac{1}{\beta}\left[1 + \eta^2\left(\frac{1-\beta^2}{2\beta}\right)^2\right]^{1/2} \qquad \text{OK.}$$

$$\beta \rightarrow \beta_{eff} = \beta\left[1 + \eta^2\left(\frac{1-\beta^2}{2\beta}\right)^2\right]^{-1/2}$$

RADIATION EFFICIENCY

$$C = \frac{\Phi}{N} = \frac{RADIATED\ \ POWER}{TOTAL\ \ INTENSITY}$$

$$\Phi = \int_{(2\pi)} J(s)d\Omega \qquad \text{(Total Flux)}$$

$$N = \int_{\sigma} S(\rho, 0)d^2\rho \qquad \text{(Source-Integrated Spectral Intensity)}$$

$$C = 1 - D(\xi)/\xi$$

$$D(\xi) = \exp(-\xi^2)\int_0^{\xi} \exp(t^2)dt \qquad \text{(Dawson's Integral)}$$

$$\xi = \frac{\sqrt{2}\,\pi w(0)}{\lambda}\beta_{eff}$$

- **IMPLICATIONS:**
  - C IS MONOTONOUSLY INCREASING IN ξ
  - $\xi^2 = \left[\frac{1}{2(k\sigma_S)^2} + \frac{2}{(k\sigma_g)^2} + 2(\sigma_S u)^2\right]^{-1}$

  - FOR QUASI-HOMOGENEOUS ($\sigma_S >> \sigma_g$) TGSM SOURCES

$$\xi^2 \approx \frac{k^2\sigma_g^2}{2} \geq \frac{k^2\sigma_g^2}{2(1+k^2\sigma_S^2\sigma_g^2u^2)} \geq \frac{k^2\sigma_g^2}{2(1+\sigma_S^2/\sigma_g^2)} \rightarrow \frac{k^2\sigma_g^2}{2}\left(\frac{\sigma_g}{\sigma_S}\right)^2$$

no twist	twist	max twist
$(u = 0)$	(u)	$(\lvert u\rvert = 1/k\sigma_g^2)$

  - QH MORE EFFICIENT THAN LASER, IF $\sigma_g^2 > 4\sigma_L^2(1 + k^2\sigma_S^2\sigma_g^2u^2)$

RADIATION EFFICIENCY

NO TWIST (GSM)
$(u = 0)$

MAX TWIST
$(|u| = 1/k\sigma_g^2)$

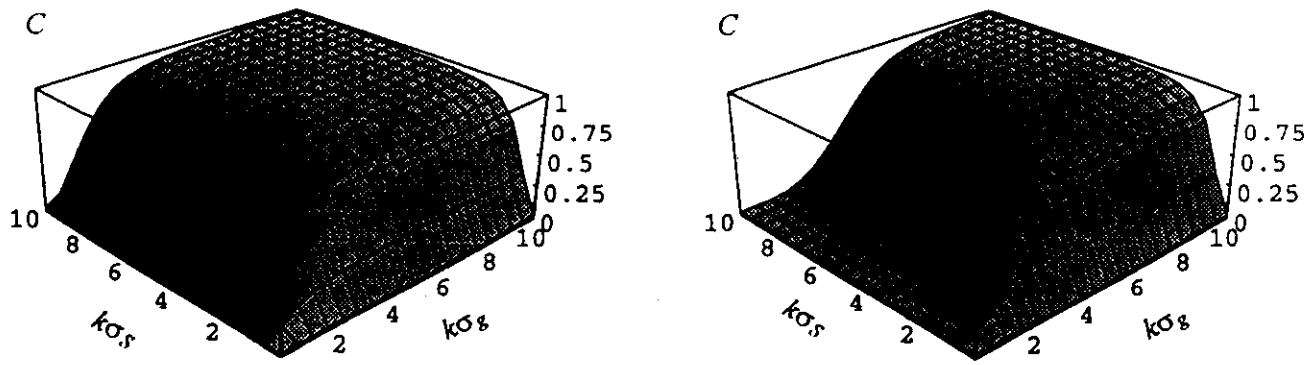

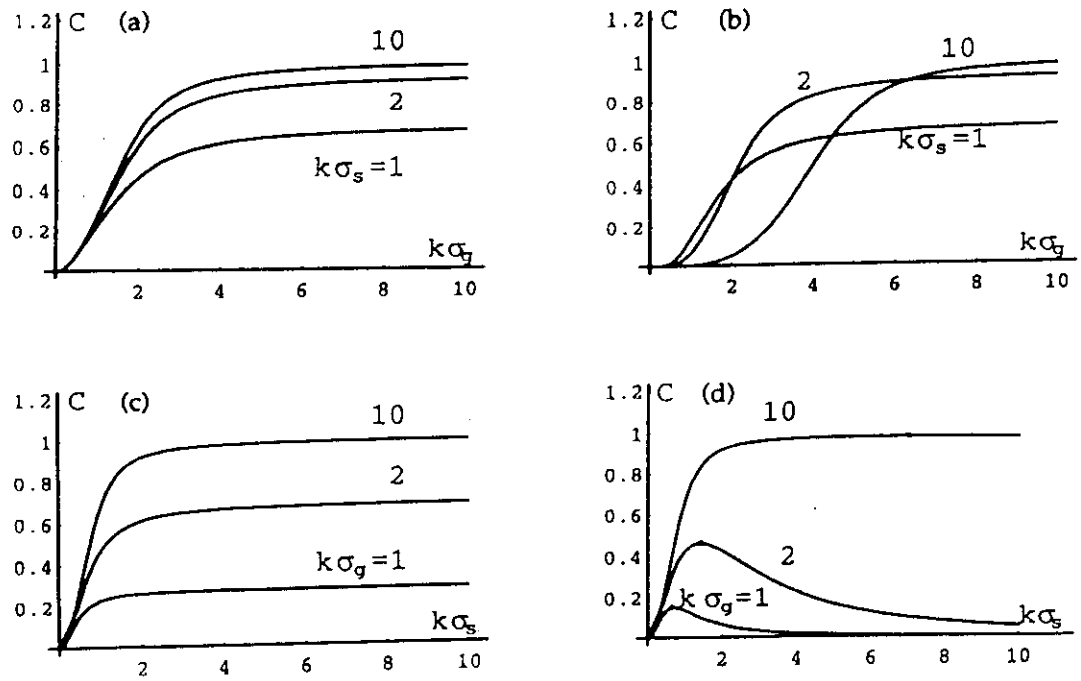

Figure 3. Radiation efficiency C as a function of $k\sigma_g$ for selected values of $k\sigma_S$ (a and b) and as a function of $k\sigma_S$ for selected values of $k\sigma_g$ (c and d), both in the no-twist case $u = 0$ (a and c) and in the maximum-twist case $|u| = 1/k\sigma_g^2$ (b and d).

RADIANCE

(WALTHER 1968)

$$B(\rho, s) = \left(\frac{k}{2\pi}\right)^2 \cos\theta \int W(\rho - \tfrac{1}{2}\rho', \rho + \tfrac{1}{2}\rho') e^{-iks\bullet\rho'} d^2\rho'$$

* ~ **WIGNER DISTRIBUTION FUNCTION**
* **INVARIANT IN ABCD SYSTEMS**
* **'TRANSFER FUNCTION'** $E(\rho, 0) = C(\sigma_S, \sigma_g, u; \rho) S(\rho, 0)$

$$B(\rho, s; 0) = (2S_0/\pi)(k\zeta\sigma_S)^2 \cos\theta \exp\left[-(k\zeta\xi\rho)^2\right]$$
$$\times \exp\left\{-2(k\zeta\sigma_S)^2\left[\sin^2\theta + 2u\sin\theta(x\sin\varphi - y\cos\phi)\right]\right\}$$

$$\zeta^2 = \left[1 + (2\sigma_S/\sigma_g)^2\right]^{-1}$$

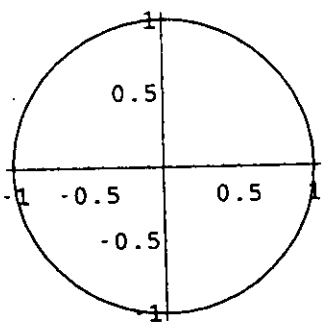

($\delta = 0$)

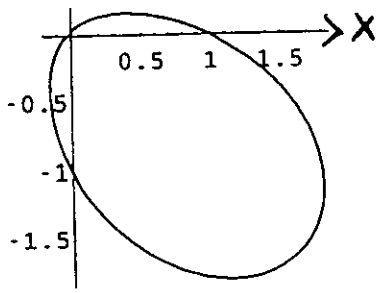

($\delta = 2$)

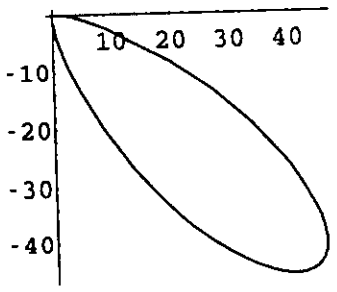

($\delta = 10$)

(WALTHER 1972)

$$B'(\rho, s) = \left(\frac{k}{2\pi}\right)^2 \cos\theta \int W(\rho', \rho) e^{-iks\bullet(\rho - \rho')} d^2\rho'$$

* **ASYMPTOTICALLY INVARIANT IN ABCD SYSTEMS** $(\lambda \to 0)$

FOCAL REGION

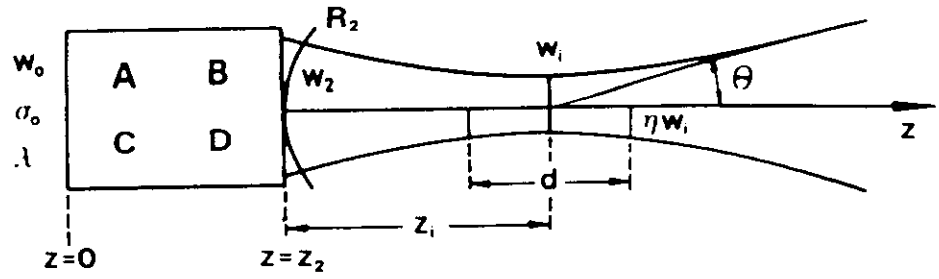

$$w(z_{out}) = w(0)\left(A^2 + B^2 z_R^{-2}\right)^{1/2}$$

$$\sigma(z_{out}) = \sigma(0)\left(A^2 + B^2 z_R^{-2}\right)^{1/2}$$

$$R(z_{out}) = \left(A^2 + B^2 z_R^{-2}\right)/\left(AC + BDz_R^{-2}\right)$$

$$u(z_{out}) = u(0)\left(A^2 + B^2 z_R^{-2}\right)^{-1}$$

where

$$z_R = \frac{\pi w^2(0)}{\lambda}\beta\left[1 + \eta^2\left(\frac{1-\beta^2}{2\beta}\right)^2\right]^{-1/2} \qquad \text{(Rayleigh range)}$$

$$\beta = \left\{1 + [w(0)/\sigma(0)]^2\right\}^{-1/2} \qquad \text{(Coherence)}$$

$$\eta = k\sigma^2(0)u(0) \qquad \text{(Twist)}$$

THIN LENS

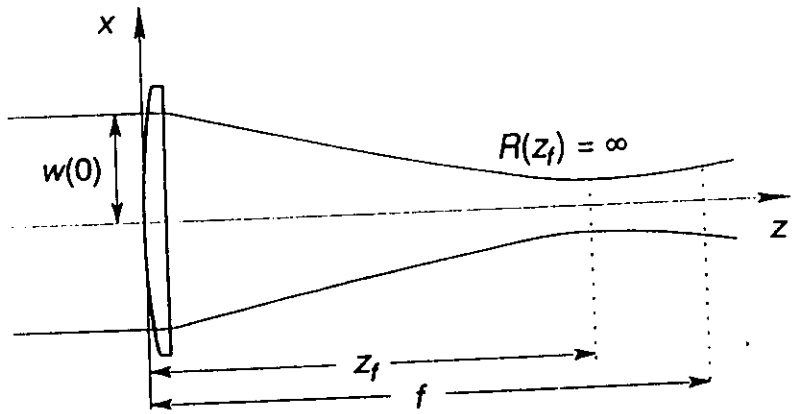

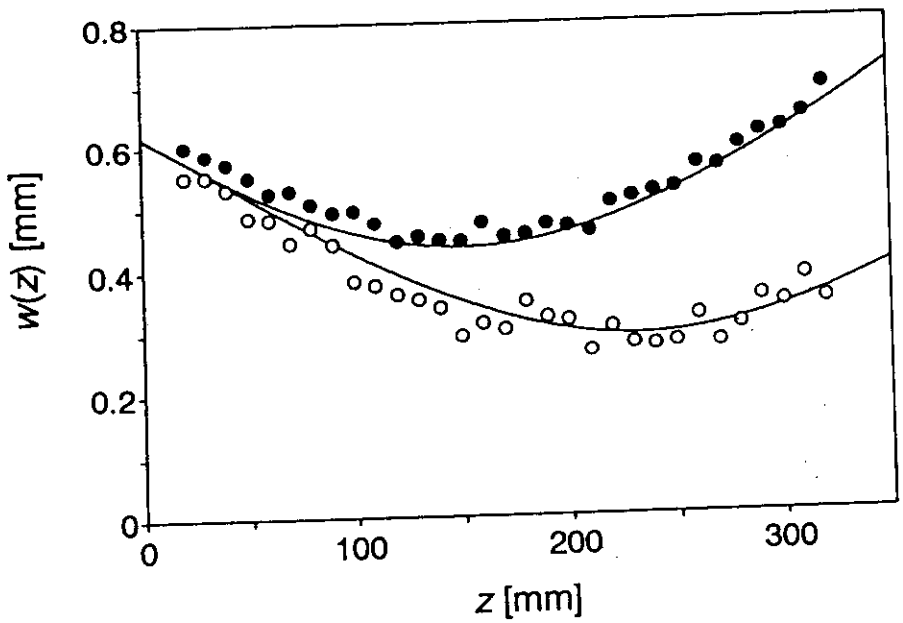

Solid dots: Twisted GSM beam
Open dots: Normal GSM beam

WHEN $f = z_R$ THE BEST FOCUS IS AT $z_f = f/2$ AND $w(z_f) = w(o)/\sqrt{2}$
THE BEAM ROTATES BY 45 DEGREES AT z_f AND BY 90 DEGREES AT f.

SPECTRAL CHANGES

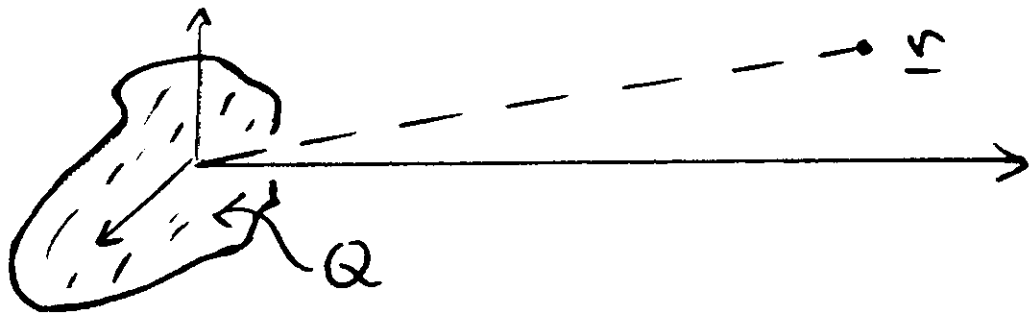

$$(\nabla_1^2+k^2)(\nabla_2^2+k^2)\,W_V(\underline{r}_1,\underline{r}_2;\omega) = (4\pi)^2 W_Q(\underline{r}_1,\underline{r}_2;\omega)$$

SPECTRUM $S_V(\underline{r},\omega) = W_V(\underline{r},\underline{r};\omega)$

SOURCE { SPECTRUM $S_Q(\underline{r},\omega) = W_Q(\underline{r},\underline{r};\omega)$
COHERENCE $\mu_Q(\underline{r}_1,\underline{r}_2;\omega)$

- **SCALING LAW** (E. Wolf, PRL 1986)
(planar sources)

  — normalized spectrum throughout far-zone same as source spectrum if

$$\mu(\underline{r}_1,\underline{r}_2;\omega) = \oint[k(\underline{r}_2-\underline{r}_1)]$$

(Example: Lambertian sources)

ILLUSTRATION (F. Gori et al., 1988)

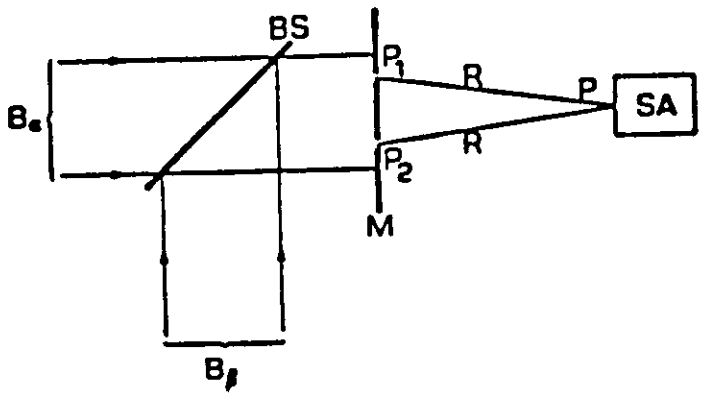

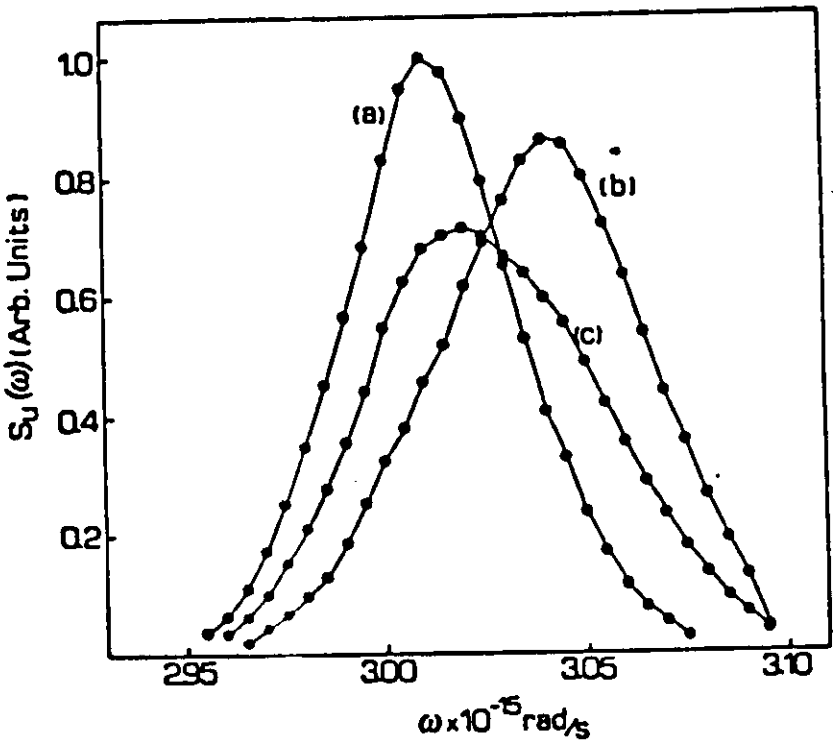

MANIFESTATIONS

- shifts of spectral lines (red or blue)
- narrowing or broadening
- splitting of lines
- imitate Doppler shifts (dynamic scatterer)

Review:

E. Wolf and D.F.V. James,

"Correlation-induced spectral changes",

Rep. Prog. Phys. 59, 771-818 (1996)

Effects of coherence in radiometry

Ari T. Friberg*
University of Rochester
The Institute of Optics
Rochester, New York 14627

Abstract. Radiometry evolved over a long period of time around rather incoherent sources of thermal nature. Only during the last few years have the effects of coherence begun to be taken into account in radiometric considerations of light sources. In this review article the fundamental concepts of conventional radiometry and of the theory of partial coherence will be first briefly recalled. The basic radiometric quantities, namely the radiance, the radiant emittance, and the radiant intensity, associated with a planar source of any state of coherence will then be introduced. It will be pointed out that the radiant intensity, representing the primary measurable quantity, obeys in all circumstances the usual postulates of conventional radiometry, whereas the radiance and the radiant emittance turn out to be much more elusive concepts. The radiometric characteristics of light from incoherent and coherent sources as well as from a certain type of partially coherent source, viz., the so-called quasihomogeneous source, will be analyzed. Quasihomogeneous sources are useful models for radiation sources that are usually found in nature. Lambertian sources will be discussed as examples.

Keywords: partial coherence; radiometry; radiance; diffraction; energy transfer; quasihomogeneity.

Optical Engineering 21(5), 927-936 (September/October 1982).

CONTENTS

1. INTRODUCTION

Radiometry, being one of the oldest branches of optics, has undergone extensive development and refinement over a period of several hundreds of years. The earliest notions of radiometry originated in the studies of Bouguer and Lambert, who in the eighteenth century formulated some empirical laws of optics.[1] Radiometry was subsequently developed in connection with the investigation of energy transfer by heat radiation. Notable contributions are especially the introduction of the concept of blackbody by Kirchhoff and Stewart and the discovery, in 1900, of the spectral distribution of blackbody radiation by Planck.[2] In its conventional form radiometry appears to have been systematized around this time, the turn of the twentieth century.

Conventional radiometry describes the transfer of radiant energy on a phenomenological basis involving intuitive notions such as tubes of light rays. In that form it has been applied to a wide variety of problems both in physics and in engineering. Yet it does not seem to be generally realized that the fundamental concepts and laws of conventional radiometry have never been derived from the presently accepted basic theories of light. Only relatively recently the accuracy and the range of validity of conventional radiometry have come under closer examination.

It is sometimes asserted that conventional radiometry describes, in some unspecified approximation, light fields generated by incoherent sources and that incoherent sources are Lambertian. Experimental evidence indicates that light sources under thermal equilibrium conditions, such as blackbody sources, radiate in accordance with Lambert's law. This fact would imply that blackbody radiation sources are incoherent, an assertion which is in disagreement with recent researches in coherence theory. Moreover, even the fields emitted by incoherent sources do not remain incoherent but instead, according to the famous van Cittert-Zernike theorem, gain coherence by the mere process of propagation. This results in a great variety of radiation patterns that can be found in nature but cannot be explained on the basis of conventional radiometry with incoherent sources. The above observations serve to illustrate the connection that must exist between the radiometric and the coherence properties of a light source.

The first attempt to incorporate the coherence properties of a light source into its radiometric description was made by Walther[3] in 1968. Considering a planar source of any state of coherence, he constructed a function that possesses several of the properties normally attributed to the radiance in conventional radiometry. This paper has become the cornerstone of virtually all of the subsequent research on the relationship between the radiometric properties of a source and its coherence properties. Other major contributions include an investigation by Marchand and Wolf[4] generalizing the

*Present address: University of Rochester, Department of Physics and Astronomy, Rochester, NY 14627.

Invited paper 5096 received June 29, 1981; revised manuscript received Jan. 18, 1982; accepted for publication Feb. 2, 1982; received by Managing Editor Feb. 10, 1982. This paper is a revision of Paper 194-04 which was presented at the SPIE seminar on Applications of Optical Coherence, Aug. 29-30, 1979, San Diego. The paper presented there appears (unrefereed) in SPIE Proceedings Vol. 194.

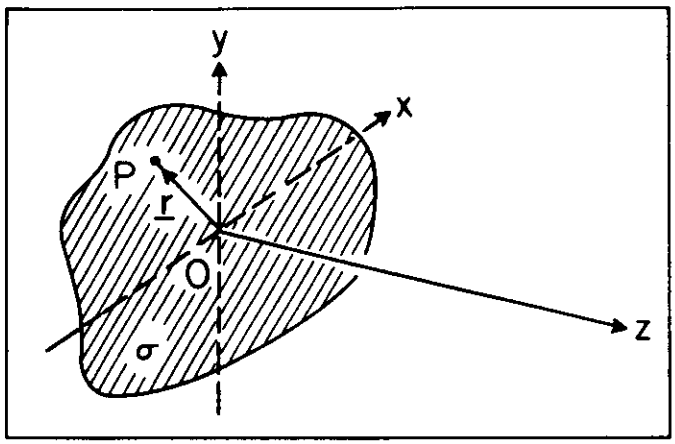

Fig. 1. A planar source σ occupying a portion of the plane z = 0 and radiating into the half space z > 0.

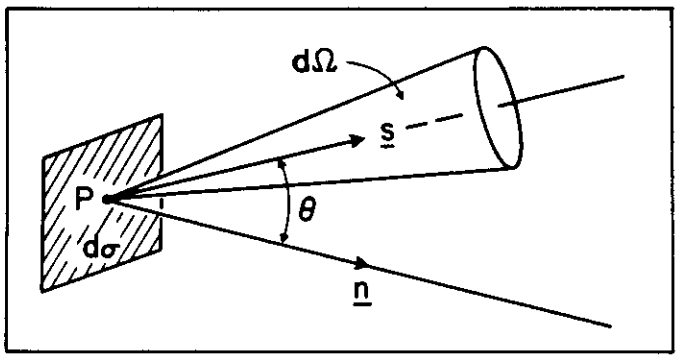

Fig. 2. Illustration of the notation relating to the traditional definition of radiance.

basic concepts of conventional radiometry to fields generated by any steady-state planar source (including fully coherent sources such as lasers), and a study by Carter and Wolf[5] on the coherence properties of Lambertian as well as non-Lambertian sources. Of great importance also is a recent investigation by Carter and Wolf,[6] in which they introduce and study a model that can be used to represent true natural radiation sources.

In the present article we will review some of the more important effects that recent research on radiometry with partially coherent light has revealed. In order to bring out the essence of these phenomena, we will make a number of simplifying assumptions. First of all, the quantum nature of light will be entirely ignored. We will also neglect all polarization effects and hence take the light field to be represented by a (fluctuating) complex scalar function. Furthermore, we will consider only fields generated by two-dimensional (planar) radiation sources.

2. SOME FUNDAMENTAL CONCEPTS

Before discussing in some detail the major effects that the coherence properties of a light source have on its radiometric characteristics, it will be convenient first to recall briefly the basic concepts and laws of conventional radiometry and of classical theory of partial coherence.

2.1. Conventional radiometry

In this article we are mainly concerned with the light energy emerging into the half space $z>0$ from a planar source σ located in the plane $z = 0$ (Fig. 1). The central quantity in the traditional radiometric description of such a source is the radiance (also known as the brightness or the specific intensity). It is defined in the following way[7]: Let $d\Phi_\omega$ represent the power, per unit frequency interval centered at frequency ω, radiated by a source element $d\sigma$ surrounding a point P into a solid angle $d\Omega$ around a direction specified by a unit vector $\underline{s}$ (Fig. 2). Then, the formula

$$d\Phi_\omega = B_\omega(\underline{r},\underline{s})\cos\theta d\Omega d\sigma , \tag{1}$$

where $\underline{r}$ denotes the position vector of the source point P and θ is the angle between the $\underline{s}$ direction and the normal $\underline{n}$ to the source, defines the radiance $B_\omega(\underline{r},\underline{s})$ at frequency ω, at the point $P(\underline{r})$, in the $\underline{s}$ direction. The radiance $B_\omega(\underline{r},\underline{s})$, which is simultaneously a function of both position and direction, thus represents the power (at frequency ω) radiated by the source per unit solid angle and per unit projected source area, the projection being onto a plane perpendicular to the $\underline{s}$ direction.

The fundamental relationship expressed by Eq. (1) can be used to obtain expressions for the other radiometric quantities. The radiant emittance, denoted by $E_\omega(\underline{r})$, is defined as the power (at frequency ω) radiated by the source per unit area around the point $P(\underline{r})$. In view of Eq. (1), it may be written as

$$E_\omega(\underline{r}) = \int_{(2\pi)} B_\omega(\underline{r},\underline{s})\cos\theta d\Omega , \tag{2}$$

where the integration extends over the 2π solid angle formed by all the possible $\underline{s}$ directions. The radiant intensity, denoted by $J_\omega(\underline{s})$, is defined, on the other hand, as the power (at frequency ω) radiated by the source per unit solid angle around the $\underline{s}$ direction. Using Eq. (1), it can be expressed in terms of the radiance as

$$J_\omega(\underline{s}) = \cos\theta \int_\sigma B_\omega(\underline{r},\underline{s})d\sigma , \tag{3}$$

where the integration extends over the source area σ. If the source is of infinite extent, the integration is to be carried over the entire source plane.

It is obvious from the definitions of the radiant emittance and the radiant intensity that the total power (at frequency ω) radiated by the source σ into the half space $z>0$, denoted by Φ_ω, is obtained from either one of the following two formulas:

$$\Phi_\omega = \int_\sigma E_\omega(\underline{r})d\sigma = \int_{(2\pi)} J_\omega(\underline{s})d\Omega . \tag{4}$$

In terms of the radiance $B_\omega(\underline{r},\underline{s})$, an expression for the total power Φ_ω would, of course, involve a double integration over the source area σ and over the solid angle 2π.

The three basic radiometric quantities defined above, namely, the radiance $B_\omega(\underline{r},\underline{s})$, the radiant emittance $E_\omega(\underline{r})$, and the radiant intensity $J_\omega(\underline{s})$, have certain characteristic properties by virtue of their physical significance. In particular, they are always non-negative for all possible values of their arguments. Moreover, $B_\omega(\underline{r},\underline{s})$ and $E_\omega(\underline{r})$ assume a zero value whenever the vector $\underline{r}$ represents a point located in the source plane outside the source area σ (if the source is of finite extent). To these properties we must add still a further requirement on the radiance $B_\omega(\underline{r},\underline{s})$ in the half space $z>0$. For this purpose we first need to generalize slightly the definition (Eq. (1)) of $B_\omega(\underline{r},\underline{s})$, where we assumed that the point $P(\underline{r})$ is located in the source plane $z = 0$. We will now allow the vector $\underline{r}$ to represent a point in any plane $z = z_1$ with $z_1 \geq 0$. Hence, Eq. (1) then defines the radiance $B_\omega(\underline{r},\underline{s})$ at a point $P(\underline{r})$ in the plane $z = z_1$. The unit vector $\underline{s}$ specifies a direction towards $z>z_1$. The dependence of $B_\omega(\underline{r},\underline{s})$ on z is left implicit for simplicity. It is normally assumed in conventional radiometry that the radiance $B_\omega(\underline{r},\underline{s})$, with $\underline{s}$ fixed, remains constant along the line through the point $P(\underline{r})$ in the direction of the fixed $\underline{s}$ vector. With the above generalized notation, this requirement may be expressed as[8]

$$\frac{d}{ds} B_\omega(\underline{r},\underline{s}) = 0 , \tag{5}$$

where d/ds denotes the directional derivative with respect to the spatial variables ($\underline{r}$ and implicit z) in the $\underline{s}$ direction. Equation (5) is known as the equation of radiative transfer in free space. It expresses the notion, tantamount to conventional radiometry, that in free space energy is propagated along straight lines.

To conclude this brief review we wish to emphasize four aspects of traditional radiometry which are evident from the above discussion. First, the radiance, the radiant emittance, and the radiant intensity are conventionally defined at a single temporal frequency of the optical field. Second, the three radiometric quantities are regarded as measurable in principle. Third, a simple additive superposition of energy from the various parts of the source is assumed to hold. And fourth, any effects due to diffraction are neglected. As we will see shortly, most of these presumptions of conventional radiometry have to be relaxed when considering partially coherent fields with diffraction and interference taking place.

2.2. Theory of partial coherence

A proper accounting for the diffraction and interference of light requires the introduction of the notion of coherence of the light field. This concept is closely related to the more or less irregular fluctuations that every practical optical field undergoes. In general, the fluctuations are much too rapid to be directly measurable by means of the usual types of detectors. However, it is often the correlations between the fluctuations rather than the fluctuations themselves which are of principal physical importance.

Let us therefore briefly discuss how the correlations of the fluctuations may be mathematically represented in a form suitable for our present purposes. It will be sufficient to consider only correlations up to the second order in the optical field variable. Let $V(\underline{r},t)$ be the complex analytic signal[9] that represents the optical field at a point P specified by the vector $\underline{r}$, at a time instant t. For simplicity $V(\underline{r},t)$ is taken to be a scalar. We assume also that the field $V(\underline{r},t)$ is statistically stationary in time. For such fields the most common quantity in the analysis of coherence effects is the so-called mutual coherence function. It is normally defined in terms of a long time average (Ref. 7, Sec. 10.3.1). In recent years it has become customary, however, to define the mutual coherence function in a more general manner by means of an average over a suitable ensemble of realizations characterizing the statistical properties of the field $V(\underline{r},t)$. If the field is not only stationary but also ergodic, then such an ensemble averaging yields the same result as the time averaging. Since most optical fields of practical interest are stationary and ergodic, we will consider only such fields from now on. We may then define the mutual coherence function by the formula

$$\Gamma(\underline{r}_1,\underline{r}_2;\tau) = \langle V(\underline{r}_1,t+\tau)V^*(\underline{r}_2,t)\rangle , \tag{6}$$

where the brackets denote either the time average or the ensemble average and the asterisk denotes the complex conjugate. Despite the appearance of the variable t on the right-hand side of Eq. (6), $\Gamma(\underline{r}_1,\underline{r}_2;\tau)$ is independent of t because of the assumed stationarity. The mutual coherence function $\Gamma(\underline{r}_1,\underline{r}_2;\tau)$ characterizes the second-order field correlations at the points specified by the vectors $\underline{r}_1$ and $\underline{r}_2$, at instants of time separated by τ.

The transfer of radiant energy from partially coherent sources is, however, more naturally described in the space-frequency rather than the space-time domain. This circumstance is a consequence of the fact that the different temporal frequency components of a statistically stationary field are uncorrelated. To obtain a measure of the optical field correlations in the space-frequency domain, we recall first that the cross-spectral density function (also known as the cross-power spectrum), denoted by $W(\underline{r}_1,\underline{r}_2;\omega)$, and the mutual coherence function $\Gamma(\underline{r}_1,\underline{r}_2;\tau)$ are related by the formula

$$W(\underline{r}_1,\underline{r}_2;\omega) = \frac{1}{2\pi}\int_{-\infty}^{\infty}\Gamma(\underline{r}_1,\underline{r}_2;\tau)e^{i\omega\tau}d\tau . \tag{7}$$

The Fourier transform relationship expressed by Eq. (7) is, of course, an optical analog of the well-known Wiener-Khintchine theorem for stationary random processes. The cross-spectral density function $W(\underline{r}_1,\underline{r}_2;\omega)$ characterizes the correlations of the optical field at frequency ω, at the two points $P(\underline{r}_1)$ and $P(\underline{r}_2)$. Further properties of $W(\underline{r}_1,\underline{r}_2;\omega)$ are discussed in a paper by Mandel and Wolf.[10]

In terms of the cross-spectral density function $W(r_1,r_2;\omega)$, one may define the quantity[10]

$$\mu(\underline{r}_1,\underline{r}_2;\omega) = \frac{W(\underline{r}_1,\underline{r}_2;\omega)}{[I(\underline{r}_1,\omega)\, I(\underline{r}_2,\omega)]^{1/2}}, \tag{8}$$

where

$$I(\underline{r},\omega) = W(\underline{r},\underline{r};\omega) \tag{9}$$

represents the averaged optical intensity at frequency ω, at the point $P(\underline{r})$. It can be shown that $\mu(\underline{r}_1,\underline{r}_2;\omega)$ is normalized so that for all values of $\underline{r}_1$, $\underline{r}_2$, and ω

$$0 \leqq |\mu(\underline{r}_1,\underline{r}_2;\omega)| \leqq 1 . \tag{10}$$

The quantity $\mu(\underline{r}_1,\underline{r}_2;\omega)$, defined by Eq. (8), is called the complex degree of spatial coherence of the light fluctuations at frequency ω, at the points $P(\underline{r}_1)$ and $P(\underline{r}_2)$. The limiting values 1 and 0 in Eq. (10) indicate that the light fluctuations at frequency ω at the points $P(\underline{r}_1)$ and $P(\underline{r}_2)$ are completely correlated or uncorrelated, respectively. If $|\mu(\underline{r}_1,\underline{r}_2;\omega)| = 1$ for all values of $\underline{r}_1$ and $\underline{r}_2$, then the optical field (at frequency ω) is said to be completely spatially coherent. On the other hand if $|\mu(\underline{r}_1,\underline{r}_2;\omega)| = 0$ for all $\underline{r}_1 \neq \underline{r}_2$, then the optical field (at frequency ω) is said to be completely spatially incoherent. These limiting cases should be regarded only as convenient mathematical idealizations rather than real physical conditions actually observed in nature. No practical optical field can be spatially incoherent in the sense defined above. A more realistic model for spatial incoherence will be introduced later.

3. RADIOMETRY WITH PLANAR SOURCES OF ANY STATE OF COHERENCE

In this section we will first obtain expressions for the basic radiometric quantities [cf. Eqs. (1)–(3)] associated with a planar source of arbitrary state of coherence, located in the plane $z = 0$. The source can be either a true primary source or a secondary one, such as an optical image for example.[11,12] In either case, there will be some field distribution across the plane $z = 0$. This distribution, occupying an area σ (which may be infinite), is what in the following will be referred to as the source σ (Fig. 1). It gives rise, by the process of optical wave propagation, to the field distribution in the half space $z > 0$. The state of coherence of the source is specified in terms of the cross-spectral density function $W^{(0)}(\underline{r}_1,\underline{r}_2;\omega)$, where $\underline{r}_1$ and $\underline{r}_2$ are the position vectors of two typical points in the plane $z = 0$ (indicated by the superscript 0), and ω denotes the temporal frequency under consideration. The resulting formulas for the radiometric quantities are consequently expressed in terms of the function $W^{(0)}(\underline{r}_1,\underline{r}_2;\omega)$. Some features of these radiometric expressions associated with a partially coherent source will be discussed and contrasted with the corresponding properties postulated in conventional radiometry.

3.1. Expressions for radiometric quantities

In order to determine the radiometric quantities associated with a partially coherent planar source, we need to consider the energy flow in the far zone of the source. This situation is a consequence of the fact that only sufficiently far away from the source can the behavior of the energy flow be unambiguously described. Let us denote by $\underline{F}(\underline{r},\omega)$ the energy flow vector associated with the optical field at the point $P(\underline{r})$. Then it can be shown that in the far zone of

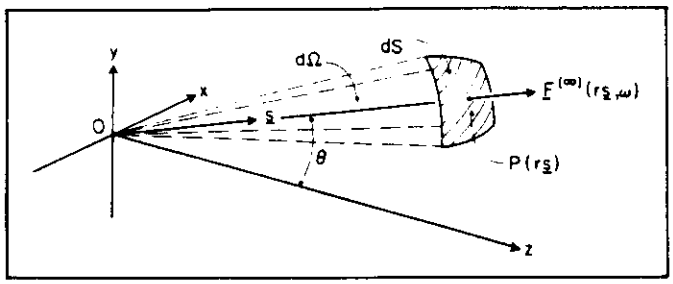

Fig. 3. Energy flow in the far zone of the source.

the source $\underline{F}(\underline{r},\omega)$ always points radially outwards from the source and that it is proportional to the optical intensity.[13] Hence, in a suitable system of units,

$$\underline{F}^{(\infty)}(r\underline{s},\omega) = I^{(\infty)}(r\underline{s},\omega)\underline{s}\,, \tag{11}$$

where $\underline{s}$ is a three-dimensional unit vector pointing to the point $P(\underline{r})$ (i.e., $\underline{s} = \underline{r}/r$ with $r = |\underline{r}|$), and the superscript ∞ indicates that the quantity has been evaluated in the far zone of the source (i.e., as $kr \to \infty$ with $k = \omega/c$, c being the speed of light in free space) (Fig. 3). The quantity $\underline{s} \cdot \underline{F}^{(\infty)}(r\underline{s},\omega)$ represents the rate per unit area, located in the direction specified by the unit vector $\underline{s}$, at which energy traverses a surface element dS on a large sphere of radius r centered at the origin. If we let $d\Omega$ denote the solid angle that dS subtends at the origin, then, in view of the relation

$$dS = r^2 d\Omega\,, \tag{12}$$

the radiant intensity $J_\omega(\underline{s})$ and the far-field flux vector $\underline{F}^{(\infty)}(r\underline{s},\omega)$ are clearly related by the formula

$$J_\omega(\underline{s}) = r^2\underline{s} \cdot \underline{F}^{(\infty)}(r\underline{s},\omega)\,. \tag{13}$$

On substituting from Eq. (11), we obtain

$$J_\omega(\underline{s}) = r^2 I^{(\infty)}(r\underline{s},\omega)\,. \tag{14}$$

The right-hand side of Eq. (14) is to be considered in the limit $kr \to \infty$, and hence it is independent of r.

The next task is to express the far-zone optical intensity $I^{(\infty)}(r\underline{s},\omega)$ in terms of the cross-spectral density function $W^{(0)}(\underline{r}_1,\underline{r}_2,\omega)$ across the source. This can be accomplished by first considering the propagation of the cross-spectral density function into the far zone and then using Eq. (9) to find the optical intensity. The cross-spectral density function is known to obey a pair of Helmholtz equations in free space. Using standard mathematical techniques, such as Green's functions or the angular spectrum method, one can show that[14]

$$I^{(\infty)}(r\underline{s},\omega) = (2\pi k)^2\cos^2\theta\,\frac{1}{r^2}\,\widetilde{W}^{(0)}(k\underline{s}_\perp,-k\underline{s}_\perp;\omega)\,, \tag{15}$$

where $\widetilde{W}^{(0)}(\underline{f}_1,\underline{f}_2;\omega)$ is the four-dimensional spatial Fourier transform of $W^{(0)}(\underline{r}_1,\underline{r}_2;\omega)$, defined by

$$\widetilde{W}^{(0)}(\underline{f}_1,\underline{f}_2;\omega) = \frac{1}{(2\pi)^4}\int_{-\infty}^{\infty}\int_{-\infty}^{\infty} W^{(0)}(\underline{r}_1,\underline{r}_2;\omega) \cdot e^{-i(\underline{f}_1\cdot\underline{r}_1 + \underline{f}_2\cdot\underline{r}_2)}d^2r_1 d^2r_2\,. \tag{16}$$

In Eq. (15), θ is the angle between the $\underline{s}$ direction and the normal to the source (i.e., the positive z axis), and $\underline{s}_\perp$ is the two-dimensional vector obtained by projecting the unit vector $\underline{s}$ onto the source plane $z = 0$.

On substituting from Eq. (15) into Eq. (14), we find the following important expression for the radiant intensity[4,13]:

$$J_\omega(\underline{s}) = (2\pi k)^2\cos^2\theta\,\widetilde{W}^{(0)}(k\underline{s}_\perp,-k\underline{s}_\perp;\omega)\,. \tag{17}$$

The formula (17), in its various forms, forms the basis for the discussion of radiation from partially coherent sources. It also represents the starting point in an effort to define the radiance and the radiant emittance associated with a partially coherent planar source. This can be seen more clearly if Eq. (17) is first rewritten, with the help of Eq. (16), in the form

$$J_\omega(\underline{s}) = \left(\frac{k}{2\pi}\right)^2\cos^2\theta\int_{-\infty}^{\infty}\int_{-\infty}^{\infty} W^{(0)}(\underline{r}_1,\underline{r}_2;\omega) \cdot e^{-ik\underline{s}_\perp\cdot(\underline{r}_1-\underline{r}_2)}d^2r_1 d^2r_2\,. \tag{18}$$

Then, introducing the difference and average coordinates

$$\underline{r}' = \underline{r}_1 - \underline{r}_2;\quad \underline{r} = \frac{1}{2}(\underline{r}_1 + \underline{r}_2) \tag{19}$$

as new integration variables, the expression (18) for the radiant intensity becomes

$$J_\omega(\underline{s}) = \left(\frac{k}{2\pi}\right)^2\cos^2\theta\int_{-\infty}^{\infty}\int_{-\infty}^{\infty} W^{(0)}\left(\underline{r} + \frac{1}{2}\underline{r}',\underline{r} - \frac{1}{2}\underline{r}';\omega\right) \cdot e^{-ik\underline{s}_\perp\cdot\underline{r}'}d^2r\,d^2r'\,. \tag{20}$$

The integration is to be taken twice independently over the entire source plane, once with respect to $\underline{r}'$ and a second time with respect to $\underline{r}$.

Comparison of Eqs. (3) and (20) suggests that the radiance $B_\omega(\underline{r},\underline{s})$ associated with a partially coherent planar source might be given by[3,4]

$$B_\omega(\underline{r},\underline{s}) = \left(\frac{k}{2\pi}\right)^2\cos\theta\int_{-\infty}^{\infty} W^{(0)}\left(\underline{r} + \frac{1}{2}\underline{r}',\underline{r} - \frac{1}{2}\underline{r}';\omega\right) \cdot e^{-ik\underline{s}_\perp\cdot\underline{r}'}d^2r'\,. \tag{21}$$

This expression for the radiance was first introduced by Walther[3] in 1968. The radiant emittance $E_\omega(\underline{r})$, obtained by substituting from Eq. (21) into Eq. (2), can then be written as[4]

$$E_\omega(\underline{r}) = \int_{-\infty}^{\infty} W^{(0)}\left(\underline{r} + \frac{1}{2}\underline{r}',\underline{r} - \frac{1}{2}\underline{r}';\omega\right)K_\omega(\underline{r}')d^2r'\,, \tag{22}$$

where

$$K_\omega(\underline{r}') = \left(\frac{k}{2\pi}\right)^2\int_{(2\pi)}\cos^2\theta e^{-ik\underline{s}_\perp\cdot\underline{r}'}d\Omega\,. \tag{23}$$

The integration in Eq. (23) may be carried out to yield[4]

$$K_\omega(\underline{r}') = \frac{k^2}{2\sqrt{2\pi}}\,\frac{J_{3/2}(kr')}{(kr')^{3/2}}\,, \tag{24}$$

where $r' = \underline{r}'$ and $J_{3/2}(x)$ is the Bessel function of the first kind and order 3/2. It can be represented in terms of trigonometric functions as

$$J_{3/2}(x) = \sqrt{\frac{2}{\pi x}}\left[\frac{\sin x}{x} - \cos x\right]. \tag{25}$$

We have thus established expressions for the basic radiometric quantities associated with a planar source of any arbitrary state of coherence. The radiance $B_\omega(\underline{r},\underline{s})$ is given by Eq. (21), the radiant emittance $E_\omega(\underline{r})$ by Eq. (22), and the radiant intensity $J_\omega(\underline{s})$ by Eq. (20). The coherence properties of the source are embodied into the cross-spectral density function $W^{(0)}(\underline{r}_1,\underline{r}_2;\omega)$ entering each of these expressions.

3.2. Properties of radiometric quantities

Equations (20)–(22) appear at first sight as the complete solution to the problem of specifying the basic radiometric quantities associated with partially coherent planar sources. Closer examination reveals, however, that some problems still remain concerning this radiometric description. It has been shown[4] that both the radiance $B_\omega(\underline{r},\underline{s})$ and the radiant emittance $E_\omega(\underline{r})$ occasionally assume negative values and that they do not necessarily always vanish outside the source area σ in the source plane. Moreover, there is no reason to expect that the radiance $B_\omega(\underline{r},\underline{s})$ would, under all circumstances, obey the equation (5) of radiative transfer in the half space $z > 0$ [cf. Ref. 3, Sec. III]. For these reasons the radiance $B_\omega(\underline{r},\underline{s})$ and the radiant emittance $E_\omega(\underline{r})$, given by Eqs. (21) and (22) respectively, cannot strictly speaking be regarded as true measures of energy flow in the traditional sense. The radiant intensity $J_\omega(\underline{s})$, given by Eq. (20), on the other hand always correctly represents the power per unit solid angle as in conventional radiometry.

Another problem associated with the radiance $B_\omega(\underline{r},\underline{s})$ is that the procedure by which it was derived above does not specify it uniquely. It is easy to find other nonequivalent expressions for the radiance such that, when substituted into Eq. (3) with the integration extending over the whole source plane (rather than just over the source area σ), they would lead to the correct expression (20) for the radiant intensity $J_\omega(\underline{s})$. One such expression was actually proposed by Walther[15] in 1973. Its derivation was originally based on a local energy balance argument involving an energy flux vector $\underline{F}(\underline{r},\omega)$ associated with the optical field. It was later rederived[16] in an interesting way by means of a set of constraints posed on the radiance $B_\omega(\underline{r},\underline{s})$. However, because of the inherent ambiguity of an energy flux vector in the near field of a source, that expression cannot be regarded as any more correct than the expression in Eq. (21). It does not possess all the features of the radiance in conventional radiometry. In particular, it too can occasionally take on negative values.[17]

In view of the fact that there are several possible definitions for the radiance function associated with a partially coherent planar source, one cannot avoid asking the following question: is it possible to find amongst all these definitions one that would satisfy all the requirements normally postulated for the radiance in conventional radiometry? It has been shown by Friberg[18,19] that no such definition, assumed to be linear in the source cross-spectral density function, can be given with sources of all states of coherence. This result has its root in the fact that the radiance $B_\omega(\underline{r},\underline{s})$ is simultaneously a function of both r and s, which are essentially Fourier conjugate variables of each other. In analogy with the principles of quantum mechanics, this result also suggests that the radiance no longer can be regarded as a measurable quantity.[18,20] In fact, the basic measurable quantity associated with radiation from partially coherent sources is the distribution of the radiant intensity $J_\omega(\underline{s})$.

In spite of the above somewhat disconcerting comments made about the radiance and the radiant emittance associated with a partially coherent source, they can nevertheless be used successfully in calculating values of truly measurable quantities. As we shall see later, in most practical cases they behave much in the same way as the radiance and the radiant emittance in conventional radiometry and provide a great deal of insight into the manner in which energy is radiated by partially coherent sources.

4. LIMITING CASES OF COHERENCE

As special cases of the general formulas (20)–(22) for the radiometric quantities, let us consider the two limiting cases when the planar source is either completely spatially incoherent or completely spatially coherent. Even though these two limits must be regarded as pure mathematical idealizations, they nonetheless provide useful information about the properties of several types of sources. A more realistic model representing a true natural source will be discussed in the next section.

4.1. Incoherent sources

In an earlier section we already encountered a definition of spatial incoherence in terms of the cross-spectral density function. For most practical purposes it is, however, more convenient to represent the cross-spectral density function of a completely spatially incoherent source in the form [Ref. 9, Sec. 4.4]

$$W^{(0)}(\underline{r}_1,\underline{r}_2;\omega) = i^{(0)}(\underline{r}_1,\omega)\delta(\underline{r}_1-\underline{r}_2), \tag{26}$$

where $\delta(\underline{r}')$ is the two-dimensional Dirac delta function, and $i^{(0)}(\underline{r},\omega) \geqq 0$ with $i^{(0)}(\underline{r},\omega) = 0$ for points located outside the source area σ. The quantity $i^{(0)}(\underline{r},\omega)$ may be loosely identified with the optical intensity distribution across the source.

Because of the delta function appearing in Eq. (26), some of the integrations in the expressions for the radiometric quantities can now be readily carried out. On substituting from Eq. (26) into Eqs. (21), (22), and (20), we find for the radiance, the radiant emittance, and the radiant intensity, respectively,[4]

$$B_\omega(\underline{r},\underline{s}) = \left(\frac{k}{2\pi}\right)^2 \cos\theta\, i^{(0)}(\underline{r},\omega), \tag{27}$$

$$E_\omega(\underline{r}) = \frac{k^2}{6\pi} i^{(0)}(\underline{r},\omega), \tag{28}$$

and

$$J_\omega(\underline{s}) = \left(\frac{k}{2\pi}\right)^2 \cos^2\theta \int_\sigma i^{(0)}(\underline{r},\omega)\,d\sigma. \tag{29}$$

In Eq. (29) we have used the fact that $i^{(0)}(\underline{r},\omega)$ is assumed to vanish outside the source area σ. It is observed from Eqs. (27) and (28) that for a spatially completely incoherent planar source the radiance and the radiant emittance are non-negative quantities and, moreover, that they assume zero values in the source plane outside the source area σ. These results indicate that in the limit of spatial incoherence there is no disagreement with conventional radiometry (except that the equation of radiative transfer may not be rigorously satisfied in the field generated by an incoherent source).

Another interesting feature is seen from Eq. (29). Denoting the radiant intensity in the forward direction (i.e., in the direction with $\theta = 0$) by $J_{\omega,0}$, Eq. (29) may be rewritten as

$$J_\omega(\underline{s}) = J_{\omega,0}\cos^2\theta. \tag{30}$$

This shows that the radiant intensity from a completely spatially incoherent source decreases, regardless of its optical intensity

distribution, in proportion to $\cos^2\theta$ and not to $\cos\theta$ as is typical of a Lambertian source.[21] In view of this result, a blackbody radiation source, whose radiant intensity distribution is well known to follow a $\cos\theta$ law, must possess some degree of spatial coherence. Recent researches have shown, indeed, that a blackbody source exhibits field correlations over distances of the order of the mean wavelength of the radiation.

4.2. Coherent sources

In the idealized case when the source is completely spatially coherent, its cross-spectral density function may be factored in the form[22]

$$W^{(0)}(\underline{r}_1,\underline{r}_2;\omega) = v^{(0)}(\underline{r}_1,\omega)v^{(0)*}(\underline{r}_2,\omega)\,. \tag{31}$$

Here $v^{(0)}(\underline{r},\omega)$ may be identified as the optical field distribution across the source. Naturally, $v^{(0)}(\underline{r},\omega)$ vanishes whenever $\underline{r}$ represents a point outside the source area σ.

With the cross-spectral density function of the source being represented by Eq. (31), the radiance, the radiant emittance, and the radiant intensity, given by Eqs. (21), (22), and (20) respectively, may be written as[4]

$$B_\omega(\underline{r},\underline{s}) = \left(\frac{k}{2\pi}\right)^2 \cos\theta \int_{-\infty}^{\infty} v^{(0)}\left(\underline{r}+\frac{1}{2}\underline{r}',\omega\right)$$

$$\cdot\, v^{(0)*}\left(\underline{r}-\frac{1}{2}\underline{r}',\omega\right)e^{-ik\underline{s}_\perp\cdot\underline{r}'}d^2r'\,, \tag{32}$$

$$E_\omega(\underline{r}) = \frac{k^2}{2\sqrt{2\pi}} \int_{-\infty}^{\infty} v^{(0)}\left(\underline{r}+\frac{1}{2}\underline{r}',\omega\right)v^{(0)*}\left(\underline{r}-\frac{1}{2}\underline{r}',\omega\right)$$

$$\cdot\, \frac{J_{3/2}(kr')}{(kr')^{3/2}}\, d^2r'\,, \tag{33}$$

and

$$J_\omega(\underline{s}) = (2\pi k)^2\cos^2\theta\,|\tilde{v}^{(0)}(k\underline{s}_\perp,\omega)|^2\,, \tag{34}$$

where $\tilde{v}^{(0)}(\underline{f},\omega)$ is the two-dimensional spatial Fourier transform of $v^{(0)}(\underline{r},\omega)$, defined by

$$\tilde{v}^{(0)}(\underline{f}) = \frac{1}{(2\pi)^2}\int_{-\infty}^{\infty} v^{(0)}(\underline{r},\omega)e^{-i\underline{f}\cdot\underline{r}}d^2r\,. \tag{35}$$

The best way to illustrate the predictions of Eqs. (32)-(34) is to consider a simple example.

Example. Let us consider a cophasal planar source with Gaussian optical intensity distribution

$$I^{(0)}(\underline{r},\omega) = I_0 e^{-\underline{r}^2/2\sigma_I^2}\,, \tag{36}$$

where I_0 and σ_I are positive parameters (Fig. 4). The optical field distribution across the source can then be written as

$$v^{(0)}(\underline{r},\omega) = \sqrt{I_0}\,e^{-\underline{r}^2/4\sigma_I^2}\,. \tag{37}$$

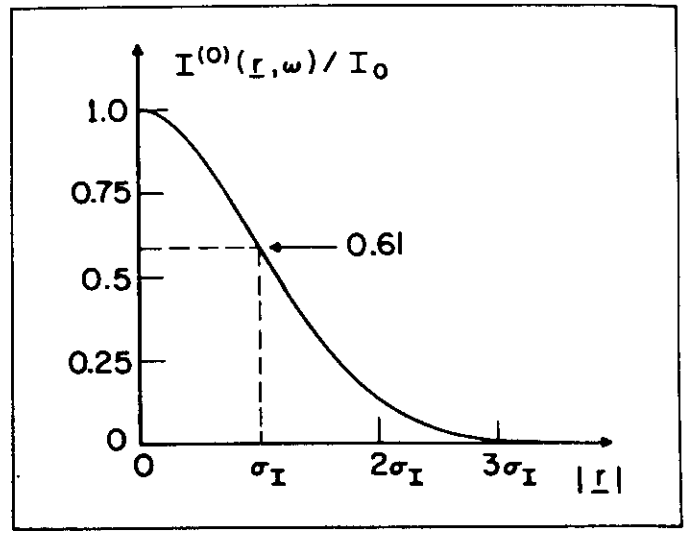

Fig. 4. Gaussian distribution of optical intensity.

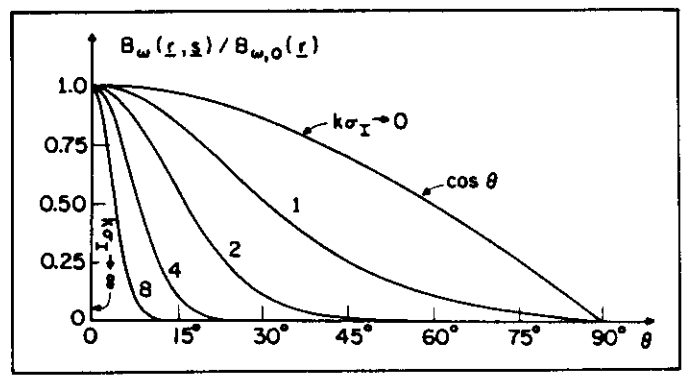

Fig. 5. Angular distribution of the normalized radiance associated with a fully coherent and cophasal planar source with Gaussian optical intensity distribution.

The waist of a fully coherent laser beam, for example, is a practical realization of the type of source represented by Eq. (37).

On substituting from Eq. (37) into Eq. (32), we find for the radiance

$$B_\omega(\underline{r},\underline{s}) = B_{\omega,0}(\underline{r})\cos\theta e^{-2(k\sigma_I)^2\sin^2\theta}\,, \tag{38}$$

where

$$B_{\omega,0}(\underline{r}) = \frac{2}{\pi}(k\sigma_I)^2 I^{(0)}(\underline{r},\omega)\,. \tag{39}$$

In deriving Eq. (38) we made use of the identity $\underline{s}^2{}_\perp = \sin^2\theta$. The radiance at any given source point is seen to be proportional to the optical intensity at that point. The graphs in Fig. 5, calculated from Eq. (38), illustrate the dependence of the radiance $B_\omega(\underline{r},\underline{s})$ on the angle θ for several values of the parameter $k\sigma_I$.

On substituting from Eq. (37) into Eqs. (35) and (34), the radiant intensity is readily found to be

$$J_\omega(\underline{s}) = J_{\omega,0}\cos^2\theta e^{-2(k\sigma_I)^2\sin^2\theta}\,, \tag{40}$$

where

$$J_{\omega,0} = (2k\sigma_I^2)^2 I_0\,. \tag{41}$$

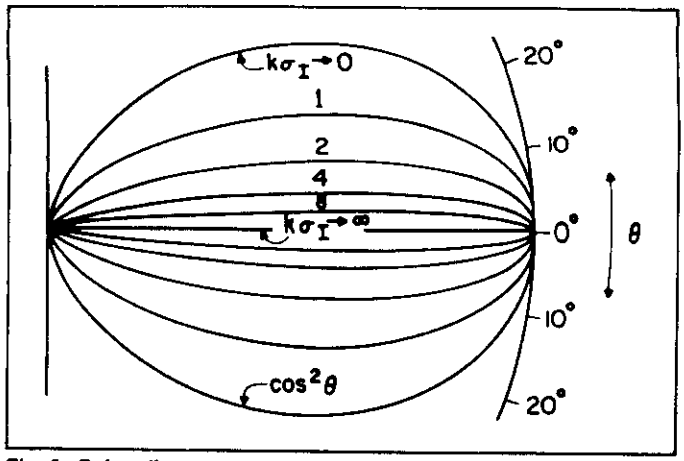

Fig. 6. Polar diagram of the normalized radiant intensity from a fully coherent and cophasal planar source with Gaussian optical intensity distribution.

Figure 6 illustrates, in the form of polar diagrams, the dependence of the radiant intensity $J_\omega(\underline{s})$ on the angle θ for several values of $k\sigma_I$. These graphs, computed according to Eq. (40), differ from the graphs in Fig. 5 by a multiplicative factor of $\cos\theta$. With a suitable value for $k\sigma_I$, Eq. (40) represents the radiant intensity generated by a fully coherent laser operating in its lowest transverse mode. For typical lasers $k\sigma_I \gg 1$, and thus the radiant intensity distribution is highly directional, centered in the forward direction. One may then approximate $\cos\theta \approx 1$ and $\sin\theta \approx \theta$. For instance, for a He-Ne laser with $\lambda = 6328\text{Å}$ and $\sigma_I = 1$ mm, the parameter $k\sigma_I = 0.99 \cdot 10^4$, and the radiant intensity $J_\omega(\underline{s})$ drops to e^{-2} times its value in the forward direction when $\theta = 1.01 \cdot 10^{-4}$ radians.

The radiant emittance $E_\omega(\underline{r})$ associated with the fully coherent and cophasal planar source with Gaussian intensity distribution can be obtained by substituting Eq. (37) into Eq. (33). After some algebra, the result is found to be

$$E_\omega(\underline{r}) = \left[1 - \frac{F(a)}{a}\right] I^{(0)}(\underline{r},\omega), \tag{42}$$

where

$$a = \sqrt{2}\,(k\sigma_I), \tag{43}$$

and

$$F(a) = e^{-a^2} \int_0^a e^{u^2}\,du. \tag{44}$$

The quantity F(a), defined by Eq. (44), is the so-called Dawson integral whose values can be found tabulated in the literature.[23] The radiant emittance is seen to be proportional to the distribution of the optical intensity across the source.

In an effort to describe the radiation characteristics of a source, it will be convenient to let

$$N_\omega = \int_{-\infty}^{\infty} I^{(0)}(\underline{r},\omega)\,d^2r \tag{45}$$

denote the integrated optical intensity across the source. Then the ratio

$$C_\omega = \Phi_\omega / N_\omega, \tag{46}$$

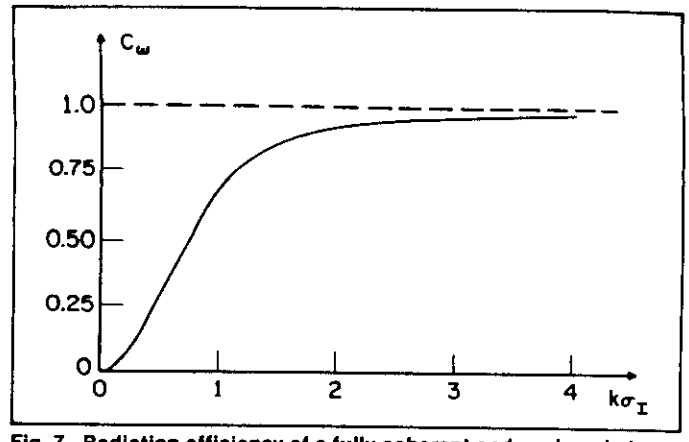

Fig. 7. Radiation efficiency of a fully coherent and cophasal planar source with Gaussian optical intensity distribution.

where Φ_ω is the total radiated power given by Eq. (4), may be called the radiation efficiency of the source at frequency ω. It can be shown that regardless of the state of coherence of the source, the radiation efficiency satisfies the inequality

$$0 \leqq C_\omega \leqq 1. \tag{47}$$

The radiation efficiency C_ω may be smaller than unity for two reasons: first, a substantial amount of the radiation may be converted into evanescent waves which do not carry energy into the far zone. And second, the source may be only partially spatially coherent.

The radiation efficiency C_ω of the fully coherent and cophasal planar source with Gaussian optical intensity distribution (Eq. (36)) is seen from Eqs. (46), (45), and (42) to be

$$C_\omega = 1 - \frac{F[\sqrt{2}\,(k\sigma_I)]}{\sqrt{2}\,(k\sigma_I)}, \tag{48}$$

where F(a) is the Dawson integral defined by Eq. (44). Figure 7 illustrates the dependence of C_ω on the parameter $k\sigma_I$. Since the source under consideration is completely spatially coherent, the less than perfect radiation efficiency is entirely due to the evanescent waves. However, for a typical laser source $C_\omega \approx 1$, as is evident from Fig. 7. Later we shall encounter sources where the loss of radiation efficiency is due to the imperfect coherence properties. One such example will be the class of the so-called quasihomogeneous sources discussed in the next section. In fact, in that case the loss due to the evanescent waves is entirely negligible when compared to the loss caused by partial spatial coherence.

Let us finally briefly examine the limiting case as $k\sigma_I \to \infty$. In this limit Eqs. (38), (40), (42), and (48) reduce to

$$\frac{B_\omega(\underline{r},\underline{s})}{B_{\omega,o}(\underline{r})} \to \frac{J_\omega(\underline{s})}{J_{\omega,o}} \to \begin{cases} 1, & \theta = 0, \\ 0, & \theta \neq 0, \end{cases} \tag{49}$$

$$E_\omega(\underline{r}) \to I^{(0)}(\underline{r},\omega), \tag{50}$$

and

$$C_\omega \to 1. \tag{51}$$

It is apparent that in this limit the source approaches a homogeneous plane wave, giving rise to a perfect unidirectional light beam undergoing no diffraction at all.

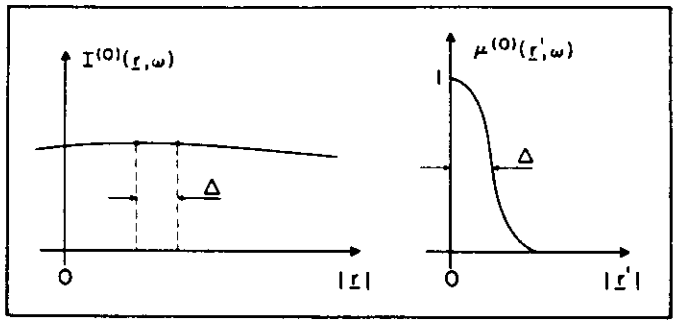

Fig. 8. Schematic illustration of the intensity and coherence variations across a quasihomogeneous source.

5. RADIOMETRY WITH QUASIHOMOGENEOUS PLANAR SOURCES

A quasihomogeneous planar source is characterized by a cross-spectral density function of the form[6]

$$W^{(0)}(\underline{r}_1,\underline{r}_2;\omega) = I^{(0)}\left[\frac{1}{2}(\underline{r}_1 + \underline{r}_2),\omega\right]\mu^{(0)}(\underline{r}_1 - \underline{r}_2;\omega), \tag{52}$$

where $I^{(0)}(\underline{r},\omega)$ represents the optical intensity distribution across the source, and $\mu^{(0)}(\underline{r}';\omega)$ is the complex degree of spatial coherence [cf. Eq. (8)], assumed to depend only on the difference $\underline{r}' = \underline{r}_1 - \underline{r}_2$. It is assumed that the intensity distribution $I^{(0)}(\underline{r},\omega)$ varies with $\underline{r}$ much more slowly than the complex degree of spatial coherence $\mu^{(0)}(\underline{r}',\omega)$ varies with $\underline{r}'$ (Fig. 8). Furthermore, it is assumed that the linear dimensions of the source are large compared with the wavelength of the light and that $|\mu^{(0)}(\underline{r}',\omega)|$ is substantially different from zero only within an $\underline{r}'$ domain that is small compared to the size of the source. The quasihomogeneous model, unlike the strictly homogeneous one, can be used to represent radiation sources of finite size frequently encountered in practice.

The radiometric quantities associated with a quasihomogeneous planar source can be readily found by substituting from Eq. (52) into the general expressions (20)–(22). The results are[6]

$$B_\omega(\underline{r},\underline{s}) = \left(\frac{k}{2\pi}\right)^2 \cos\theta I^{(0)}(\underline{r},\omega)\int_{-\infty}^{\infty}\mu^{(0)}(\underline{r}',\omega)\, e^{-ik\underline{s}_\perp\cdot\underline{r}'}\, d^2r', \tag{53}$$

$$E_\omega(\underline{r}) = I^{(0)}(\underline{r},\omega)\int_{-\infty}^{\infty}\mu^{(0)}(\underline{r}',\omega)K_\omega(\underline{r}')d^2r', \tag{54}$$

and

$$J_\omega(\underline{s}) = k^2\cos^2\theta\,\tilde{I}^{(0)}(0,\omega)\int_{-\infty}^{\infty}\mu^{(0)}(\underline{r}',\omega)\, e^{-ik\underline{s}_\perp\cdot\underline{r}'}\, d^2r', \tag{55}$$

where $K_\omega(\underline{r}')$ is given by Eq. (24), and $\tilde{I}^{(0)}(0,\omega)$ is the value, at the origin $\underline{f} = 0$, of the two-dimensional spatial Fourier transform of the source intensity distribution, defined by

$$\tilde{I}^{(0)}(\underline{f},\omega) = \frac{1}{(2\pi)^2}\int_{-\infty}^{\infty} I^{(0)}(\underline{r},\omega)e^{-i\underline{f}\cdot\underline{r}}\, d^2r. \tag{56}$$

It is seen from Eq. (53) that the radiance $B_\omega(\underline{r},\underline{s})$ is proportional to the optical intensity $I^{(0)}(\underline{r},\omega)$ and to the two-dimensional spatial Fourier transform of the complex degree of spatial coherence $\mu^{(0)}(\underline{r},\omega)$ of the light across the source. Because $\mu^{(0)}(\underline{r},\omega)$ is a nonnegative definite quantity,[10] its Fourier transform is always nonnegative by the classic theorem of Bochner.[24] Hence, the radiance $B_\omega(\underline{r},\underline{s})$ associated with a quasihomogeneous planar source is a nonnegative quantity that vanishes outside the source area. Moreover, it can be shown[25] that the radiance $B_\omega(\underline{r},\underline{s})$, given by Eq. (53), remains essentially constant along any given $\underline{s}$ direction over a distance ℓ that satisfies the condition

$$\ell \ll \left(\frac{2\cos^4\theta}{\sin\theta}\right)\left(\frac{k}{|f|_{max}}\right)^3\lambda. \tag{57}$$

Here θ is the angle that the $\underline{s}$ direction makes with the positive z axis, $k = 2\pi/\lambda$, and $|\underline{f}|_{max}$ is, roughly speaking, the magnitude of the largest spatial frequencies of the source intensity distribution [cf. Eq. (56)]. Since the optical intensity across a quasihomogeneous source varies very little over distances of the order of wavelength, the ratio $k/|f|_{max}$ is large compared to unity. Consequently, the radiance associated with a quasihomogeneous source satisfies the equation (5) of radiative transfer to a good approximation. In the limits as the source approaches a strictly homogeneous source or the angle $\theta \to 0$, the upper bound for ℓ set by Eq. (57) approaches infinity, indicating that in these cases the equation of radiative transfer is rigorously obeyed.[25]

Comparing the expression (54) for the radiant emittance $E_\omega(\underline{r})$ to the definition (46) of the radiation efficiency C_ω, one sees that[6,26]

$$E_\omega(\underline{r}) = C_\omega I^{(0)}(\underline{r},\omega), \tag{58}$$

where

$$C_\omega = \int_{-\infty}^{\infty}\mu^{(0)}(\underline{r}',\omega)K_\omega(\underline{r}')d^2r'. \tag{59}$$

Hence, the radiant emittance $E_\omega(\underline{r})$ associated with a quasihomogeneous planar source is proportional to the source intensity distribution, with the proportionality factor being determined by the complex degree of spatial coherence $\mu^{(0)}(\underline{r}',\omega)$. In view of Eq. (47), the radiant emittance $E_\omega(\underline{r})$ never exceeds the value of the optical intensity $I^{(0)}(\underline{r},\omega)$.

An interesting result[6] is readily seen from Eq. (55): the angular distribution of the radiant intensity $J_\omega(\underline{s})$ is proportional to the two-dimensional spatial Fourier transform of the complex degree of spatial coherence of the light across the source and to the square of the cosine of the angle that the $\underline{s}$ direction makes with the positive z axis. Thus, the coherence properties of a quasihomogeneous source completely determine the angular distribution of the radiant intensity generated by the source. This important result is one part of a remarkable reciprocity theorem,[6] the other part of which asserts that the complex degree of spatial coherence of the light in the far zone of a quasihomogeneous source is, apart from a simple geometrical factor, equal to the normalized spatial Fourier transform of the optical intensity across the source. This second part of the theorem can be regarded as a generalization of the famous van Cittert-Zernike theorem to quasihomogeneous planar sources.

5.1. Examples of quasihomogeneous planar sources

We will illustrate the general expressions (53)–(55) of the radiometric quantities pertaining to quasihomogeneous planar sources by several examples.

5.1.1. Gaussian correlated source

Let us assume that the complex degree of spatial coherence of the light in the source plane is given by

$$\mu^{(0)}(\underline{r}',\omega) = e^{-\underline{r}'^2/2\sigma_\mu^2}, \tag{60}$$

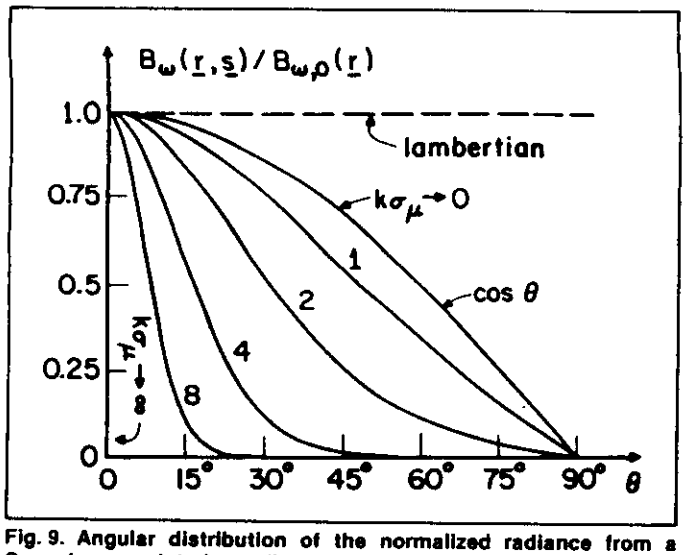

Fig. 9. Angular distribution of the normalized radiance from a Gaussian correlated quasihomogeneous planar source.

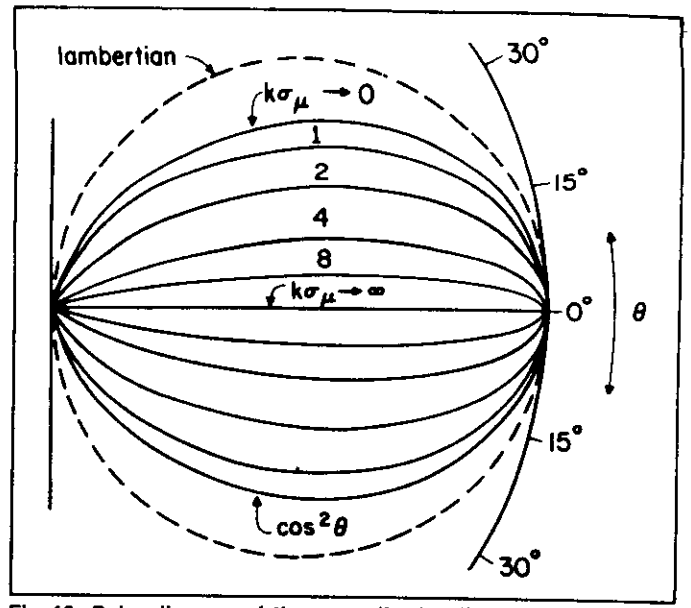

Fig. 10. Polar diagram of the normalized radiant intensity from a Gaussian correlated quasihomogeneous planar source [after Carter and Wolf[6]].

where σ_μ is a positive parameter. The exact form of the optical intensity distribution $I^{(0)}(\underline{r},\omega)$ across the source is of no consequence as long as it meets the requirements stated at the beginning of this section. On substituting from Eq. (60) into Eq. (53), we find for the radiance

$$B_\omega(\underline{r},\underline{s}) = B_{\omega,0}(\underline{r})\cos\theta e^{-\frac{1}{2}(k\sigma_\mu)^2\sin^2\theta}, \tag{61}$$

where

$$B_{\omega,0}(\underline{r}) = \frac{(k\sigma_\mu)^2}{2\pi} I^{(0)}(\underline{r},\omega). \tag{62}$$

The graphs in Fig. 9, computed from Eq. (61), illustrate the dependence of $B_\omega(\underline{r},\underline{s})$ on the angle θ for several values of the parameter $k\sigma_\mu$. It is observed that the larger the effective coherence area of the source is, the more directional the radiance $B_\omega(\underline{r},\underline{s})$ becomes. The broken line corresponds to a Lambertian source. Substitution from Eq. (60) into Eq. (55) yields for the radiant intensity[6,27]

$$J_\omega(\underline{s}) = J_{\omega,0}\cos^2\theta e^{-\frac{1}{2}(k\sigma_\mu)^2\sin^2\theta}, \tag{63}$$

where

$$J_{\omega,0} = 2\pi(k\sigma_\mu)^2\widetilde{I}^{(0)}(0,\omega). \tag{64}$$

Here, $\widetilde{I}^{(0)}(0,\omega)$ is given by Eq. (56) with $\underline{f} = 0$. Figure 10 illustrates, in the form of polar diagrams calculated according to Eq. (63), the distribution of the radiant intensity $J_\omega(\underline{s})$ as a function of the angle θ for several values of $k\sigma_\mu$. It is evident from these graphs that there is a profound modification in the directionality of the radiant intensity when the correlation distance σ_μ is increased from zero to a value of about a wavelength.[27] The broken line corresponding to the radiant intensity from a Lambertian source is included for comparison.

The radiation efficiency of a Gaussian correlated quasihomogeneous planar source is found by substituting from Eq. (60) into Eq. (59). The result is[6]

$$C_\omega = 1 - \frac{F[k\sigma_\mu/\sqrt{2}\,]}{k\sigma_\mu/\sqrt{2}}, \tag{65}$$

where F(a) is the Dawson integral defined by Eq. (44). The radiation efficiency C_ω, calculated from Eq. (65), is presented in Fig. 11 as a function of $k\sigma_\mu$. It is seen to increase monotonically from a value zero, when $k\sigma_\mu = 0$ (incoherent source), to its maximum value unity, when $k\sigma_\mu = \infty$ (coherent source). Hence, the loss in radiation efficiency is due to imperfect spatial coherence properties of the light across the source.

5.1.2. Blackbody source

Consider an opening of area A made into one of the walls of a cavity inside which optical radiation is at thermal equilibrium. We assume that the linear dimensions of the opening are large compared to the mean wavelength of the radiation field. The opening can be regarded as a planar source within which the optical intensity (at frequency ω) is a constant, denoted by $I_{\omega,0}$, and the complex degree of spatial coherence is[5]

$$\mu^{(0)}(\underline{r}',\omega) = \frac{\sin kr'}{kr'}, \tag{66}$$

where $r' = |\underline{r}'|$. For such a source, which is a special case of the so-called Bessel correlated sources,[28] Eqs. (53) and (55) yield for the radiance and the radiant intensity

$$B_\omega(\underline{r},\underline{s}) = \frac{1}{2\pi} I_{\omega,0}, \tag{67}$$

and

$$J_\omega(\underline{s}) = \frac{A}{2\pi} I_{\omega,0}\cos\theta, \tag{68}$$

respectively. The radiation efficiency is found[26] to be $C_\omega = 1/2$. Equations (67) and (68) show that the radiance is a constant within the source area and that the radiant intensity follows a $\cos\theta$ law. Both these features are characteristic of a Lambertian source. This result then indicates that a Lambertian source is not completely spatially incoherent but exhibits, according to Eq. (66), field correlations over distances of the order of the wavelength of the light.

6. SUMMARY AND DISCUSSION

In this article we have reviewed some of the more important

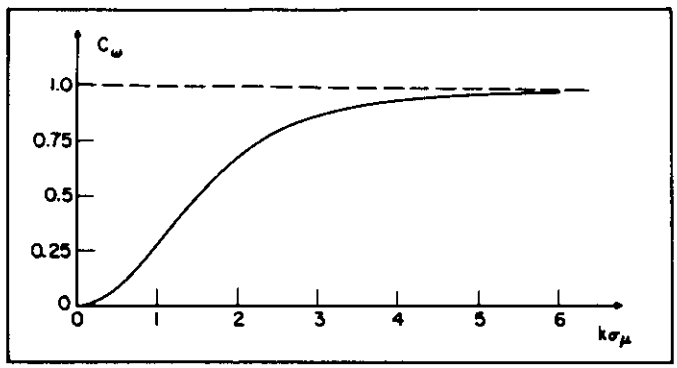

Fig. 11. Radiation efficiency of a Gaussian correlated quasihomogeneous planar source [after Carter and Wolf[6]].

features of radiation emanating from planar sources of any prescribed state of coherence. It is evident from the discussion that the coherence properties of a source play an essential role in determining its radiation characteristics. When comparing radiometry of partially coherent light with conventional radiometry, it is observed that in both cases energy transfer is naturally treated frequency by frequency. However, many other aspects of conventional radiometry cannot directly be taken over into the generalized radiometry. In particular, the radiance and the radiant emittance can no longer be considered as measurable quantities with their intuitive physical interpretations postulated in conventional radiometry. The primary measurable quantity associated with radiation from partially coherent sources is the angular distribution of the radiant intensity.

We have discussed the radiometric description of planar sources of any state of coherence and analyzed in some detail the limiting cases of spatially completely incoherent and spatially completely coherent sources. We have also presented, with illustrative examples, the radiometric characteristics of a source model, the so-called quasihomogeneous model, that can be used in many instances to represent true natural sources. Still more refined source models, which we have not been able to touch upon in this article, have been proposed in the literature. One example is the so-called Schell model source,[29-31] which represents a broader class of radiation sources than does the quasihomogeneous model. When the area occupied by the source is sufficiently large and the intensity variation across the source sufficiently slow, the predictions based on the Schell model are essentially the same as those obtained from the quasihomogeneous model. Further details and relevant references can be found in some recent related review articles.[20,32,33]

All throughout this article we have been concerned with the determination of the radiometric characteristics of a source assuming that its coherence properties are known. The inverse problem, i.e., determining the distributions of the optical intensity and the complex degree of spatial coherence across the source from the measured radiation data and especially from the angular distribution of the radiant intensity, has recently acquired increased attention.[5,33-35] The solution of the inverse problem is important both from a practical point of view and from a mathematical point of view, but it does not fall into the category of topics to be covered under the present title. In Ref. 36 some aspects of the uniqueness of the relationship between the cross-spectral density function across a planar source and the angular distribution of the radiant intensity will be considered.

7. ACKNOWLEDGMENTS

The author wishes to thank E. Wolf for several helpful discussions concerning this manuscript. Financial support from the U.S. Army Research Office and from the Academy of Finland is gratefully acknowledged.

8. REFERENCES

1. Geist, J., Opt. Eng. 15(6), 537 (1976).
2. Planck, M., *The Theory of Heat Radiation*, Dover, New York (1959).
3. Walther, A., J. Opt. Soc. Am. 58, 1256 (1968).
4. Marchand, E. W. and Wolf, E., J. Opt. Soc. Am. 64, 1219 (1974).
5. Carter, W. H. and Wolf, E., J. Opt. Soc. Am. 65, 1067 (1975).
6. Carter, W. H. and Wolf, E., J. Opt. Soc. Am. 67, 785 (1977).
7. Born, M. and Wolf, E., *Principles of Optics*, fifth edition, Sec. 4.8.1., Pergamon, Oxford and New York (1975).
8. Chandrasekhar, S., *Radiative Transfer*, Chap. I, Eq. (47), Dover, New York (1960).
9. Beran, M. J. and Parrent, G. B., Jr., *Theory of Partial Coherence*, Sec. 2.1., Society of Photo-Optical Instrumentation Engineers, Bellingham, WA (1974).
10. Mandel, L. and Wolf, E., J. Opt. Soc. Am. 66, 529 (1976).
11. Wolf, E. and Carter, W. H., J. Opt. Soc. Am. 68, 953 (1978).
12. Carter, W. H. and Wolf, E., Opt. Commun. 25, 288 (1978).
13. Wolf, E., J. Opt. Soc. Am. 68, 1597 (1978).
14. Marchand, E. W. and Wolf, E., J. Opt. Soc. Am. 62, 379 (1972).
15. Walther, A., J. Opt. Soc. Am. 63, 1622 (1973).
16. Walther, A., Opt. Lett. 3, 127 (1978).
17. Marchand, E. W. and Wolf, E., J. Opt. Soc. Am. 64, 1273 (1974).
18. Friberg, A. T., in *Coherence and Quantum Optics IV*, ed. Mandel, L. and Wolf, E., Plenum, New York (1978).
19. Friberg, A. T., J. Opt. Soc. Am. 69, 192 (1979).
20. Wolf, E., J. Opt. Soc. Am. 68, 6 (1978).
21. Marchand, E. W. and Wolf, E., Opt. Commun. 6, 305 (1972).
22. Perina, J., *Coherence of Light*, Sec. 4.2., Van Nostrand, London (1971).
23. Abramowitz, M. and Stegun, I.A., *Handbook of Mathematical Functions*, p. 319, Dover, New York (1965).
24. Goldberg, R. R., *Fourier Transforms*, Chap. 5, Cambridge University Press, Cambridge, England (1965).
25. Friberg, A. T., Opt. Acta 28, 261 (1981).
26. Wolf, E. and Carter, W. H., in *Coherence and Quantum Optics IV*, ed. Mandel, L. and Wolf, E., Plenum, New York (1978).
27. Wolf, E. and Carter, W. H., Opt. Commun. 13, 205 (1975).
28. Baltes, H. P., Steinle, B., and Antes, G., Opt. Commun. 18, 242 (1976).
29. Schell, A. C., "The Multiple Plate Antenna," Doctoral Dissertation, Sec. 7.5., Massachusetts Institute of Technology (1971).
30. Baltes, H. P., Steinle, B. and Antes, G., in *Coherence and Quantum Optics IV*, ed. Mandel, L. and Wolf, E., Plenum, New York (1978).
31. Baltes, H. P. and Steinle, B., Nuovo Cimento B 41, 428 (1977).
32. Baltes, H. P., Appl. Phys. 12, 221 (1977).
33. Baltes, H. P., Geist, J., and Walther, A., in *Inverse Source Problems in Optics*, ed. Baltes, H. P., Springer, New York and Berlin (1978).
34. Baltes, H. P. and Steinle, B., Lett. Nuovo Cimento 18, 313 (1977).
35. McGuire, D., Opt. Commun. 29, 17 (1979).
36. Friberg, A. T., Proc. SPIE 194, 71 (1979). A revised version of this paper appears in Opt. Eng. 21(2), 362 (1982).

Radiation from partially coherent sources

Ari T. Friberg*
Pellila
SF-31600
Jakioinen, Finland

Abstract. Although the theory of partial coherence was formulated in a reasonably general form about a quarter of a century ago, it was not until a few years ago that this theory began to be applied to problems of radiation from partially coherent sources. In this review article, the properties of the radiant intensity generated by a planar source of any state of coherence will be discussed. It will be first recalled that the radiant intensity can be expressed as a two-dimensional spatial Fourier transform of a correlation function of the field in the source plane, averaged over the source area. The characteristics of the radiation from several model sources will then be analyzed. With the help of these results, certain equivalence theorems relating to the radiant intensity from planar sources of entirely different degrees of spatial coherence will be reviewed and the underlying physical principles will be elucidated. A number of illustrative examples will also be given. Finally some very recent work, which has led to the construction of planar sources with controllable degrees of spatial coherence, will be described. Experiments carried out with these sources will be discussed; they verify the main relationships between the coherence properties of the source and the directionality of the light it generates.

Keywords: coherence of planar sources; directionality.

Optical Engineering 21(2), 362-369 (March/April 1982).

CONTENTS

1. INTRODUCTION

In an earlier article,[1] we have reviewed some of the more important effects that have been discovered during the last ten years or so in connection with the studies of radiometry with partially coherent light. In that article we presented expressions for the basic radiometric quantities associated with a planar source of arbitrary state of coherence and discussed, with illustrative examples, the limiting cases of completely coherent and incoherent sources as well as some partially coherent model sources that have been proposed in the literature. We noted that the angular distribution of the radiant intensity is the primary measurable quantity pertaining to radiation from partially coherent sources. In the present article, we will pursue further the considerations of the radiation characteristics of steady-state planar sources; in particular, we will analyze more deeply the properties of the radiant intensity generated by a planar source of any state coherence. Some very recent experiments aimed at testing the theoretical predictions will also be briefly discussed.

To get some insight as to the type of phenomena we will be talking about in this paper, let us consider a simple example.[2] Suppose one compares the radiation generated, on one hand, by a thermal light source and, on the other hand, by a typical gas laser (Fig. 1). The angular distribution of the radiant intensity from a thermal source is well known to follow Lambert's law, whereas the distribution of the radiant intensity from a typical laser is quite different, being sharply peaked in the forward direction. Now, a thermal source is spatially almost completely incoherent, and a laser is, of course, spatially highly coherent. Hence, this example seems to indicate that there is a close relationship between the state of coherence of the source and the directionality of the light it generates. This, indeed, is the case, as recent researches on radiation from partially coherent sources have shown.

Illustrative as the above example may be, it does not fully clarify the matter. One might be tempted to conclude from it that complete spatial coherence is a sufficient condition for the generation of highly directional light beams. This is obviously incorrect, as can be easily seen by considering the diffraction of an expanded laser beam from a circular opening.[3] If the radius of the opening is of the order of the wavelength, the resulting radiant intensity distribution—the classic Airy pattern—shows a substantial divergency angle. More surprising, however, is the fact that not only is complete spatial coherence not a sufficient condition, but it is not even a necessary condition for the attainment of high directionality. This result was recently demonstrated by Collett and Wolf,[4,5] who describe several planar sources which are rather incoherent in the global sense and yet generate precisely the same angular distribution of the radiant intensity as a fully coherent laser. This research has also led to the novel concept of partially coherent light beams.[6]

*Present address: Department of Physics and Astronomy, University of Rochester, Rochester, New York 14627.

Paper 5078 received Dec. 8, 1980; accepted for publication July 16, 1981; received by Managing Editor July 27, 1981. This paper is a revision of Paper 194-05 which was presented at the SPIE seminar on Applications of Optical Coherence Aug. 29–30, 1979, San Diego, CA. The paper presented there appears (unrefereed) in SPIE Proceedings Vol. 194.

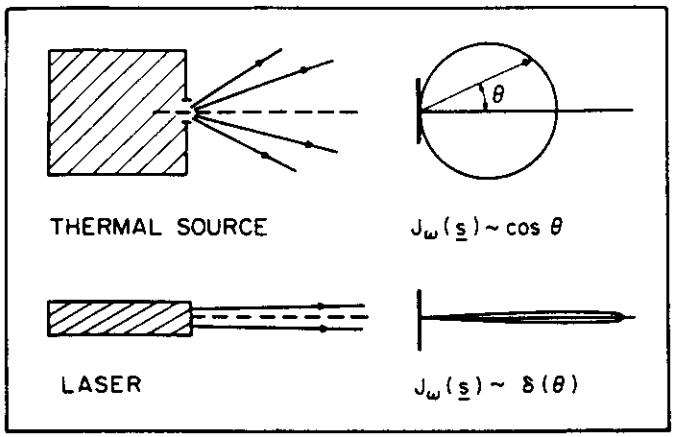

Fig. 1. Schematic illustration of the angular distribution of the radiant intensity from a thermal light source and from a typical laser.

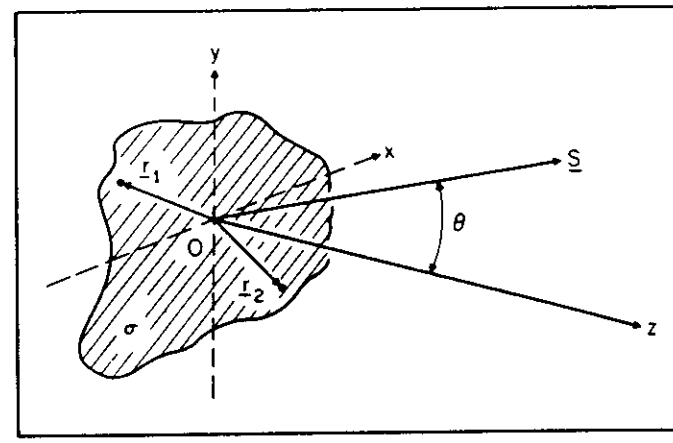

Fig. 2. Illustration of the notation relating to radiation from partially coherent planar sources.

In the present article, we continue to use the same notation as in the previous article.[1] We consider a planar source, either a primary or a secondary one, occupying an area σ (which may be infinite) in the plane $z = 0$ and radiating into the half-space $z > 0$ (Fig. 2). The light generated by the source is represented by a fluctuating complex analytic signal, taken to be a scalar function of position and time and assumed to be stationary and ergodic. Because the different temporal frequency components of a stationary random function are uncorrelated,[7] it is sufficient to consider the transfer of energy at a single temporal frequency, ω say, of the optical field. The state of coherence of the radiation source is therefore conveniently specified by the cross-spectral density function[7] $W^{(0)}(\underline{r}_1, \underline{r}_2; \omega)$ of the light across the plane $z = 0$. The vectors $\underline{r}_1$ and $\underline{r}_2$ represent a typical pair of points in the source plane $z = 0$ (indicated by the superscript 0). Equivalently, the coherence properties of the source may be expressed in terms of the complex degree of spatial coherence $\mu^{(0)}(\underline{r}_1, \underline{r}_2; \omega)$ and the optical intensity $I^{(0)}(\underline{r}, \omega)$ of the light across the plane $z = 0$. They are related to the cross-spectral density function $W^{(0)}(\underline{r}_1, \underline{r}_2; \omega)$ by the following formulas:[7]

$$I^{(0)}(\underline{r}, \omega) = W^{(0)}(\underline{r}, \underline{r}; \omega) , \tag{1}$$

$$\mu^{(0)}(\underline{r}_1, \underline{r}_2; \omega) = \frac{W^{(0)}(\underline{r}_1, \underline{r}_2; \omega)}{\left[I^{(0)}(\underline{r}_1, \omega)\, I^{(0)}(\underline{r}_2, \omega)\right]^{1/2}} . \tag{2}$$

Several properties of these functions as well as their relationship to some of the more commonly known quantities in the theory of partial coherence, such as the mutual coherence function and the complex degree of coherence, are discussed in Ref. 7.

The primary object of interest in this paper is the angular distribution of the radiant intensity generated by the planar source σ. The radiant intensity, denoted by $J_\omega(\underline{s})$, is defined as the power (at frequency ω) radiated by the source per unit solid angle around a direction specified by the unit vector $\underline{s}$ (Fig. 2). The total power (at frequency ω) radiated by the planar source σ into the half-space $z > 0$ may thus be obtained from

$$\Phi_\omega = \int_{(2\pi)} J_\omega(\underline{s})\, d\Omega , \tag{3}$$

where the integration extends over the 2π solid angle formed by all the $\underline{s}$ directions pointing into the half-space $z > 0$. Denoting, moreover, by

$$N_\omega = \int_{-\infty}^{\infty} I^{(0)}(\underline{r}, \omega)\, d^2r \tag{4}$$

the integrated optical intensity (at frequency ω) across the source, one may define the ratio

$$C_\omega = \Phi_\omega / N_\omega \tag{5}$$

as the radiation efficiency of the source at frequency ω. Irrespective of the state of coherence of the source, it can be shown to satisfy the inequality $0 \leqq C_\omega \leqq 1$.

2. RADIANT INTENSITY FROM PLANAR SOURCES OF ANY STATE OF COHERENCE

In this section we will first present several different formulas expressing the radiant intensity generated by the planar source σ described in the introduction (Fig. 2). The state of coherence of the source, which may be quite arbitrary, is specified by the cross-spectral density function $W^{(0)}(\underline{r}_1, \underline{r}_2; \omega)$ of the light across the source plane $z = 0$. The different formulas for the radiant intensity, each having their own distinct advantages, will then be used to elucidate various aspects of radiation from partially coherent planar sources.

2.1. Expressions for the radiant intensity

The radiant intensity $J_\omega(\underline{s})$ generated by a planar source in the direction specified by a unit vector $\underline{s}$ (Fig. 2) has been shown to be given by[1,8,9]

$$J_\omega(\underline{s}) = (2\pi k)^2 \cos^2\theta\, \widetilde{W}^{(0)}(k\underline{s}_\perp, -k\underline{s}_\perp; \omega) , \tag{6}$$

where $k = \omega/c$, with c being the speed of light in free space, and $\widetilde{W}^{(0)}(\underline{f}_1, \underline{f}_2; \omega)$ is the four-dimensional spatial Fourier transform of $W^{(0)}(\underline{r}_1, \underline{r}_2; \omega)$, defined by

$$\widetilde{W}^{(0)}(\underline{f}_1, \underline{f}_2; \omega) = \frac{1}{(2\pi)^4} \int_{-\infty}^{\infty} \int_{-\infty}^{\infty} W^{(0)}(\underline{r}_1, \underline{r}_2; \omega) \cdot e^{-i(\underline{f}_1 \cdot \underline{r}_1 + \underline{f}_2 \cdot \underline{r}_2)} d^2r_1\, d^2r_2 . \tag{7}$$

Moreover, in Eq. (6), θ is the angle that the unit vector $\underline{s}$ makes with the positive z-axis, and $\underline{s}_\perp$ denotes the two-dimensional vector obtained by projecting $\underline{s}$ onto the source plane $z = 0$.

On substituting from Eq. (7) into Eq. (6), we obtain

$$J_\omega(\underline{s}) = \left(\frac{k}{2\pi}\right)^2 \cos^2\theta \int_{-\infty}^{\infty} \int_{-\infty}^{\infty} W^{(0)}(\underline{r}_1, \underline{r}_2; \omega) \cdot e^{-ik\underline{s}_\perp \cdot (\underline{r}_1 - \underline{r}_2)} d^2r_1\, d^2r_2 . \tag{8}$$

Let us next introduce the difference and average coordinates

$$\underline{r}' = \underline{r}_1 - \underline{r}_2; \quad \underline{r} = \frac{1}{2}(\underline{r}_1 + \underline{r}_2) \tag{9}$$

and define

$$C_v(\underline{r}', \omega) = \int_{-\infty}^{\infty} W^{(0)}\left(\underline{r} + \frac{1}{2}\underline{r}', \underline{r} - \frac{1}{2}\underline{r}'; \omega\right) d^2r \ . \tag{10}$$

where the integration extends throughout the source plane $z = 0$. With this notation, Eq. (8) may be rewritten as[9,10]

$$J_\omega(\underline{s}) = k^2 \cos^2\theta \, \tilde{C}_v(k\underline{s}_\perp, \omega) \ , \tag{11}$$

where $\tilde{C}_v(\underline{f}, \omega)$ is the two-dimensional spatial Fourier transform of $C_v(\underline{r}', \omega)$, namely,

$$\tilde{C}_v(\underline{f}, \omega) = \frac{1}{(2\pi)^2} \int_{-\infty}^{\infty} C_v(\underline{r}', \omega) \, e^{-i\underline{f}\cdot\underline{r}'} \, d^2r' \ . \tag{12}$$

The quantity $C_v(\underline{r}', \omega)$, defined by Eq. (10), is called the source-averaged cross-spectral density function of the light in the source plane. In view of the physical significance of $W^{(0)}(\underline{r}_1, \underline{r}_2; \omega)$, the function $C_v(\underline{r}', \omega)$ is clearly proportional to the average value of the correlations of the light fluctuations at frequency ω for all pairs of points $\underline{r}_1$ and $\underline{r}_2$ in the source plane whose relative "separation" is $\underline{r}' = \underline{r}_1 - \underline{r}_2$, the average being taken over the whole source.

It will be convenient to introduce still a third expression for the radiant intensity. For that purpose, let us define the quantity

$$\eta^{(0)}(\underline{r}', \omega) = \frac{C_v(\underline{r}', \omega)}{C_v(0, \omega)} = \frac{C_v(\underline{r}', \omega)}{N_\omega} \ . \tag{13}$$

where the second equality follows the Eqs. (10), (1), and (4). It can be shown that $\eta^{(0)}(\underline{r}', \omega)$ satisfies the conditions[11]

$$\eta^{(0)}(0, \omega) = 1; \quad |\eta^{(0)}(\underline{r}', \omega)| \leqq 1 \ , \tag{14}$$

regardless of the state of coherence of the source. Substitution from Eq. (13) into Eq. (11) yields for the radiant intensity

$$J_\omega(\underline{s}) = k^2 \cos^2\theta \, N_\omega \tilde{\eta}^{(0)}(k\underline{s}_\perp, \omega) \ , \tag{15}$$

where $\tilde{\eta}^{(0)}(\underline{f}, \omega)$ is, of course, the two-dimensional spatial Fourier transform of $\eta^{(0)}(\underline{r}', \omega)$ [cf. Eq. (12)]. With Eqs. (14) and (15) in mind, it is natural to call the quantity $\eta^{(0)}(\underline{r}', \omega)$ the coefficient of directionality[11] of the planar source at frequency ω.

We have thus three formally different expressions for the radiant intensity from a planar source, namely those given by Eqs. (6), (11), and (15). The formulas in Eqs. (6) and (15) are useful when describing certain recent equivalence theorems[4,11] which imply that sources of entirely different states of coherence may nonetheless produce exactly the same distributions of the radiant intensity. A consequence of such an equivalence is, for example, that sources which are far from being spatially completely coherent generate light beams that are just as directional as a Gaussian laser beam.[5] The expression in Eq. (11), on the other hand, turns out to be very convenient when discussing the implications of the analytic properties of the radiant intensity.

2.2. Implications of the expressions for the radiant intensity

Let us consider, first, Eq. (6). According to that formula, only those spatial frequencies of $W^{(0)}(\underline{r}_1, \underline{r}_2; \omega)$, which obey the constraints $\underline{f}_1 = -\underline{f}_2 = k\underline{s}_\perp$, contribute to the radiant intensity. Such a pair $(\underline{f}, -\underline{f})$ is commonly called an antidiagonal pair of spatial frequencies, and the corresponding spatial Fourier component $\tilde{W}^{(0)}(\underline{f}, -\underline{f}; \omega)$ is referred to as an antidiagonal element of $\tilde{W}^{(0)}(\underline{f}_1, \underline{f}_2; \omega)$. Moreover, since $|k\underline{s}_\perp| \leqq |k\underline{s}| = k$, only spatial frequencies for which $|\underline{f}| \leqq k$, the so-called low spatial frequencies, appear in the expression (6) for the radiant intensity. With this terminology we may thus say that the radiant intensity from a planar source is uniquely determined by the low-frequency antidiagonal elements of the four-dimensional spatial Fourier transform of the cross-spectral density function $W^{(0)}(\underline{r}_1, \underline{r}_2; \omega)$ of the light across the source plane.[4]

An interesting conclusion may be immediately drawn from the above result: any two planar sources, whose cross-spectral density functions are such that their four-dimensional spatial Fourier transforms have identical low-frequency antidiagonal elements, will generate identical distributions of the radiant intensity. This is the original form of the equivalence theorem, formulated by Collett and Wolf,[4] pertaining to planar sources of arbitrary states of coherence. Such equivalent sources will, of course, in general generate fields with entirely different far-zone coherence properties, because the far-field coherence is determined by all the low-frequency elements of $\tilde{W}^{(0)}(\underline{f}_1, \underline{f}_2; \omega)$, not just by the antidiagonal ones.[12]

Let us now turn our attention to Eq. (15) and reformulate the above equivalence theorem in a manner that affords a simple and intuitive explanation of the underlying physical reasons for the equivalence. The following result is seen at once from Eq. (15): any two planar sources, which have the same coefficients of directionality $\eta^{(0)}(\underline{r}', \omega)$ and whose integrated optical intensities N_ω are the same, will generate identical distributions of the radiant intensity. This new version of the equivalence theorem, with some additional mathematical refinements, was formulated by Collett and Wolf.[11] To fully appreciate the physical insight provided by this new formulation, let us express the coefficient of directionality $\eta^{(0)}(\underline{r}', \omega)$ in terms of the complex degree of spatial coherence $^{(0)}(\underline{r}_1, \underline{r}_2; \omega)$ and the optical intensity $I^{(0)}(\underline{r}, \omega)$ By substituting from Eq. (2) into Eq. (10) and using the result in Eq. (13), the following expression is obtained:

$$\eta^{(0)}(\underline{r}', \omega) = \frac{1}{N_\omega} \int_{-\infty}^{\infty} \mu^{(0)}\left(\underline{r} + \frac{1}{2}\underline{r}', \underline{r} - \frac{1}{2}\underline{r}', \omega\right) \left[I^{(0)}\left(\underline{r} + \frac{1}{2}\underline{r}', \omega\right) I^{(0)}\left(\underline{r} - \frac{1}{2}\underline{r}', \omega\right)\right]^{1/2} d^2r \ . \tag{16}$$

This formula shows that the coefficient of directionality depends not only on the distribution of the complex degree of spatial coherence, but also on the optical intensity distribution of the light across the source. The coefficient of directionality may be thought of as being obtained by means of an integral of the complex degree of spatial coherence, appropriately weighting each contribution to the integral by an intensity-dependent factor. For instance, two planar sources with the same integrated optical intensities N_ω may have quite different distributions of the complex degree of spatial coherence $\mu^{(0)}(\underline{r}_1, \underline{r}_2; \omega)$ and of the optical intensity $I^{(0)}(\underline{r}, \omega)$, and yet they generate the same distributions of the radiant intensity, provided only that for each $\underline{r}'$ the integral in Eq. (16) is the same for both of them. In such a case, the differences in the complex degrees of spatial coherence are compensated by the differences in the optical intensities. Concrete illustrations of these remarks will be provided shortly.

Finally, let us briefly consider the implications of Eq. (11). It shows that the radiant intensity (at frequency ω) produced by a planar source of any state of coherence is proportional to the product of $\cos^2\theta$ and the two-dimensional spatial Fourier transform of the source-averaged cross-spectral density function $C_v(\underline{r}', \omega)$ of the field in the source plane. Since $k = \omega/c = 2\pi/\lambda$, where λ is the wavelength corresponding to the frequency ω, the radiant intensity is also inversely proportional to the square of the wavelength of the light. If the planar source σ under consideration is of finite extent, the source-averaged cross-spectral density function $C_v(\underline{r}', \omega)$, in view of

Eq. (10), obviously vanishes identically outside some finite $\underline{r}'$ domain. According to some theorems on Fourier transforms, the function $\tilde{C}_V(\underline{f},\omega)$ in such a case possesses certain unique analytic properties. Without going into the details of the mathematics, we will mention a few conclusions that can be drawn by such analytic considerations. In the first place, it can be shown that[5]

$$J_\omega(\underline{s}) \to 0, \text{ as } \theta \to \pi/2 , \tag{17}$$

to at least the second order in $\cos\theta$. Hence a finite planar source does not radiate in any direction parallel to the source plane. This result also implies that, strictly speaking, no *finite* planar source radiating in accordance with Lambert's law can exist. However, many light sources encountered in practice are Lambertian to a good approximation.

Another important conclusion that follows immediately from the analytic properties of the radiant intensity produced by a finite planar source is related to the inverse problem of determining the source coherence properties from the measurements of the radiant intensity. The following very strong theorem has been proven by Wolf:[9] the exact knowledge of the radiant intensity for all $\underline{s}$ directions filling any finite solid angle, however small, uniquely determines the complete source-averaged cross-spectral density function $C_V(\underline{r}',\omega)$ of the light in the source plane. According to Eq. (13), the coefficient of directionality $\eta^{(0)}(\underline{r}',\omega)$ and the integrated optical intensity N_ω of the planar source are readily obtained once $C_V(\underline{r}',\omega)$ is known. In particular, one can take the finite solid angle appearing in the above theorem to be the whole 2π solid angle formed by all the possible $\underline{s}$ directions. These results then imply that the quantities $C_V(\underline{r}',\omega)$, $\eta^{(0)}(\underline{r}',\omega)$, and N_ω associated with a planar source giving rise to any prescribed distribution of the radiant intensity $J_\omega(\underline{s})$ (assumed to have been produced by some *finite* planar source) can be uniquely specified.

It should be noted that even though the radiant intensity $J_\omega(\underline{s})$ uniquely determines the source-averaged cross-spectral density function $C_V(\underline{r}',\omega)$, the cross-spectral density function $W^{(0)}(\underline{r}_1,\underline{r}_2;\omega)$ itself is not necessarily unique across the source. This remark is in keeping with the earlier observations that planar sources of entirely different states of coherence may generate identical distributions of the radiant intensity. However, it can be shown that in the special case of a nonradiating finite planar source (i.e., a source for which $J_\omega(\underline{s})$ has a zero value for all the possible $\underline{s}$ directions), the cross-spectral density function $W^{(0)}(\underline{r}_1,\underline{r}_2;\omega)$ must vanish whenever $\underline{r}_1 \neq \underline{r}_2$. Hence every *finite* planar source, other than a strictly spatially incoherent one, necessarily radiates. This result also implies that a finite planar source cannot generate a field that consists of a pure surface wave. Analogous considerations pertaining to true primary planar sources were presented by Friberg.[13]

3. QUASIHOMOGENEOUS SOURCE THAT GENERATES A KNOWN DISTRIBUTION OF RADIANT INTENSITY

As an application of the general discussion presented in the previous section, we will consider here the following two related problems:[11] first, how to specify a quasihomogeneous planar source that will produce the same radiant intensity as any given planar source,[14] and, second, how to specify a quasihomogeneous planar source that will generate any prescribed distribution of the radiant intensity, assuming that the radiant intensity was produced by some finite planar source.

For that purpose, we first recall that a quasihomogeneous planar source is characterized by a cross-spectral density function of the form[1,15]

$$W^{(0)}(\underline{r}_1,\underline{r}_2;\omega) = I^{(0)}\left[\frac{1}{2}(\underline{r}_1+\underline{r}_2),\omega\right]\mu^{(0)}(\underline{r}_1-\underline{r}_2;\omega), \tag{18}$$

where $I^{(0)}(\underline{r},\omega)$ is the optical intensity distribution, and $\mu^{(0)}(\underline{r}',\omega)$, assumed to depend only on the difference $\underline{r}' = \underline{r}_1 - \underline{r}_2$, is the complex degree of spatial coherence of the light in the source plane. It is assumed, moreover, that $I^{(0)}(\underline{r},\omega)$ varies with $\underline{r}$ much more slowly than $\mu^{(0)}(\underline{r}',\omega)$ varies with $\underline{r}'$, and that the linear dimensions of the source are large compared to both the wavelength of the light and the effective coherence interval of the light across the source. On substituting from Eq. (18) into Eq. (16), the coefficient of directionality of a quasihomogeneous planar source (denoted by subscript Q) is readily found to be

$$\eta_Q^{(0)}(\underline{r}',\omega) = \mu_Q^{(0)}(\underline{r}',\omega) , \tag{19}$$

where use was made of the result

$$N_{\omega,Q} = \int_{-\infty}^{\infty} I_Q^{(0)}(\underline{r},\omega)\,d^2r , \tag{20}$$

with $I_Q^{(0)}(\underline{r},\omega)$ being the optical intensity distribution of the quasihomogeneous source. Eq. (19) shows that the coefficient of directionality of a quasihomogeneous planar source is precisely equal to its complex degree of spatial coherence.

Consider now some given planar source σ of any state of coherence whatever. Its coefficient of directionality, denoted by $\eta_\sigma^{(0)}(\underline{r}',\omega)$, may be computed from Eq. (16), and its integrated optical intensity, denoted by $N_{\omega,\sigma}$, is readily obtained from Eq. (4). The radiant intensity distribution produced by this source is therefore known, it being given by Eq. (15). Now, according to the equivalence theorem discussed earlier, a quasihomogeneous planar source whose coefficient of directionality $\eta_Q^{(0)}(\underline{r}',\omega)$ and integrated optical intensity $N_{\omega,Q}$ satisfy the conditions

$$\eta_Q^{(0)}(\underline{r}',\omega) = \eta_\sigma^{(0)}(\underline{r}',\omega);\ N_{\omega,Q} = N_{\omega,\sigma} , \tag{21}$$

will generate precisely the same distribution of the radiant intensity as the given planar source σ. With the help of Eqs. (19) and (20), these conditions take the form[11]

$$\mu_Q^{(0)}(\underline{r}',\omega) = \eta_\sigma^{(0)}(\underline{r}',\omega);\ \int_{-\infty}^{\infty} I_Q^{(0)}(\underline{r},\omega)\,d^2r = N_{\omega,\sigma} . \tag{22}$$

These results show that there is, in fact, an infinite number of quasihomogeneous sources that produce the same radiant intensity as any given source. They all have the same complex degree of spatial coherence, uniquely specified by the first condition in Eq. (22), but their optical intensity distributions may differ, provided that they are sufficiently smooth and satisfy the second condition in Eq. (22).

To illustrate the above comments, let us determine a quasihomogeneous source that will produce the same radiant intensity as a completely coherent and cophasal square source of uniform intensity I_0. Taking the sides to be of length 2ℓ, one easily finds for such a source

$$\eta_\sigma^{(0)}(\underline{r}',\omega) = \begin{cases} (1-|x'|/2\ell)(1-|y'|/2\ell), \text{ if } |x'| \leqq 2\ell \text{ and } |y'| \leqq 2\ell , \\ 0, \text{ otherwise} , \end{cases} \tag{23}$$

where $\underline{r}' = (x',y')$. The integrated optical intensity $N_{\omega,\sigma}$ is, of course, equal to $4\ell^2 I_0$. The radiant intensity distribution generated by the source under consideration is known to be

$$J_\omega(\underline{s}) = \left(\frac{k}{2\pi}\right)^2 (4\ell^2)^2 I_0 \cos^2\theta \left(\frac{\sin ks_x\ell}{ks_x\ell}\right)^2 \left(\frac{\sin ks_y\ell}{ks_y\ell}\right)^2 , \tag{24}$$

where $\underline{s} = (s_x,s_y,s_z)$ with $s_z = \cos\theta$. Now, according to Eq. (22), a quasihomogeneous planar source, whose complex degree of spatial coherence is given by the right-hand side of Eq. (23), will also give rise to the radiant intensity of Eq. (24). The complex degree of spatial coherence $\mu_Q^{(0)}(\underline{r}',\omega)$ of the quasihomogeneous source, with $y' = 0$,

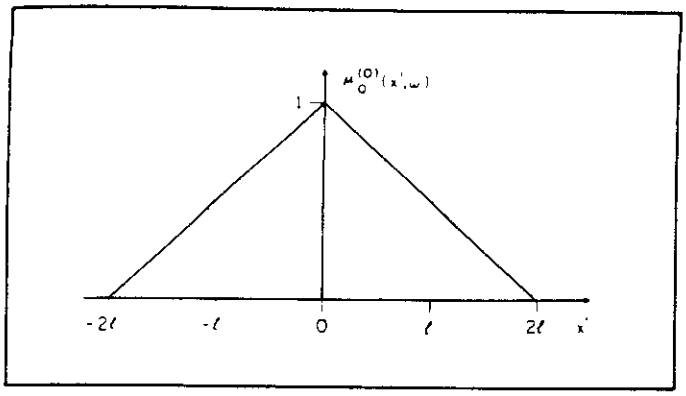

Fig. 3. The complex degree of spatial coherence, with y' = 0, of a quasi-homogeneous planar source that produces the same distribution of the radiant intensity as a uniform, completely coherent, and cophasal square source of sides 2ℓ.

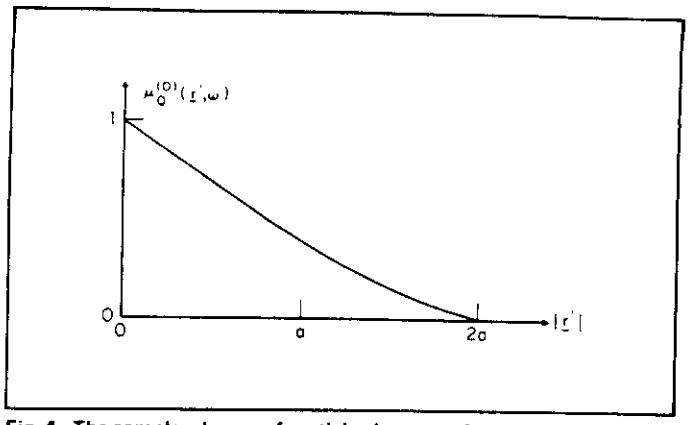

Fig. 4. The complex degree of spatial coherence of a quasihomogeneous planar source that produces the classic Airy pattern of the radiant intensity (after Collett and Wolf[11]).

is illustrated in Fig. 3. The actual shape of the optical intensity distribution across this equivalent source is irrelevant, as long as it meets the requirements of quasihomogeneity and integrates to $4\ell^2 I_0$. Equivalent quasihomogeneous sources corresponding to more complicated examples, possibly illuminated with partially coherent light, can be specified in a similar manner.

Let us now turn our attention to the second problem stated at the beginning of this section. As we have already explained, a prescribed distribution of the radiant intensity (assumed to have been generated by some finite source σ) uniquely determines the source-averaged cross-spectral density function, denoted here by $C_{V,\sigma}(\underline{r}',\omega)$ for convenience. According to Eq. (13), this in turn uniquely determines the coefficient of directionality $\eta_\sigma^{(0)}(\underline{r}',\omega)$ and the integrated optical intensity $N_{\omega,\sigma}$ of the source. Now, by substituting these on the right-hand side of the conditions in Eq. (22), we obtain a quasihomogeneous source that also will produce the prescribed distribution of the radiant intensity. As before, the complex degree of spatial coherence of such a quasihomogeneous source is unique, but its optical intensity distribution may vary.

As an example, we will take the prescribed distribution of the radiant intensity to be the famous Airy pattern

$$J_\omega(\underline{s}) = \left(\frac{k}{2\pi}\right)^2 (\pi a^2)^2 I_0 \cos^2\theta \left[\frac{2J_1(ka\sin\theta)}{ka\sin\theta}\right]^2 , \tag{25}$$

where $J_1(x)$ is the Bessel function of the first kind and first order. The quantities a and I_0 are positive parameters. A quasihomogeneous planar source producing the radiant intensity, given by Eq. (25), can be shown[11] to have a complex degree of spatial coherence

$$\mu_Q^{(0)}(\underline{r}',\omega) = \begin{cases} \dfrac{2}{\pi}\left[\cos^{-1}\left(\dfrac{r'}{2a}\right) - \left(\dfrac{r'}{2a}\right)\sqrt{1-\left(\dfrac{r'}{2a}\right)^2}\right], & \text{if } r' \leqq 2a , \\ 0, \text{ otherwise} , \end{cases} \tag{26}$$

where $r' = |\underline{r}'|$. Its optical intensity distribution must have an integral over the entire source equal to $(\pi a^2) I_0$. The complex degree of spatial coherence, given by Eq. (26), is illustrated in Fig. 4.

4. MODEL SOURCES

To become more familiar with the various concepts introduced earlier in this article, we will now discuss several partially coherent model sources. In addition to the quasihomogeneous sources,[15] we will also consider the so-called Schell model sources.[16,17] A Schell model source is characterized by a cross-spectral density function of the form

$$W^{(0)}(\underline{r}_1,\underline{r}_2;\omega) = \left[I^{(0)}(\underline{r}_1,\omega)\, I^{(0)}(\underline{r}_2,\omega)\right]^{1/2} \mu^{(0)}(\underline{r}_1 - \underline{r}_2;\omega) . \tag{27}$$

Here $I^{(0)}(\underline{r},\omega)$ is the optical intensity distribution, and $\mu^{(0)}(\underline{r}',\omega)$, assumed to depend only on the difference $\underline{r}' = \underline{r}_1 - \underline{r}_2$, is the complex degree of spatial coherence of the light in the source plane. The Schell model sources, like the quasihomogeneous ones, are a generalization of the statistically homogeneous sources. If the optical intensity distribution across the source varies sufficiently slowly from point to point, as is the case with many natural radiation sources, the Schell model sources become essentially quasihomogeneous.

We will consider three types of quasihomogeneous sources and one type of Schell model source. The quasihomogeneous sources are taken to have a distribution of the complex degree of spatial coherence, which is either of Gaussian or of exponential form, or it is specified in terms of Bessel functions. These distributions are, respectively,

$$\mu^{(0)}(\underline{r}',\omega) = e^{-\underline{r}'^2/2\sigma_\mu^2} , \tag{28}$$

$$\mu^{(0)}(\underline{r}',\omega) = e^{-|\underline{r}'|/D} , \tag{29}$$

$$\mu^{(0)}(\underline{r}',\omega) = \frac{2}{\sqrt{\pi}}\,\Gamma\left(\nu+\frac{3}{2}\right)\frac{j_\nu(k|\underline{r}'|)}{\left(\frac{1}{2}k|\underline{r}'|\right)^\nu} \tag{30}$$

Here σ_μ and D are positive parameters, $\Gamma(x)$ denotes the gamma function, and $j_\nu(x)$ is the spherical Bessel function of the first kind and of order ν, with $\nu \geqq -1/2$. The exact forms of the optical intensity distributions $I^{(0)}(\underline{r},\omega)$ across these sources are of no importance in the present context, as long as they meet the requirements of quasihomogeneity. The Schell model source, on the other hand, is taken to have both its complex degree of spatial coherence and its optical intensity of Gaussian form; i.e., $\mu^{(0)}(\underline{r}',\omega)$ is the same as Eq. (28), and $I^{(0)}(\underline{r},\omega)$ is given by

$$I^{(0)}(\underline{r},\omega) = I_0 e^{-\underline{r}^2/2\sigma_I^2} , \tag{31}$$

where I_0 and σ_I are positive parameters.

We will determine the coefficient of directionality $\eta^{(0)}(\underline{r}',\omega)$, the distribution of the radiant intensity $J_\omega(\underline{s})$, and the radiation efficiency C_ω associated with these four model sources. The results, some of which can be found in Refs. 1, 5, 11, 15, 18–22, and some of which are new, are given in tabulated form (Table I).

A few comments are perhaps in order regarding the entries in Table I. In the first place, if $\sigma_I \gg \sigma_\mu$ then $\Delta \to \sigma_\mu$, and the Gaussian Schell model source reduces to a Gaussian correlated quasihomo-

TABLE I. Radiation from Partially Coherent Model Sources.

MODEL	QUASIHOMOGENEOUS			SCHELL
INTENSITY	NOT RELEVANT			GAUSSIAN
COHERENCE	GAUSSIAN	EXPONENTIAL	BESSEL	GAUSSIAN
COEFFICIENT OF DIRECTIONALITY	$e^{-\underline{r}'^2/2\sigma_\mu^2}$	$e^{-\lvert\underline{r}'\rvert/D}$	$\frac{2}{\sqrt{\pi}}\,\Gamma(\nu+\frac{3}{2})\frac{J_\nu(k\lvert\underline{r}'\rvert)}{(\frac{1}{2}k\lvert\underline{r}'\rvert)^\nu}$	$e^{-\underline{r}'^2/2\Delta^2}$ $\frac{1}{\Delta^2}=\frac{1}{\sigma_\mu^2}+\frac{1}{(2\sigma_I)^2}$
RADIANT INTENSITY	$J_{\omega,o}\cos^2\theta e^{-\frac{1}{2}(k\sigma_\mu)^2\sin^2\theta}$ $J_{\omega,o}=\frac{(k\sigma_\mu)^2}{2\pi}\int I^{(0)}(\underline{r},\omega)\,d^2r$	$J_{\omega,o}\cos^2\theta[1+(kD)^2\sin^2\theta]^{-\frac{3}{2}}$ $J_{\omega,o}=\frac{(kD)^2}{2\pi}\int I^{(0)}(\underline{r},\omega)\,d^2r$	$J_{\omega,o}\cos^{2\nu+1}\theta$ $J_{\omega,o}=\frac{1}{\pi}(\nu+\frac{1}{2})\int I^{(0)}(\underline{r},\omega)\,d^2r$	$J_{\omega,o}\cos^2\theta e^{-\frac{1}{2}(k\Delta)^2\sin^2\theta}$ $J_{\omega,o}=(k\Delta\sigma_I)^2 I_o$
RADIATION EFFICIENCY	$1-\frac{F(k\sigma_\mu/\sqrt{2})}{k\sigma_\mu/\sqrt{2}}$ $F(a)=e^{-a^2}\int_0^a e^{u^2}du$	$1-\frac{1}{(kD)}\sin^{-1}\left(\frac{kD}{\sqrt{1+(kD)^2}}\right)$	$\frac{2\nu+1}{2\nu+2}$	$1-\frac{F(k\Delta/\sqrt{2})}{k\Delta/\sqrt{2}}$ $F(a)=e^{-a^2}\int_0^a e^{u^2}du$

geneous source. On the other hand, if $\sigma_\mu\to\infty$, then it represents a completely coherent and cophasal planar source with Gaussian optical intensity distribution. In that case, $\Delta\to 2\sigma_I$, and the results are found to be identical to those given in Refs. 1, 4, and 11. If, moreover, $k\sigma_I \gg 1$, then such a source represents a Gaussian laser, and one may, of course, approximate $\cos\theta\approx 1$ and $\sin\theta\approx\theta$. Several special cases of the Bessel correlated quasihomogeneous sources are also of interest. For $\nu=-1/2$, the complex degree of spatial coherence is found from Eq. (30) to be $J_0(kr')$, where $r'=|\underline{r}'|$ and $J_0(x)$ is the Bessel function of the first kind and order zero. Hence the source exhibits a finite (non-zero) correlation distance, and yet its radiation efficiency is seen to be zero. At first sight this appears to contradict our earlier remark that every finite planar source (other than a strictly spatially incoherent one) necessarily radiates.[13] The resolution of this dilemma is, of course, that the Bessel correlated quasihomogeneous source with $\nu=-1/2$ is of infinite extent. For $\nu=0$, the right-hand side of Eq. (30) reduces to $\sin kr'/kr'$, leading to a Lambertian planar source.[1,23] For $\nu=1/2$, Eq. (30) gives, on the other hand, a complex degree of spatial coherence of the form $2J_1(kr')/kr'$, where $J_1(x)$ is the Bessel function of the first kind and order one. The radiant intenslty from such a source is seen to follow a $\cos^2\theta$-law, identical to that from a spatially incoherent source (when spatial incoherence is defined in terms of the non-normalizable Dirac delta function).[1,8,23]

5. PARTIALLY COHERENT SOURCES THAT PRODUCE THE SAME RADIANT INTENSITY AS A LASER

We have already described a procedure by which one can specify the characteristics of a quasihomogeneous planar source that will generate the same distribution of the radiant intensity as any given planar source. We illustrated this procedure by determining a quasihomogeneous source which produces the same radiant intensity as a uniform, fully coherent, and cophasal square source. In this section, we will discuss a broader class of partially coherent sources, each with a different coherence area and a different optical intensity distribution, giving rise to a radiant intensity distribution identical to that of a fully coherent Gaussian laser beam.[5]

Let us first compute the radiant intensity distribution generated by a laser source with a flat output mirror, operating in its lowest-order transverse mode. Neglecting the diffraction effects caused by the edges of the output mirror, the radiant intensity may be found from Table I by setting $\sigma_\mu=\infty$ for the Gaussian Schell model source. Writing σ_L and I_L in place of σ_I and I_o to indicate that these quantities pertain to the laser, the optical intensity distribution across the output mirror is

$$I_L^{(0)}(\underline{r},\omega) = I_L e^{-\underline{r}^2/2\sigma_L^2}, \tag{32}$$

and the resulting radiant intensity distribution is readily found to be[1,4,5]

$$J_{\omega,L}(\underline{s}) = (2k\sigma_L^2)^2 I_L\cos^2\theta e^{-2(k\sigma_L)^2\sin^2\theta}. \tag{33}$$

By comparing the formula of Eq. (33) to the expression of the radiant intensity given in Table I for the Gaussian Schell mode. source, the following important theorem follows at once:[5] any Schell model source, whose optical intensity distribution and complex degree of spatial coherence are both Gaussian and whose parameters σ_μ, σ_I, and I_o satisfy the conditions

$$\frac{1}{\sigma_\mu^2}+\frac{1}{(2\sigma_I)^2}=\frac{1}{(2\sigma_L)^2};\quad I_o=\left(\frac{\sigma_L}{\sigma_I}\right)^2 I_L, \tag{34}$$

will generate precisely the same distribution of the radiant intensity, namely that of Eq. (33), as a fully coherent and cophasal planar laser source with the Gaussian optical intensity distribution of Eq. (32). Even though all sources satisfying the conditions (34) will generate the same radiant intensity distributions, their far-field coherence properties will, as we have discussed earlier, in general be different.

It is evident from the first condition of Eq. (34) that the parameters σ_μ and σ_I of any Gaussian Schell model source producing the radiant intensity of Eq. (33) must satisfy the inequalities $\sigma_I \geqq \sigma_L$ and $\sigma_\mu \geqq 2\sigma_L$. Hence the width of the optical intensity distribution across any such Schell model source can be no smaller than the width of the laser intensity distribution, and the width of the complex degree of spatial coherence must be at least twice the width of the laser intensity.

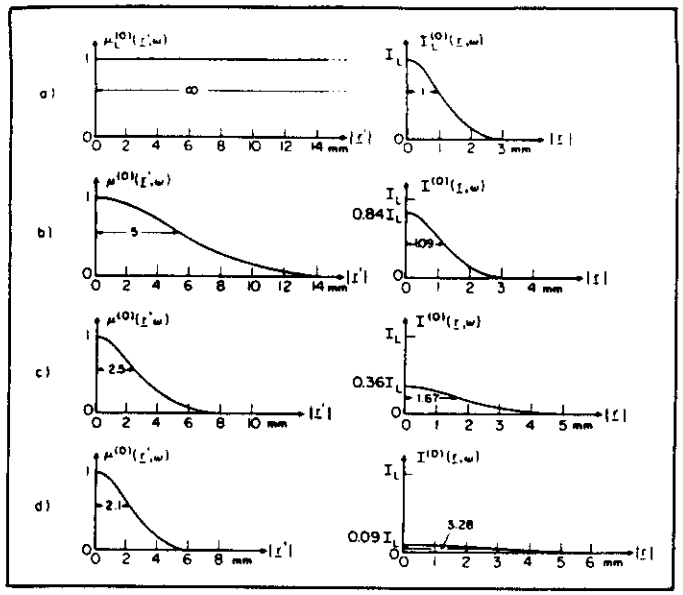

Fig. 5. Illustrating the coherence and intensity distributions across partially coherent Gaussian Schell model sources (b, c, and d) giving rise to the same radiant intensity distribution as a fully coherent laser source (a). The radiant intensity is given by Eq. (33) with $\sigma_L = 1$ mm and I_L arbitrary (after Wolf and Collett[5]).

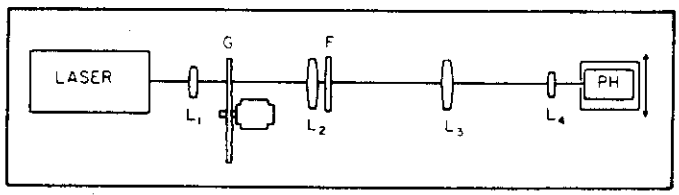

Fig. 6. Schematic illustration of the Gori system (after De Santis, Gori, Guattari, and Palma[27]).

Choosing $\sigma_\mu \approx 2\sigma_L$ and $\sigma_I \gg \sigma_\mu$, the resulting Schell model source is essentially quasihomogeneous.[4] This source is precisely the one which would have been obtained by using the procedure, described earlier, of specifying equivalent quasihomogeneous planar sources.

In Fig. 5, we present the distributions of the optical intensity and the complex degree of spatial coherence of the light across several different Gaussian Schell model sources, each source generating the same radiant intensity as a fully coherent Gaussian laser source. The graphs clearly illustrate the trade-off taking place between the source coherence and the source intensity, so as to produce identical distributions of the radiant intensity.

6. SOURCES WITH CONTROLLABLE DISTRIBUTIONS OF INTENSITY AND COHERENCE

Even though the properties of radiation from partially coherent sources have been the subject of active research for more than ten years, experimental investigations as to the practical realization of such sources and the testing of the theoretical predictions have only very recently begun. Among the suggested ways of producing a controllable partially coherent source are, for example, a suitable superposition of independent laser beams[24] and the scattering of light by a liquid crystal under the application of a dc electric field.[21,25,26] Most of the experimental effort so far has concentrated on direct verification of the predicted relationship between the coherence properties of a source and the directionality of the light it generates. The first experimental results, supporting the equivalence theorem which implies that certain partially coherent planar sources may produce light fields just as directional as a laser beam, were obtained by DeSantis, Gori, Guattari, and Palma[27] using an optical

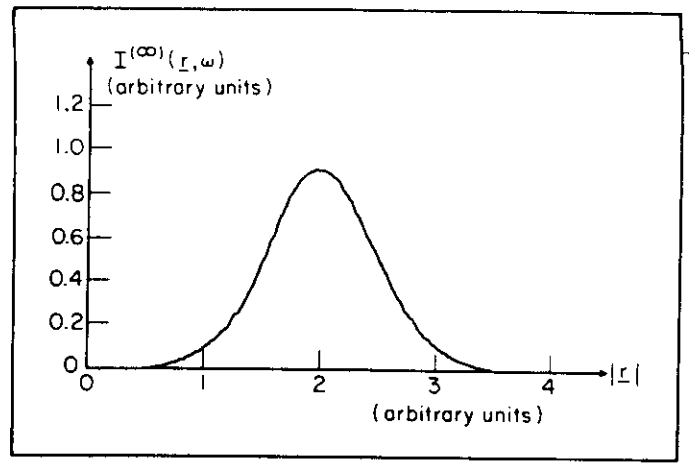

Fig. 7. Recording of the optical intensity distribution in the far field of a fully coherent Gaussian laser source (after De Santis, Gori, Guattari, and Palma[27]).

system resembling an ordinary collimator. Because of the importance of the results and the ingenuity of the device, we will briefly describe the experiment carried out by Gori and his coworkers.

The Gori system is illustrated in Fig. 6. G is a rotating ground glass, F is a Gaussian amplitude filter, and L_1-L_4 are simple lenses. Consider first the ground glass G and the amplitude filter F removed. The field, originating in the laser, can be made to emerge from the lens L_2 with no phase curvature and with a Gaussian optical intensity distribution, if the focal lengths f_1 and f_2 of the lenses L_1 and L_2 as well as their separation are chosen properly. Hence, in this case, the lens L_2 realizes a fully coherent Gaussian planar source. Its optical intensity distribution may thus be represented by Eq. (32), with the constants I_L and σ_L being determined by the system parameters. The lens L_3 produces in its back focal plane the far-field distribution of the coherent field emerging from the lens L_2, and the lens L_4 forms an enlarged image of that distribution on the photodetector PH. The intensity profile scanned along a line perpendicular to the optical axis in the far-field distribution of the coherent Gaussian source (i.e., the plane of the lens L_2) is presented in Fig. 7.

After examining the coherent case, the rotating ground glass G and the Gaussian amplitude filter F are reinserted. A Gaussian spot of laser light is produced on the ground glass by the lens L_1. If the spot diameter is large compared to the inhomogeneity scale of the glass, it can be considered as a spatially incoherent planar source with a Gaussian intensity distribution.[28] Let us denote the value of the intensity on the optical axis by I_S and the rms width of the intensity distribution by σ_S. The lens L_2 is placed a distance f_2, i.e., the focal length of L_2, from the ground glass G, and the filter F, with a field transmission function of rms width σ_F, is adjacent to the lens L_2. Using the van Cittert-Zernike theorem and the usual optical propagation laws, the cross-spectral density function of the field emerging from the filter F can be shown to be[27]

$$W^{(0)}(\underline{r}_1, \underline{r}_2; \omega) = \frac{I_S (k\sigma_S)^2}{4\pi f_2^2} e^{-(k\sigma_S/2f_2)^2(\underline{r}_1 - \underline{r}_2)^2} e^{-(\underline{r}_1^2 + \underline{r}_2^2)/2\sigma_F^2} . \quad (35)$$

This formula implies that the plane of the filter F acts as a Gaussian Schell model source. Its complex degree of spatial coherence is given by Eq. (28), and its optical intensity is given by Eq. (31), with the constants I_0, σ_I, and σ_μ being related to the system parameters I_S, σ_S, f_2, and σ_F by the formulas

$$I_0 = \frac{I_S (k\sigma_S)^2}{4\pi f_2^2} ; \sigma_I = \frac{\sigma_F}{\sqrt{2}} ; \sigma_\mu = \frac{\sqrt{2} f_2}{k\sigma_S} . \quad (36)$$

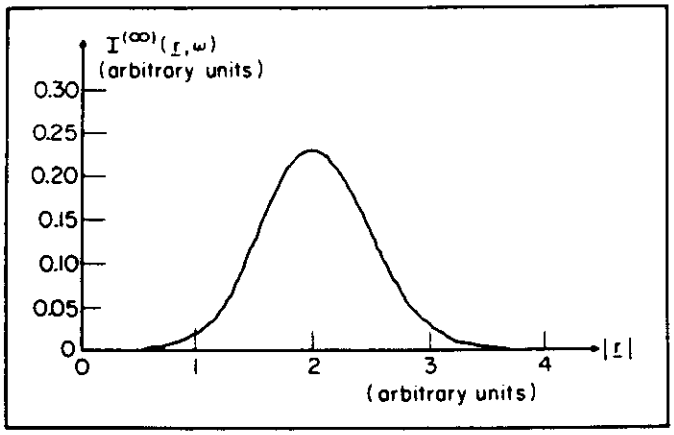

Fig. 8. Recording of the optical intensity distribution in the far field of a Guassian Schell model source realized by means of the Gori system (after De Santis, Gori, Guattari, and Palma[27]).

Now, according to the discussion in the previous section, if the parameters I_0, σ_I, and σ_μ associated with the light emerging from the filter F satisfy the conditions (34), then such a source produces exactly the same far-field intensity distribution as the fully coherent Gaussian source characterized by the parameters I_L and σ_L. The intensity profile scanned along a line perpendicular to the optical axis in the far field produced by a source of this type (i.e., the field emerging from the filter F) with suitably chosen system parameters is shown in Fig. 8. The arbitrary units used for the intensity and for the distance from the optical axis are the same in both Figs. 7 and 8. It is observed that the measured far-field intensity distributions presented in these figures show a remarkable similarity, thus providing evidence in support of the theoretical predictions.

It is of interest to note that the Gori system described above can be used to produce a whole class of partially coherent sources with controllable distributions of intensity and spatial coherence. By varying the system parameters I_S, σ_S, f_2, and σ_F, the constants I_0, σ_I, and σ_μ may be altered thus changing the spatial coherence and intensity profiles of the Gaussian Schell model source, located in the plane of the filter F. An additional degree of freedom could be provided by using, in place of the laser illuminated rotating ground glass G, some partially coherent light source with known spatial coherence and intensity properties.

Further experimental studies with regard to the highly directional character of the radiation patterns produced by certain types of quasihomogeneous sources have been carried out by Farina, Narducci, and Collett.[29] Their interest has been to investigate the problem with a minimum number of optical elements, so as to reduce extraneous effects and the possibility of experimental error. Using phase screens illuminated by a collimated laser light as quasihomogeneous sources, they have observed that the radiated fields are very directional, as predicted by the theory, in spite of the globally incoherent character of the light in the source plane. They have also observed that changing the intensity distribution across the source plane does not essentially alter the radiation pattern, as long as the intensity distribution meets the requirements of quasihomogeneity. Some preliminary measurements concerning the reciprocity theorem[1,15] pertaining to quasihomogeneous planar sources were also made.

7. SUMMARY AND DISCUSSION

In this review article we have discussed various aspects of the radiant intensity generated by a planar source of any state of coherence. Among the more important results mentioned is an equivalence theorem which implies that sources with entirely different coherence properties may, nevertheless, produce identical distributions of the radiant intensity. This theorem was illustrated by means of several examples, including a class of partially coherent sources which give rise to a radiation field that is just as directional as a fully coherent laser beam. Several model sources were analyzed in terms of convenient new concepts, such as the coefficient of directionality and the radiation efficiency. Finally, some experimental work, aimed at the practical realization of partially coherent sources with controllable coherence and intensity properties and at the testing of the theoretical predictions regarding their radiation characteristics, was briefly described.

Even though the number of experimental results regarding radiation from partially coherent sources is still rather limited, it appears safe to say that such measurements have verified the main relationships between the coherence properties of a source and the directionality of the light it generates. In particular, the fact that complete spatial coherence is not a necessary requirement for the generation of highly directional light beams has been experimentally confirmed. However, to obtain convincing experimental evidence about many other phenomena predicted by the theory, a subtantial amount of further effort is required.

As is well known, fully coherent laser beams give rise to pronounced speckle effects that are often very disturbing. In many applications, a very directional light beam with low spatial coherence would have several advantages over the fully coherent laser beam. For these reasons, especially after it was shown that a globally rather incoherent source may produce a light beam which is just as directional as a laser beam, highly directional partially coherent light beams appear to be likely subjects of future research.

8. ACKNOWLEDGMENTS

It is a pleasure to thank E. Wolf for several helpful discussions concerning the manuscript. Financial support from the U.S. Army ERADCOM, Ft. Monmouth, New Jersey, and from the Academy of Finland is gratefully acknowledged.

9. REFERENCES

1. Friberg, A. T., Proc. SPIE 194, 55(1979).
2. Wolf, E., J. Opt. Soc. Am. 68, 6(1978).
3. Parrent, G. B., Jr. and Thompson, B. J., *Physical Optics Notebook*, SPIE, Bellingham, WA (1969).
4. Collett, E. and Wolf, E., Opt. Lett. 2, 27(1978).
5. Wolf, E. and Collett, E., Opt. Commun. 25, 293(1978).
6. Foley, J. T. and Zubairy, M. S., Opt. Commun. 26, 297(1978).
7. Mandel, L. and Wolf, E., J. Opt. Soc. Am. 66, 529(1976).
8. Marchand, E. W. and Wolf, E., J. Opt. Soc. Am. 64, 1219(1974).
9. Wolf, E., J. Opt. Soc. Am. 68, 1597(1978).
10. Carter, W. H., Opt. Commun. 26, 1(1978).
11. Collett, E. and Wolf, E., J. Opt. Soc. Am. 69, 942(1979).
12. Marchand, E. W. and Wolf, E., J. Opt. Soc. Am. 62, 379(1972).
13. Friberg, A. T., J. Opt. Soc. Am. 68, 1281(1978).
14. De Santis, P., Gori, F. and Palma, C., Opt. Commun. 28, 151(1979).
15. Carter, W. H. and Wolf, E., J. Opt. Soc. Am. 67, 785(1977).
16. Schell, A. C., "The multiple plate antenna," Doctoral Dissertation, Massachusetts Institute of Technology (1971), Section 7.5.
17. Steinle, B. and Baltes, H. P., J. Opt. Soc. Am. 67, 241(1977).
18. Baltes, H. P., Steinle, B. and Antes, G., Opt. Commun. 18, 242(1976).
19. Antes, G., Baltes, H. P., and Steinle, B., Helv. Phys. Acta 49, 759(1976).
20. Baltes, H. P. and Steinle, B., Nuovo Cimento B, 41, 428(1977).
21. Carter, W. H. and Bertolotti, M., J. Opt. Soc. Am. 68, 329(1978).
22. Baltes, H. P., Steinle, B. and Antes, G., "Radiometric and correlation properties of bounded planar sources," in *Coherence and Quantum Optics IV*, eds. Mandel, L. and Wolf, E., Plenum, New York (1978).
23. Carter, W. H. and Wolf, E., J. Opt. Soc. Am. 65, 1067(1975).
24. Gori, F. and Palma, C., Opt. Commun. 27, 185(1978).
25. Scudieri, F., Bertolotti, M. and Bartolino, R., Appl. Opt. 13, 181(1974).
26. Bertolotti, M., Scudieri, F. and Verginelli, S., Appl. Opt. 15, 1842(1976).
27. De Santis, P., Gori, F., Guattari, G. and Palma, C., Opt. Commun. 29, 256 (1979).
28. Martienssen, W. and Spiller, E., Am. J. Phys. 32, 919(1964).
29. Farina, J. D., Narducci, L. M. and Collett, E., Opt. Commun. 32, 203(1980).

Proceedings of the

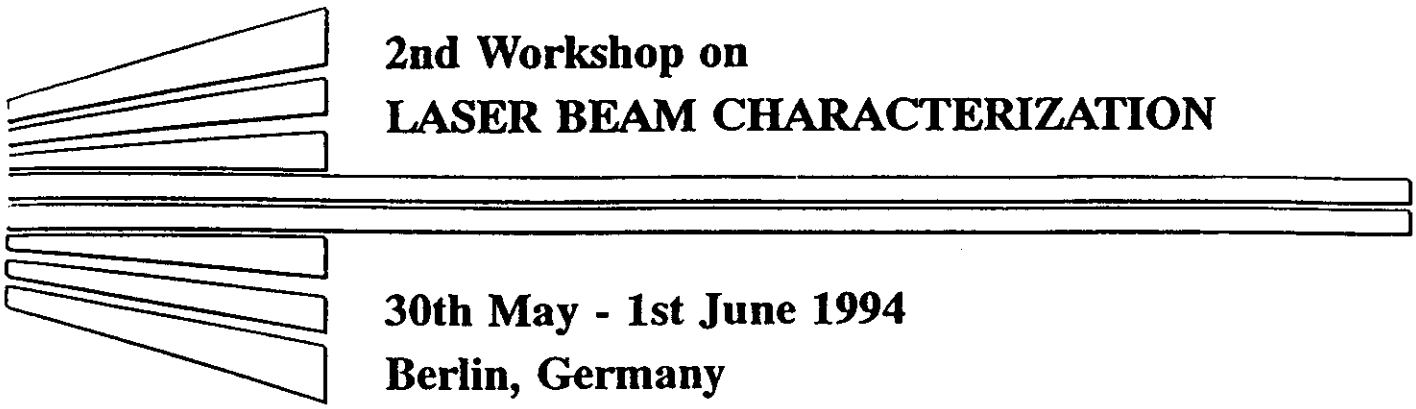

2nd Workshop on
LASER BEAM CHARACTERIZATION

30th May - 1st June 1994
Berlin, Germany

Editors:
H. Weber, N. Reng, J. Lüdtke, P. M. Mejías

This workshop was funded by the German Ministry of Research and Technology (BMFT).

PARTIALLY COHERENT BEAMS

Ari T. Friberg

Department of Technical Physics, Helsinki University of Technology
Rakentajanaukio 2C, FIN-02150 Espoo, Finland

Abstract

A tutorial review of partially coherent beams in optical systems is presented. The main theoretical concepts, some principal applications, versatile practical implementation techniques, and the most significant physical effects brought on by a reduced optical coherence are discussed and illustrated with examples.

1. Introduction

With the rapidly expanding use of lasers e.g. in communication, information technology, process industry, and medicine, the importance of beam optics has increased considerably. The physical properties of the radiation emitted by many novel laser types can be efficiently controlled, and so in recent years the need has arisen to understand the characteristics and behavior of partially coherent beam fields in advanced optical systems. In this tutorial paper we review some of the characteristic features of such beams with a particular emphasis on the effects of partial spatial coherence.

For clarity the main ideas and phenomena are presented in simple terms, but important consequences are mentioned and references are given to the more comprehensive accounts. After reviewing the basic notions of optical coherence in the space-time and space-frequency domains, the so-called coherent-mode decomposition is introduced and the formulation is applied to the determination of the transverse mode structure of multimode laser beams. Various exact and approximate properties of the beam-like wavefields in free space are analyzed, and partially coherent beam synthesis methods are discussed. Central to this work is the hybrid acousto-optic technique that can be employed to control efficiently (in real time) the coherence properties and intensity distributions of optical beams. The most widely used theoretical and experimental model fields are the Gaussian Schell-model (GSM) beams that constitute, in essence, extensions of the fully coherent Gaussian laser beams into the realm of variable-coherence optics. The principal propagation techniques and coherence-influenced physical effects in optical systems are elucidated using the GSM beams. Finally, the main concepts and results associated with the partially coherent nondiffracting beams are recalled.

2. Optical coherence theory

Optical coherence phenomena are customarily described in terms of the space-time correlation functions but in many situations, such as generalized radiometry, a corresponding space-frequency representation of optical coherence seems more appropriate. We begin by briefly reviewing these two coherence formulations, discuss their relationship, and point out some important consequences that follow from it.

Let $V(\mathbf{r},t)$ be the complex analytic signal [1,2] that represents a statistically stationary and ergodic scalar field. The main space-time correlation quantity then is the mutual coherence function

$$\Gamma(\mathbf{r}_1,\mathbf{r}_2;\tau)=\langle V^*(\mathbf{r}_1,t)V(\mathbf{r}_2,t+\tau)\rangle, \tag{1}$$

where the brackets denote (time or ensemble) averaging. When the mutual coherence function is divided by the averaged optical intensity

$$I(\mathbf{r})=\Gamma(\mathbf{r},\mathbf{r};0)=\langle|V(\mathbf{r},t)|^2\rangle \tag{2}$$

in the form

$$\gamma(\mathbf{r}_1, \mathbf{r}_2; \tau) = \Gamma(\mathbf{r}_1, \mathbf{r}_2; \tau)/[I(\mathbf{r}_1)I(\mathbf{r}_2)]^{1/2}, \tag{3}$$

a classic quantity known as the complex degree of coherence is obtained. This function is normalized so that for all values of its arguments

$$0 \leq |\gamma(\mathbf{r}_1, \mathbf{r}_2; \tau)| \leq 1, \tag{4}$$

and the lower and upper limits correspond, respectively, to complete incoherence and complete coherence in the space-time domain. A field that is fully coherent in this sense throughout some domain is necessarily monochromatic [3]. Physically the mutual coherence function $\Gamma(\mathbf{r}_1, \mathbf{r}_2; \tau)$ characterizes the (second-order) field correlations at points $\mathbf{r}_1$ and $\mathbf{r}_2$ and at time instants separated by τ. The function $\Gamma(\mathbf{r}_1, \mathbf{r}_2; \tau)$ has several unique properties that derive from its nature as a correlation function [4]. The normalized form $\gamma(\mathbf{r}_1, \mathbf{r}_2; \tau)$ quantifies the degree of the field correlations and it can be measured e.g. in the usual Young's two-pinhole experiment [2–4]; the fringe visibility is proportional to the modulus while the locations of the intensity maxima determine the phase, and τ represents the difference in time delays owing to wave propagation to the observation point from the pinholes at $\mathbf{r}_1$ and $\mathbf{r}_2$.

Since the stationary random process $V(\mathbf{r}, t)$ cannot die out as $t \to \pm\infty$, the field does not possess a temporal Fourier transform. We may, however, introduce purely formally as a generalized function the Fourier transform

$$\tilde{V}(\mathbf{r}, \omega) = \frac{1}{2\pi} \int_{-\infty}^{\infty} V(\mathbf{r}, t) \exp(i\omega t) \mathrm{d}t, \tag{5}$$

for which $\tilde{V}(\mathbf{r}, \omega) = 0$ when $\omega < 0$, and after inverting it make use of this definition in Eq. (1). Since the left-hand side of Eq. (1) is independent of t, it follows that the (statistical) average $\langle \tilde{V}^*(\mathbf{r}_1, \omega) \tilde{V}(\mathbf{r}_2, \omega') \rangle$ must vanish unless $\omega = \omega'$, and so [5]

$$\langle \tilde{V}^*(\mathbf{r}_1, \omega) \tilde{V}(\mathbf{r}_2, \omega') \rangle = W(\mathbf{r}_1, \mathbf{r}_2; \omega) \delta(\omega - \omega'), \tag{6}$$

where the factor $W(\mathbf{r}_1, \mathbf{r}_2; \omega)$ multiplying the Dirac delta function $\delta(\omega - \omega')$ is the cross-spectral density associated with the field. On substituting the above expression into Eq. (1) we then find at once that

$$\Gamma(\mathbf{r}_1, \mathbf{r}_2; \tau) = \int_0^{\infty} W(\mathbf{r}_1, \mathbf{r}_2; \omega) \exp(-i\omega\tau) \mathrm{d}\omega. \tag{7}$$

This formula shows that the mutual coherence function $\Gamma(\mathbf{r}_1, \mathbf{r}_2; \tau)$ likewise is a complex analytic signal. Equations (6) and (7) together constitute the essense of the extended Wiener-Khintchine theorem [5], namely that the different (generalized) Fourier components of a stationary field are uncorrelated and that the mutual coherence function $\Gamma(\mathbf{r}_1, \mathbf{r}_2; \tau)$ and the cross-spectral density function $W(\mathbf{r}_1, \mathbf{r}_2; \omega)$ form a Fourier-conjugate pair.

It is evident that the cross-spectral density $W(\mathbf{r}_1, \mathbf{r}_2; \omega)$ characterizes the (second-order) scalar field correlations at points $\mathbf{r}_1$ and $\mathbf{r}_2$ and at frequency ω. This function is the primary quantity in most applications of the modern coherence theory and below we will apply it extensively in partially coherent beam analysis. We assume that Eq. (7) can be inverted and the result is

$$W(\mathbf{r}_1, \mathbf{r}_2; \omega) = \frac{1}{2\pi} \int_{-\infty}^{\infty} \Gamma(\mathbf{r}_1, \mathbf{r}_2; \tau) \exp(i\omega\tau) \mathrm{d}\tau. \tag{8}$$

The 'diagonal element' of the cross-spectral density, i.e. the function

$$S(\mathbf{r}, \omega) = W(\mathbf{r}, \mathbf{r}; \omega) \tag{9}$$

is the spectrum (or spectral density) of the optical field at point $\mathbf{r}$ and at frequency ω. If the cross-spectral density function is normalized as

$$\mu(\mathbf{r}_1, \mathbf{r}_2; \omega) = W(\mathbf{r}_1, \mathbf{r}_2; \omega)/[S(\mathbf{r}_1, \omega) S(\mathbf{r}_2, \omega)]^{1/2}, \tag{10}$$

then for all values of $\mathbf{r}_1$, $\mathbf{r}_2$, and ω

$$0 \leq |\mu(\mathbf{r}_1, \mathbf{r}_2; \omega)| \leq 1. \tag{11}$$

The quantity $\mu(\mathbf{r}_1, \mathbf{r}_2; \omega)$ is called the complex degree of spectral (or spatial) coherence [5]. As before, the (mathematical) limiting values 0 and 1 above indicate that the light fluctuations at points $\mathbf{r}_1$ and $\mathbf{r}_2$ are fully uncorrelated or fully correlated, respectively, but this time at the temporal frequency ω of the stationary field. If the condition of complete spectral coherence is satisfied in some volume, the cross-spectral density $W(\mathbf{r}_1, \mathbf{r}_2; \omega)$ factors in $\mathbf{r}_1$ and $\mathbf{r}_2$ [6, 7]. It is interesting to note that the quantity $\mu(\mathbf{r}_1, \mathbf{r}_2; \omega)$ can also be measured in a Young's experiment if the pinholes are covered by narrow-band spectral filters [8]. The situation is illustrated in Fig. 1. When the filter passbands are made arbitrarily small, the maximum visibility of the interference fringes formed in the observation plane by the filtered light will not, in general, tend to unity, but rather (at a symmetric point for which $\tau = 0$, and assuming sufficiently long integration time) it is equal to the absolute value of the complex degree of spectral coherence of the incident light at the two pinholes and at the center frequency of the filters.

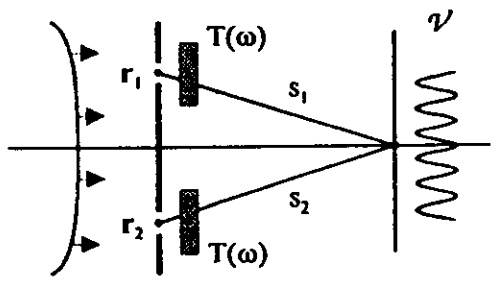

Figure 1. The spectral filters $T(\omega)$ modify the incident cross-spectral density (and therefore also the space-time correlations) but leave the complex degree of spectral coherence unaltered. For narrow-band filters centered at ω_0, the exiting complex degree of coherence is [8] $\gamma(\mathbf{r}_1, \mathbf{r}_2; \tau) = \mu(\mathbf{r}_1, \mathbf{r}_2; \omega_0)\theta(\tau)$, where $\theta(\tau)$ is solely determined by $T(\omega)$ and obeys $\theta(0) = 1$.

As the filtering example demonstrates, the two quantities $\gamma(\mathbf{r}_1, \mathbf{r}_2; \tau)$ and $\mu(\mathbf{r}_1, \mathbf{r}_2; \omega)$ measure different types of coherence. For example, being fully coherent in one domain does dot imply the same in the other domain. The two complex coherence degrees are, however, intimately related as can be seen by deriving a functional dependence between them. More specifically, we first find from Eqs. (7) and (10) that

$$\Gamma(\mathbf{r}_1, \mathbf{r}_2; \tau) = \int_0^\infty [S(\mathbf{r}_1, \omega) S(\mathbf{r}_2, \omega)]^{1/2} \mu(\mathbf{r}_1, \mathbf{r}_2; \omega) \exp(-i\omega\tau) \mathrm{d}\omega. \tag{12}$$

Using Eq. (2) and the fact that $\mu(\mathbf{r}, \mathbf{r}; \omega) = 1$ for all ω [cf. Eqs. (9) and (10)], the (averaged) optical intensity at point $\mathbf{r}$ is found to be

$$I(\mathbf{r}) = \int_0^\infty S(\mathbf{r}, \omega) \mathrm{d}\omega. \tag{13}$$

This expression is merely a statement of the obvious physical situation that the total intensity is made up of all the spectral contributions. If we define the normalized spectrum as

$$s(\mathbf{r}, \omega) = S(\mathbf{r}, \omega) / \int_0^\infty S(\mathbf{r}, \omega) \mathrm{d}\omega, \tag{14}$$

then Eq. (12) readily implies that

$$\gamma(\mathbf{r}_1, \mathbf{r}_2; \tau) = \int_0^\infty [s(\mathbf{r}_1, \omega) s(\mathbf{r}_2, \omega)]^{1/2} \mu(\mathbf{r}_1, \mathbf{r}_2; \omega) \exp(-i\omega\tau) \mathrm{d}\omega. \tag{15}$$

This is an important relation which shows, first of all [cf. Eq. (7)], that the two quantities $\gamma(\mathbf{r}_1, \mathbf{r}_2; \tau)$ and $[s(\mathbf{r}_1, \omega) s(\mathbf{r}_2, \omega)]^{1/2} \mu(\mathbf{r}_1, \mathbf{r}_2; \omega)$ form a Fourier-transform pair. It also readily leads to expressions, in terms of the normalized spectrum $s(\mathbf{r}, \omega)$ and the complex degree of spectral coherence $\mu(\mathbf{r}_1, \mathbf{r}_2; \omega)$, for the quantities [1, 2, 4] that are traditionally used to characterize the spatial coherence and the temporal coherence, viz. $\gamma(\mathbf{r}_1, \mathbf{r}_2; 0)$ and $\gamma(\mathbf{r}, \mathbf{r}; \tau)$, respectively.

An illustrative special case is the uniform and isotropic blackbody radiation source, which obeys Lambert's law $J(\theta,\omega) \propto \cos\theta$ at each frequency. In such a case the complex degree of spectral coherence (e.g. at a sufficiently large planar opening) is uniquely given by [9]

$$\mu(\mathbf{r}_1,\mathbf{r}_2;\omega) = \frac{\sin k|\mathbf{r}_2-\mathbf{r}_1|}{k|\mathbf{r}_2-\mathbf{r}_1|}, \tag{16}$$

where $k = \omega/c$ is the wave number and c is the vacuum speed of light. Since the (space-independent) normalized spectrum is known to follow Planck's law

$$s(\omega) = \frac{15}{\pi^4}\left(\frac{\hbar}{KT}\right)^4 \frac{\omega^3}{\exp(\hbar\omega/KT)-1}, \tag{17}$$

where T is the temperature, K is Boltzmann's constant, and $\hbar$ is Planck's constant divided by 2π, the associated space-time complex degree of coherence $\gamma(\mathbf{r}_1,\mathbf{r}_2;\tau)$ is obtained at once from Eq. (15). The resulting temporal and spatial coherence properties are illustrated in Fig. 2. It is recalled [10] that blackbody radiance (brightness) assumes its maximum at $\omega_{max} \approx 2.82\,(KT/\hbar)$ and, according to Fig. 2, the temporal coherence is seen to extend over a range of just about up to $\tau \sim 2\pi/\omega_{max}$. Of course it is obvious that Lambertian radiation fields do not constitute beams, but these sources have played a central role in elucidating the foundation of spectral radiometry with partially coherent light [11]. We note also that, strictly, the expressions above correspond to the trace of the 3×3 electric cross-spectral density tensor which can be argued to be compatible with the scalar physical optics [9, 12]. In literature, the exact electromagnetic correlation properties of blackbody radiation are analyzed and illustrated [2, 12].

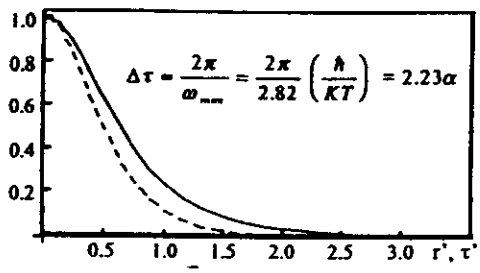

Figure 2. Graphs of blackbody temporal coherence $|\gamma(0,\tau')|$ as a function of $\tau' = \tau/\alpha$ (solid line) and spatial coherence $\gamma(\mathbf{r}',0)$ as a function of $r' = r/\alpha c$ (dashed line), obtained by numerical integration from Eqs. (15)–(17). The temporal coherence function obeys $|\gamma(0,-\tau')| = |\gamma(0,\tau')|$. The parameter $\alpha = \hbar/KT$.

So far we have not taken into consideration the fact that optical fields are (electromagnetic) wave fields. Therefore in free space the mutual coherence function $\Gamma(\mathbf{r}_1,\mathbf{r}_2;\tau)$ obeys a coupled pair of wave equations, whereas the cross-spectral density $W(\mathbf{r}_1,\mathbf{r}_2;\omega)$ satisfies two Helmholtz equations [11]

$$(\nabla_j^2 + k^2)W(\mathbf{r}_1,\mathbf{r}_2;\omega) = 0, \qquad (j = 1,2), \tag{18}$$

where k is the wave number associated with frequency ω. In half-space problems, often encountered in optics, exact solutions to Eq. (18) can be furnished in terms of the angular spectrum (or plane-wave) representation or the (1st and 2nd) Rayleigh integral formulas [13]. In the context of optical systems, the function $W(\mathbf{r}_1,\mathbf{r}_2;\omega)$ is normally required only in planes z = constant and the paraxial approximation for beam-like fields is usually employed. With rotationally symmetric optical systems (containing no losses or gains), the general solution for the planar cross-spectral density function is expressible using the extended Fresnel diffraction integral as

$$\begin{aligned} W(\rho_1,\rho_2;z_{out}) &= (k/2\pi B)^2 \exp\left[-\frac{ikD}{2B}(\rho_1^2-\rho_2^2)\right] \iint W(\rho_1',\rho_2';0) \\ &\quad \times \exp\left[-\frac{ikA}{2B}(\rho_1'^2-\rho_2'^2)\right] \exp\left[\frac{ik}{B}(\rho_1\cdot\rho_1'-\rho_2\cdot\rho_2')\right] \mathrm{d}^2\rho_1'\mathrm{d}^2\rho_2', \end{aligned} \tag{19}$$

where $\mathbf{r} = (\rho, z)$ for $(j = 1,2)$, and A, B, C, and D are the (real) elements of the system ray-transfer matrix; the input plane is taken at $z = 0$ (the frequency ω is not shown explicitly). In nonsymmetric aligned cases the ABCD matrix M is a 4×4 (symplectic) matrix, but the diffraction integral can still be written in a convenient block form; with tilt or decenter, 5×5 ray matrices are needed [14].

The propagation equations for the stationary second-order correlation functions are another obvious reason why the spatial and temporal coherence properties cannot be independent. In fact, Sudarshan [15] has shown that in free space the coupled wave equations for the mutual coherence function $\Gamma(\mathbf{r}_1, \mathbf{r}_2; \tau)$ can be turned into differential equations that are of first order in time (though nonlocal in space). These equations have then been solved to produce explicit formulas for the mutual coherence function, as well as for the cross-spectral density $W(\mathbf{r}_1, \mathbf{r}_2; \omega)$ and the spectrum $S(\mathbf{r}, \omega)$, in terms of a spatial integral over the mutual intensity $\Gamma(\mathbf{r}_1, \mathbf{r}_2; 0)$ [16]. In nonstationary wave fields, such as pulses, the situation is more complicated. Likewise, the vector nature of random electromagnetic fields brings in additional difficulties. Although the electromagnetic correlation tensors, various relations among them, and the degree of polarization have long been studied [1–4], the effects of polarization in narrow optical beams have not so far received much attention. The far field of a blackbody radiator was recently shown to be unpolarized in all directions [17].

3. New space-frequency theory and the coherent-mode representation

The cross-spectral density function $W(\mathbf{r}_1, \mathbf{r}_2; \omega)$ can be introduced either via Eq. (6) or Eq. (8), but both methods are somewhat unsatisfactory. The temporal Fourier transform $\tilde{V}(\mathbf{r}, \omega)$ does not exist as an ordinary function [cf. Dirac delta function in Eq. (6)], and a great deal of mathematical sophistication is expended to deal with this problem. The possible approaches include generalized harmonic analysis, stochastic Fourier-Stieltjes integral, or use of generalized function theory [18]. In Eq. (8), on the other hand, the cross-spectral density is obtained through space-time correlations, which seems an added unphysical complexity. For these reasons a new space-frequency representation of optical coherence was developed a few years ago by Wolf [18–21]. This theory also leads to certain natural modes of partially coherent fields that have found several applications [21].

We assume that the cross-spectral density $W(\mathbf{r}_1, \mathbf{r}_2; \omega)$ is a continuous function of ω and contains a finite amount energy in the volume of interest [18, 19], i.e.

$$\iint |W(\mathbf{r}_1, \mathbf{r}_2; \omega)|^2 \mathrm{d}^3 r_1 \mathrm{d}^3 r_2 < \infty, \tag{20}$$

and consequently $W(\mathbf{r}_1, \mathbf{r}_2; \omega)$ is a Hilbert-Schmidt kernel [20]. The cross-spectral density is evidently Hermitian [cf. Eq. (6)]

$$W(\mathbf{r}_2, \mathbf{r}_1; \omega) = W^*(\mathbf{r}_1, \mathbf{r}_2; \omega), \tag{21}$$

and it can also be shown to satisfy the non-negative definiteness condition [20, Appendix A]

$$\iint W(\mathbf{r}_1, \mathbf{r}_2; \omega) f^*(\mathbf{r}_1) f(\mathbf{r}_2) \mathrm{d}^3 r_1 \mathrm{d}^3 r_2 \geq 0, \tag{22}$$

where $f(\mathbf{r})$ is any square-integrable function. This expression obviously leads at once e.g. to the general result that the radiant intensity produced by a fluctuating planar source is a non-negative quantity. Equations (20)–(22) together imply, by Mercer's theorem, that the cross-spectral density function admits the convergent expansion [18–21]

$$W(\mathbf{r}_1, \mathbf{r}_2; \omega) = \sum_n \lambda_n(\omega) \psi_n^*(\mathbf{r}_1, \omega) \psi_n(\mathbf{r}_2, \omega), \tag{23}$$

where $\psi_n(\mathbf{r}, \omega)$ are the eigenfunctions and $\lambda_n(\omega)$ the eigenvalues of the Fredholm integral equation

$$\int W(\mathbf{r}_1, \mathbf{r}_2; \omega) \psi_n(\mathbf{r}_1, \omega) \mathrm{d}^3 r_1 = \lambda_n(\omega) \psi_n(\mathbf{r}_2, \omega). \tag{24}$$

The eigenvalues are real and non-negative, $\lambda_n(\omega) \geq 0$, and the eigenfunctions can be taken orthonormal in the volume of field analysis. For a given cross-spectral density there may be one, many, or infinite non-zero eigenvalues. It is clear that with obvious modifications the discussion above applies also to two and one-dimensional field distributions.

The important point now is the following. If one defines a statistical ensemble of monochromatic functions $\{U(\mathbf{r},\omega)\exp(-i\omega t)\}$ such that [18,19]

$$U(\mathbf{r},\omega) = \sum_n a_n(\omega)\psi_n(\mathbf{r},\omega), \tag{25}$$

where the coefficients satisfy $\langle a_n^*(\omega)a_m(\omega)\rangle = \lambda_n(\omega)\delta_{nm}$, then on comparison with Eq. (23) it readily follows that

$$W(\mathbf{r}_1,\mathbf{r}_2;\omega) = \langle U^*(\mathbf{r}_1,\omega)U(\mathbf{r}_2,\omega)\rangle. \tag{26}$$

Hence this result shows that, contrary to popular belief, the cross-spectral density of a stationary optical field can be expressed as a correlation of ordinary functions in the space-frequency domain.

Several physically significant consequences can be pointed out. Since the various contributions in Eq. (23) factor in $\mathbf{r}_1$ and $\mathbf{r}_2$, each term corresponds to a spatially completely coherent field (at the given frequency) [6]. This can also readily be verified on substituting the contributions into Eq. (10). Use of the coupled propagation equations in conjunction with the eigenfunction orthogonality leads to the result that each eigenfunction $\psi_n(\mathbf{r},\omega)$ — and therefore by linearity also the function $U(\mathbf{r},\omega)$ — satisfies the Helmholtz equation in free space. For these reasons the terms in Eq. (23) are spatially coherent modes (natural modes of oscillation), and the expansion is known as the coherent-mode decomposition of the cross-spectral density. The higher-order coherence functions of the optical fields in the space-frequency domain were discussed quite recently [21].

4. Gaussian Schell-model sources and beams

Perhaps the most widely used model fields in modern coherence theory are the Gaussian Schell-model (GSM) sources and the beam-like radiation fields that they generate [22–27]. These beam-fields can be analyzed in closed form and they are readily produced in a controlled manner in the laboratory [28,29]. The GSM sources bridge continuously the gap between the spatially incoherent (thermal) sources and the usual fully coherent laser sources.

The general Schell-model sources are characterized by the fact that the spectral degree of coherence in Eq. (10) depends only on the separation between the points $\mathbf{r}_1$ and $\mathbf{r}_2$, i.e. $\mu(\mathbf{r}_1,\mathbf{r}_2;\omega) = g(\mathbf{r}_2-\mathbf{r}_1,\omega)$. For Gaussian Schell-model sources both the spectral intensity $S(\mathbf{r},\omega)$ and the (real) spectral coherence degree $g(\mathbf{r}',\omega)$ (with $\mathbf{r}' = \mathbf{r}_2-\mathbf{r}_1$) are Gaussian functions. Hence the planar GSM sources (across the waist plane, say $z=0$) are defined by

$$W(\rho_1,\rho_2;\omega) = [S(\rho_1,\omega)S(\rho_2,\omega)]^{1/2}g(\rho_2-\rho_1,\omega), \tag{27}$$

where

$$S(\rho,\omega) = S(\omega)\exp(-2\rho^2/w_S^2), \tag{28}$$

$$g(\rho',\omega) = \exp(-\rho'^2/2\sigma_g^2). \tag{29}$$

Here again $\mathbf{r}_j = (\rho_j, z)$ for $(j=1,2)$, $S(\omega)$ is the on-axis spectrum, and w_S and σ_g are positive parameters (that may depend on ω). It is evident that the spectrum $S(\omega)$ will also affect the (total) beam intensity distribution generated by the source [30]. When $w_S \gg \sigma_g$, the GSM source is globally incoherent, but it may still be locally coherent or incoherent depending on whether $\sigma_g \gg \lambda$ or $\sigma_g \approx \lambda$, where λ is the wavelength. The effectively incoherent limit above corresponds to a special case of the so-called quasihomogeneous sources, for which the spectral intensity $S(\rho,\omega)$ varies in space slowly enough so as to remain essentially constant over regions in which the spectral coherence degree $g(\rho',\omega)$ has sensible values [11,31]. The symmetric GSM source (27)–(29) can be generalized in an obvious way to anisotropic (but orthogonal) cases, that lead to several interesting results on far-field radiation [32,33].

The planar GSM sources (and beams) have an important place in the modern coherence theory also because for them the coherent modes are explicitly known. Substitution of Eqs. (27)–(29) into the integral

equation (24) leads, after considerable algebra, to the separable solution (i.e. identical expressions along both x and y axes) [34,35]

$$\psi_n(x,\omega) = (2/\pi w_S^2\beta)^{1/4}(2^n n!)^{-1/2} H_n(\sqrt{2}x/w_S\sqrt{\beta}) \exp(-x^2/w_S^2\beta), \tag{30}$$

$$\lambda_n(\omega) = S(\omega)\sqrt{2\pi}w_S[\beta/(1+\beta)][(1-\beta)/(1+\beta)]^n, \tag{31}$$

where $\beta = [1 + (\sigma_g/w_S)^{-2}]^{-1/2}$, and $H_n(x)$ are the Hermite polynomials. The parameter $\alpha = \sigma_g/w_S$ appearing in β is the (non-normalized) global degree of coherence; β itself is bound such that $\beta = 1$ implies full spatial coherence and $\beta \to 0$ in the incoherent limit. The eigenfunctions are seen to be the Hermite-Gaussian functions characteristic also of the usual Fox-Li modes of laser resonators [36]. In the coherent limit ($\sigma_g \gg \sigma_S$) the lowest eigenvalue $\lambda_0(\omega)$ is dominant, whereas in the other extreme ($\sigma_g \ll \sigma_S$) a great many modes contribute. The number of oscillating modes can be connected with the information content (degrees of freedom) carried by the beam [37].

The propagation of GSM fields can be studied on a mode-by-mode basis [35,42]. Besides extensions of the GSM models to the anisotropic sources and quite recently also to include certain coherence-induced twists (handedness) [38], another special case for which the coherent modes are explicitly known is the Bessel J_0-correlated Schell-model source [39]. The coherent modes associated with any (finite) Schell-model source have been proven to form a complete set [40], although generally they will have to be evaluated numerically. A considerable simplification, however, takes place in the homogeneous short-correlation limit in which the eigenmodes are normalized harmonic functions and the eigenvalues are samples from the spatial frequency spectrum of the cross-spectral density [41].

5. Determination of beam's transverse modes

Let us briefly consider the determination of the spatial modes associated with a partially coherent beam. The transverse mode structure can not be obtained from the planar intensity data alone, as is evidenced e.g. by the fact that the spectral intensity in Eqs. (27)–(29) is the same regardless of the coherence parameter σ_g. If the laser oscillates simultaneously in several transverse (and longitudinal) modes, the frequencies of each mode are slightly different. The spectral width of the beam is, however, usually so small that the detector integrates over all frequencies. Therefore the resulting cross-spectral density (or actually the mutual intensity) is as expressed by Eq. (23), with ω denoting the mean frequency and the coherent modes $\psi_n(\rho,\omega)$ being products of functions of the form of Eq. (30).

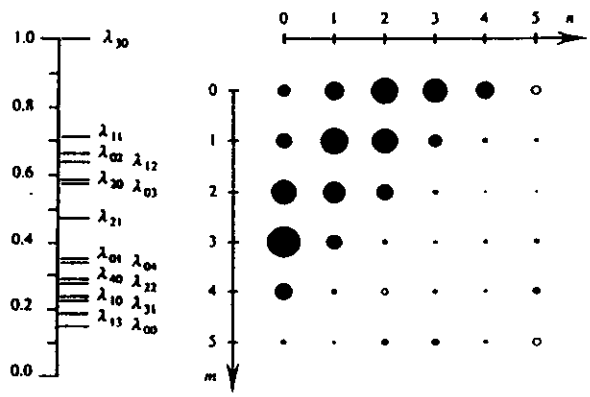

Figure 3. Graphical illustrations of the observed transverse mode eigenvalues. On left side: the normalized modal weights. On right side: the solid disk areas are proportional to modal weights, and hollow circles represent modes for which the calculated result was negative. Clearly the fundamental TEM_{00} mode is not dominant.

The spot sizes of all Hermite-Gaussian modes are the same. On propagation the spot size evolves as usual and the mode function also acquires the typical phase curvature, likewise the same for each mode. However, within the paraxial approximation the functions remain the coherent modes associated with the cross-spectral density [43]. So if we denote the eigenfunction (omitting the frequency ω for brevity)

across some plane z = constant by $\psi_n(\rho, z) = \phi_n(\rho, z)\exp[i\alpha_n(\rho, z)]$, where $\phi_n(\rho, z)$ and $\alpha_n(\rho, z)$ are real, the integral equation (24) evidently reduces to [44–46]

$$\int W_R(\rho_1, \rho_2; z)\phi_n(\rho_1, z)\mathrm{d}^2\rho_1 = \lambda_n\phi_n(\rho_2, z), \tag{32}$$

where $W_R(\rho_1, \rho_2; z)$ is as in Eq. (23) but contains only the weighted superpositions of the (amplitude) functions $\phi_n(\rho, z)$. This is now a central expression. If the function $W_R(\rho_1, \rho_2; z)$ is measured interferometrically, we could simply integrate Eq. (32) to find the eigenvalues λ_n. However, the problem is that we don't know the spot-size parameter w that is implicit in the eigenfunctions $\phi_n(\rho, z)$ [cf. Eq. (30)]. Therefore one must measure the real kernel $W_R(\rho_1, \rho_2; z)$ with respect to fixed points, at which the function $\phi_n(\rho, z)$ does not vanish. Then Eq. (32) can first be solved numerically for the spot size w, and once this is known the eigenvalues can be integrated straightforwardly. In numerical simulations the method proved amazingly stable, even in the presence of considerable noise [44].

In Fig. 3 we present experimental results obtained for a stable commercial multimode He-Ne laser (Siemens model LGK 7621 MM). The real spatial coherence kernel $W_R(\rho_1, \rho_2; z)$ was measured on a 20×20 grid using Young's interferometer with computer-controlled crossed-slit apertures. The possible sign changes of $W_R(\rho_1, \rho_2; z)$ can be observed from the phase jumps (by π radians) in the interference pattern. Several significant modes are found in a relatively symmetric pattern, with λ_{30} the strongest, in agreement with the observed increases in the far-field beam spread. Using the observed modes with significant amplitudes, the function $W_R(\rho_1, \rho_2; z)$ can be reconstructed numerically. In this manner, the calculated intensity and spatial coherence distributions are compared with the corresponding directly measured distributions and the results are in excellent agreement [45,46].

6. Beam synthesis and coherence control

In view of the van Cittert-Zernike theorem [11], the spatial coherence properties of a wave field can be modified simply through apertures and propagation [28,29], but the resulting beams usually are weak. Since also the coherent modes of optical fields are difficult to control, more efficient methods of beam synthesis have been developed. Gori and coworkers [47–49] express the GSM wave fields as incoherent superpositions of elliptical Gaussian component beams, which are spatially displaced and propagate parallel to each other. This technique has clarified greatly the directionality of partially coherent wave fields [48]. In another superposition method the component beams may occupy the same area in the waist plane, but they propagate in different directions [50]. This is a flexible method that can be implemented using synthetic acousto-optic holograms. Both superposition techniques can also be extended so as to produce the recent coherence-induced twists [38].

Consider, for example, an anisotropic GSM source of the type of Eqs. (27)–(29), with w_x and w_y being the spot sizes in the x and y directions, and similarly σ_x and σ_y being the orthogonal transverse coherence lengths. The decomposition of this field (at $z = 0$) by means of Gaussian beams propagating in different directions is of the form

$$W(\rho_1, \rho_2; 0) = \iint P(\theta_x, \theta_y)U^*(\rho_1; \theta_x, \theta_y)U(\rho_2; \theta_x, \theta_y)\mathrm{d}\theta_x\mathrm{d}\theta_y, \tag{33}$$

where

$$U(\rho; \theta_x, \theta_y) = \sqrt{S(\omega)}\exp(-x^2/w_x^2)\exp(-y^2/w_y^2)\exp(ik\theta_x x)\exp(ik\theta_y y), \tag{34}$$

$$P(\theta_x, \theta_y) = (2\pi)^{-1}k^2\sigma_x\sigma_y\exp[-(k\sigma_x)^2\theta_x^2/2]\exp[-(k\sigma_y)^2\theta_y^2/2], \tag{35}$$

as can be verified by direct integration (for paraxial fields the limits may formally be taken to infinity). Physically, the integration variables θ_x and θ_y give the deflection angles of the coherent (elliptic Gaussian) beam components.

The cross-spectral density $W(\rho_1, \rho_2; 0)$ in Eq. (33) can be efficiently generated with an experimental setup [50,51] shown in Fig. 4. An incident coherent Gaussian beam with the desired ellipticity (w_x, w_y) is

converted into a set of coherent, but mutually uncorrelated (because of Doppler shifts) Gaussian beams by a synthetic grating that propagates in the acousto-optic deflector (AO). To generate an approximate GSM beam, the envelope of the discrete set of beams (diffraction orders of the progressive grating) is made Gaussian by appropriately optimizing the grating profile. Thus a sampled version of the decomposition (33)–(35) is produced by two crossed deflectors. In practice, it is convenient to realize the acousto-optic grating in a hybrid form: A Raman-Nath regime grating (period Λ_H, generated by H) with a Gaussian power spectrum is used to phase modulate a sinusoidal Bragg-regime carrier grating (period $\Lambda_C \ll \Lambda_H$, generated by C) that deflects the incident beam by an angle $2\theta_B$ (where $\theta_B \approx \lambda/2\Lambda_C$). The phase-modulation grating, which carries the information, is analogous to the Dammann grating in optics and it is illustrated in Fig. 5. The partially coherent, modulated beam then propagates in the direction of the (negative) first diffraction order of the carrier grating.

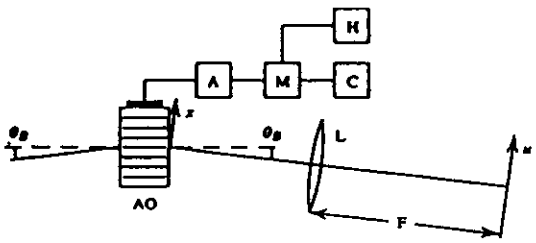

Figure 4. Experimental setup. AO = acousto-optic deflector, C = driver, H = information source, M = mixer, A = amplifier.

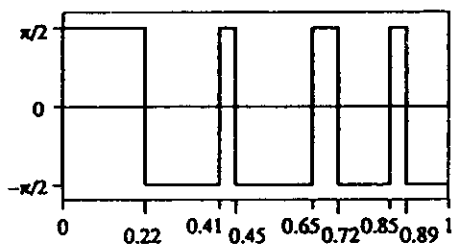

Figure 5. Phase profile of an optimized binary phase grating with approximately Gaussian power spectrum.

When the coherent Gaussian component beams propagate to the back focal plane of the Fourier-transforming lens L (focal length F), they each acquire a certain width $w_F = \lambda F/\pi w_0$ (where w_0 is the width at the deflector) and separation $u_0 = \lambda F/\Lambda_H$ between the adjacent beam centers. Two distinctly different modes of operation are now available. If $w_F \ll u_0$ (or equivalently $\pi w_0/\Lambda_H \gg 1$), the diffracted beams are well separated and one may speak of beam-splitting mode [52]. All individual beams are now fully coherent, but mutually uncorrelated. If, on the other hand, $w_F \gg u_0$, the beams will partially overlap and one is working in beam profile shaping mode. In this mode, the degree of spatial coherence within the superposition field can take a variety of different values and functional forms. In addition to the efficient GSM beam synthesis and control [50,51], potential applications include Gaussian to flat-top conversion [53]. If the optimized phase-grating data are stored in a computer, the intensity and coherence properties of the output beam can be reconfigured within the access time of the acousto-optic deflector.

7. GSM beams in optical systems

We shall return now to the GSM source (27)–(29) and analyze the evolution of the beam it generates in free space and through optical systems. On propagation from the source plane [i.e. the waist $z = 0$, at which $R(0) = \infty$] in accordance with Eq. (19) in free space (viz. $A = 1$, $B = z$, $C = 0$, and $D = 1$), the planar cross-spectral density associated with the wavefield is

$$\begin{aligned} W(\rho_1, \rho_2; z) &= S(\omega) w_S^2 w^{-2}(z) \exp[-(\rho_1^2 + \rho_2^2)/w^2(z)] \\ &\quad \times \exp[-(\rho_1 - \rho_2)^2/2\sigma^2(z)] \exp[-ik(\rho_1^2 - \rho_2^2)/2R(z)], \end{aligned} \tag{36}$$

where $w(z)$ is the beam's spot size, $R(z)$ is the radius of wavefront curvature, and $\sigma(z)$ is the transverse coherence length. If we define, as before, $\alpha = \sigma(z)/w(z)$ and $\beta = [1 + \alpha^{-2}]^{-1/2}$, then α and β are known to remain invariant for the GSM beams [23]. Therefore, the spot size and transverse coherence evolve in the same way and we may introduce a new quantity, called simply the beam parameter [54],

as $b(z) = \pi n w^2(z)\beta/\lambda$, where n is the refractive index and the coherence information is in β. With these definitions the GSM beam parameters obey in a homogeneous medium the propagation equations [54]

$$b(z) = b_0[1 + (z/b_0)^2], \tag{37}$$

$$R(z) = z[1 + (b_0/z)^2], \tag{38}$$

where $b_0 = \pi n w_S^2 \beta/\lambda$ is the beam parameter at the waist. These equations are seen to be highly analogous with those characterizing the usual Gaussian laser beam (limit $\sigma_g \to \infty$, or $\beta \to 1$).

Particularly important in the passage of GSM beams through symmetric ABCD systems is a quantity $q(z)$, known sometimes as the generalized complex ray. It is defined in terms of the real, coherence-dependent parameters $R(z)$ and $b(z)$ by the formula [54,55]

$$\frac{1}{q(z)} = \frac{1}{R(z)} - \frac{i}{b(z)}, \tag{39}$$

and it satisfies the extended Kogelnik's ABCD law

$$q_{out} = \frac{Aq_0 + B}{Cq_0 + D}, \tag{40}$$

proved e.g. by symmetry considerations [24], by induction [55], and also explicitly (for arbitrary input parameters) using the cascaded Fresnel diffraction integral (19) [56]. The transformation law (40) implies that a GSM beam remains a GSM beam in optical systems, only the parameters describing it vary.

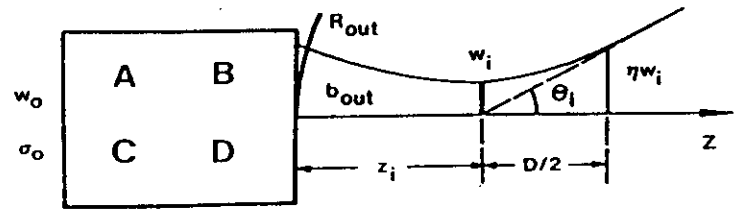

Figure 6. Observable quantities associated with a GSM beam emerging from an arbitrary ABCD system.

On exit the GSM beam forms a waist at some distance z_i (positive when converging) from the system (see Fig. 6). Without any loss of generality, we may in analysis extend the ABCD system to begin from the input beam waist. Separating the real and imaginary parts of Eq. (40) and using Eq. (39), one first finds expressions for the output beam parameters R_{out} and b_{out} and these be inverted to yield z_i and the waist parameter b_i. Expressed in terms of the matrix elements A, B, C, and D, the results are [54–56]

$$z_i = -\frac{A^2 + B^2 b_0^{-2}}{AC + BDb_0^{-2} + (ACb_0^2 + BD)^{-1}}, \tag{41}$$

$$m^2 = \frac{A^2 + B^2 b_0^{-2}}{1 + (ACb_0 + BDb_0^{-1})^2}, \tag{42}$$

where in the latter formula we have introduced $m = \sqrt{b_i/b_0} = w_i/w_0$ as the image magnification. The other observable quantities of interest in the exit beam waist region are

$$\sigma_i = m\sigma_0, \tag{43}$$

$$D = 2m^2 b_0 \sqrt{\eta^2 - 1}, \tag{44}$$

$$\Theta_i = \arctan(\lambda/\pi n m w_0 \beta), \tag{45}$$

where σ_i is the image coherence width, D is the depth of focus (defined as twice the distance in which the beam expands from w_i to $\eta\, w_i$), and Θ_i is the usual far-field diffraction angle. Equations (41)–(45) provide a complete description of the GSM beam passage through symmetric paraxial systems.

Several consequences and extensions are of interest. It follows from Eqs. (41)–(45) that the quantities z_i, m, and D depend only on b_0 (i.e. on $\pi n w_0^2 \beta/\lambda$), whereas the quantities w_i, σ_i, and Θ_i depend also on w_0 and σ_0. An obvious generalization to an anisotropic case then shows, for example, that an elliptic GSM beam for which $w^2\beta/\lambda$ is the same in both orthogonal directions, retains its shape in a symmetric optical system [49,56]. Various equivalence relations are similarly obtained e.g. for the far-field radiation using Eqs. (42) and (45). Evidently in nondispersive (color-corrected) optical systems the coherence dependence can be compensated by scaling the wavelength as λ/β. The coherent case ($\beta = 1$) corresponds to a Gaussian laser, while in the incoherent limit ($\beta \to 0$) we obtain $b_0 \to 0$ and Eqs. (41) and (42) reduce to $z_i \to -B/D$ and $|m| \to 1/|D|$. These expressions correspond exactly to the geometrical-optics results for an ensemble of radiating point sources, distributed according to a Gaussian weight function. In the asymptotic limit as $\lambda \to 0$ (with α and β fixed) we have $b_0 \to \infty$, and Eqs. (41) and (42) yield $z_i \to -A/C$ and $|m| \to 0$. These expressions represent a point image in the system backfocal plane, i.e. the GSM beam behaves as an infinite plane wave [56].

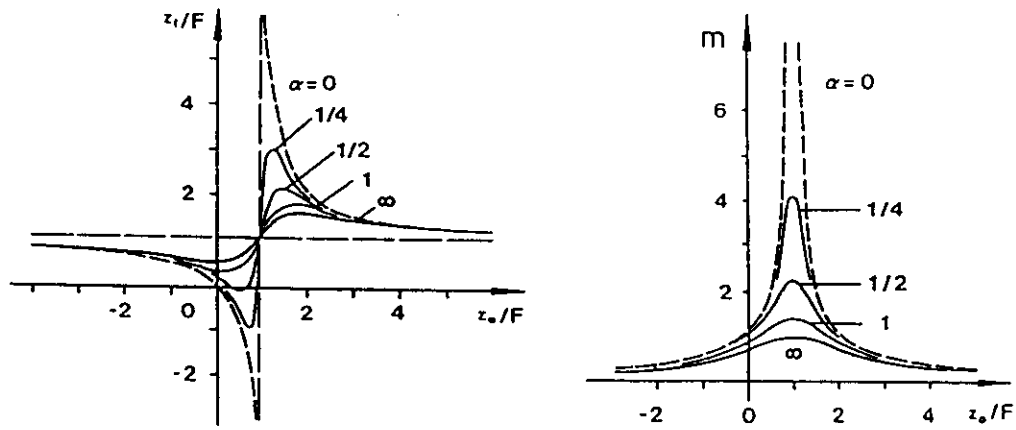

Figure 7. Dependence of the thin-lens image location z_1/F (left) and magnification m (right) on the incident GSM beam waist distance z_0/F and the spatial coherence parameter α.

As an important example we consider a thin lens of focal length F, placed at a distance z_0 from the GSM input beam waist. On substituting the ABCD matrix elements in Eqs. (41) and (42), we find after considerable algebra the following coherence-dependent thin-lens imaging equations [54,55]:

$$\frac{1}{z_i} = \frac{1}{F} - \frac{1}{z_0 + b_0^2/(z_0 - F)}, \tag{46}$$

$$m = \left[\left(1 - \frac{z_0}{F}\right)^2 + \left(\frac{b_0}{F}\right)^2\right]^{-1/2}. \tag{47}$$

Once the magnification is known, the other quantities are obtained from Eqs. (43)–(45). The results (46) and (47) are illustrated in Fig. 7 for several values of the global degree of coherence $\alpha = \sigma_0/w_0$, while keeping w_0 and λ fixed ($\pi w_0^2/\lambda F = 1$). It is seen that the magnification increases as the spatial coherence is reduced, and the image beam waist moves closer to the position predicted by geometrical optics (set $b_0 = 0$). The difference between the geometrical-optics and the actual image locations is known as the focus shift, usually large in low Fresnel-number optical systems. The coherence-induced variations in the GSM beam image size and position have been verified experimentally [57], and these phenomena obviously affect e.g. the transverse coupling of partially coherent beams into optical fibers.

8. Propagation-invariant partially coherent beams

It has been pointed out [58,59] that there exist exact free-space solutions of the Helmholtz equation, which are propagation-invariant in the sense that the spectral intensity distribution $S(\rho, z)$ is independent of the axial coordinate z. These solutions differ from the usual shape-invariant optical fields such as laser beams in that also the transverse scale of $S(\rho, z)$ is z-independent. Thus these solutions, which are characterized by the fact that they consist entirely of plane-wave components that propagate along the surface of a cone, have been called diffraction-free beams (or conical fields). Such a term is somewhat misleading since these wave fields are not really beams at all in the traditional sense (consider the power flow) but rather interference patterns, and because all these solutions contain an infinite amount of energy, which is indeed a necessary condition for exact propagation invariance. Nevertheless, practical finite-aperture approximations of such beams are efficiently generated e.g. by computer holography and they are of considerable interest, for example, in metrology and precision alignment. The simplest diffraction-free beam, and the only rotationally symmetric one, is the classic (lowest-order) Bessel beam $S(\rho, z) = J_0^2(\alpha\rho)$, where α is a parameter such that $0 \leq \alpha \leq k$ (this α is not to be confused with the coherence degree). The Bessel beam has a narrow central maximum (half-width $\rho_{\mathrm{HW}} \approx \alpha^{-1}$), which retains its shape over an appreciable distance ($z_{\max} \approx 2\pi R\rho_{\mathrm{HW}}/\lambda$, if the radius of the aperture is R).

In partially coherent optics we consider the cross-spectral density function $W(\mathbf{r}_1, \mathbf{r}_2)$ that obeys the coupled Helmholtz equations (18). We take the requirement for the propagation invariance to be

$$W(\rho_1, \rho_2; z) = W(\rho_1, \rho_2; 0) \tag{48}$$

for all $z \geq 0$ [60]. This requirement poses an invariance condition on both the transverse intensity and the transverse spatial coherence. On expanding the cross-spectral density in the form of a double angular spectrum representation, expressing it in polar coordinates, and further requiring that the condition (48) be satisfied, one can show that the angular correlations between all plane-wave components must necessarily vanish in the radial direction; this condition may, in fact, be considered as the defining property of the partially coherent propagation-invariant fields. Making use of this result the general expression for the propagation-invariant partially coherent beams then is [60]

$$\begin{aligned} W(\mathbf{r}_1, \mathbf{r}_2) \;=\; & \int_0^{k/2\pi} \iint_0^{2\pi} f^2 S(f, \theta_1, \theta_2) \exp\{i(z_2 - z_1)[k^2 - (2\pi f)^2]^{1/2}\} \\ & \times \exp[i2\pi f(x_2 \cos\theta_2 - x_1 \cos\theta_1 + y_2 \sin\theta_2 - y_1 \sin\theta_1)] \mathrm{d}f \mathrm{d}\theta_1 \mathrm{d}\theta_2, \end{aligned} \tag{49}$$

where $S(f, \theta_1, \theta_2)$ is an arbitrary function and the upper limit of the f-integration has been set to exclude the evanescent waves that cannot satisfy the invariance requirement.

Besides the coherent diffraction-free fields, the general expression (49) has a number of interesting special cases. If we assume that the angular correlations between the plane-wave components vanish also in the azimuthal direction, and moreover, that the angular spectrum is nonzero and of constant strength on a single radial ring only, the general propagation-invariant beam formula reduces to the Bessel-correlated field

$$W(\mathbf{r}_1, \mathbf{r}_2) = S_0 \exp[i\beta(z_2 - z_1)] J_0[\alpha|\rho_1 - \rho_2|], \tag{50}$$

where S_0 = constant and $\alpha^2 + \beta^2 = k^2$. This wavefield is of a uniform intensity but it has a sharply peaked, invariant transverse coherence distribution; it can be viewed as the counterpart of the coherent Bessel beam in variable-coherence optics. Incidentally, this particular wave solution happens to be one of the few fields for which the coherent modes of the cross-spectral density are known explicitly [39]. Propagation-invariant wavefields that possess rapidly varying profiles of both the spectral intensity and the spatial coherence also exist [60]. Such fields, and the more general self-imaging wavefields, constitute the partially coherent modes of a planar Fabry-Perot resonator [61]. Finally we note that the exact partially coherent propagation-invariant field (49) satisfies, in a plane-to-plane propagation, remarkably also the corresponding (single) paraxial propagation equation for the planar cross-spectral density $W(\rho_1, \rho_2; z)$ [62]. The wavefield remains shape-invariant in all lossless ABCD systems, but the property of strict propagation invariance is conserved only if the system is afocal.

9. Conclusions

We have demonstrated that optical coherence manifests itself differently in the different domains. The concepts associated with spectral (spatial) coherence are relatively new. The spatial coherence properties of confined optical beams can be analyzed mathematically and experimentally, and directional beams of this type can be produced efficiently in practice with any desired spectral intensity and coherence profiles. The coherence properties were shown to modify the beam evolution characteristics, both in the context of passage through optical systems (focused waves) and with invariant fields. Partially coherent sources and the beam-like fields they radiate have in the recent past also contributed to a variety of other topics, including spectral radiometry and radiative transfer [38] as well as correlation-induced spectral shifts and partially coherent spectroscopy [63].

Acknowledgements

The author is a Senior Fellow with the Academy of Finland. Collaboration in many parts of this research with J. Turunen and E. Tervonen is gratefully acknowledged. Thanks are owed also to M. Kaivola and S. Yu. Popov for assistance.

References

[1] M. Born and E. Wolf, *Principles of Optics*, 5th ed. (Pergamon, Oxford, 1975), Chap. 10.

[2] L. Mandel and E. Wolf, "Coherence properties of optical fields", *Rev. Mod. Phys.* 37, 231–287 (1965).

[3] M.J. Beran and G.B. Parrent, Jr., *Theory of Partial Coherence* (Prentice-Hall, Englewood Cliffs, NJ, 1964), Chap. 4.

[4] J. Perina, *Coherence of Light*, 2nd ed. (D. Reidel Publ. Co., Dordrecht, Holland, 1985).

[5] L. Mandel and E. Wolf, "Spectral coherence and the concept of cross-spectral purity", *J. Opt. Soc. Am.* 66, 529–535 (1976).

[6] L. Mandel and E. Wolf, "Complete coherence in the space-frequency domain", *Opt. Commun.* 36, 247–249 (1981).

[7] M.J. Bastiaans, "A frequency-domain treatment of partial coherence", *Optica Acta* 24, 261–274 (1977).

[8] E. Wolf, "Young's interference fringes with narrow-band light", *Opt. Lett.* 8, 250–252 (1983).

[9] W.H. Carter and E. Wolf, "Coherence properties of lambertian and non-lambertian sources", *J. Opt. Soc. Am.* 65, 1067–1071 (1975).

[10] R.W. Boyd, *Radiometry and the Detection of Optical Radiation* (Wiley, New York, 1983), Chap. 4.

[11] E. Wolf, "Coherence and radiometry", *J. Opt. Soc. Am.* 68, 6–17 (1978).

[12] H.P. Baltes, "Coherence and the radiation laws", *Appl. Phys.* 12, 221–244 (1977)

[13] G.C. Sherman, "Introduction to the angular-spectrum representation of optical fields", in *Applications of Mathematics in Modern Optics*, ed. W.H. Carter, *Proc. SPIE* 358, 31–38 (1982).

[14] A.E. Siegman, *Lasers* (University Science Books, Mill Valley, CA, 1986), Chap. 15.

[15] E.C.G. Sudarshan, "Quantum theory of partial coherence", *J. Math. Phys. Sci.* 3, 121–175 (1969).

[16] E. Wolf and A.J. Devaney, "On a relationship between spectral properties and spatial coherence properties of light", *Opt. Lett.* 6, 168–170 (1981).

[17] D.F.V. James, "Polarization of light radiated by black-body sources", *Opt. Commun.* (in press, 1994).

[18] E. Wolf, "A new description of second-order coherence phenomena in the space-frequency domain", in *Optics in Four Dimensions — 1980*, eds. M.A. Machado and L.M. Narducci (American Institute of Physics, New York, 1981), Conference proceedings No. 65, pp. 42–48.

[19] E. Wolf, "New spectral representation of random sources and of the partially coherent fields that they generate", *Opt. Commun.* 38, 3–6 (1981).

[20] E. Wolf, "New theory of partial coherence in the space-frequency domain. Part I: Spectra and cross spectra of steady-state sources", *J. Opt. Soc. Am.* 72, 343–351 (1982); "Part II: Steady-state fields and higher-order correlations", *J. Opt. Soc. Am. A* 3, 76–85 (1986).

[21] G.S. Agarwal and E. Wolf, "Higher-order coherence functions in the space-frequency domain", *J. Mod. Opt.* 40, 1489–1496 (1993).

[22] J.T. Foley and M.S. Zubairy, "The directionality of gaussian Schell-model beams", *Opt. Commun.* 26, 297–300 (1978).

[23] A.T. Friberg and R.J. Sudol, "Propagation parameters of gaussian Schell-model beams", *Opt. Commun.* 41, 383–387 (1982); "The spatial coherence properties of Gaussian Schell-model beams", *Optica Acta* 30, 1075–1097 (1983).

[24] R. Simon, E.C.G. Sudarshan, and N. Mukunda, "Generalized rays in first-order optics: Transformation properties of Gaussian Schell-model fields", *Phys. Rev. A* 29, 3273–3279 (1984); "Partially coherent beams and a generalized ABCD-law", *Opt. Commun.* 65, 322–328 (1988).

[25] S. Lavi, R. Prochaska, and E. Keren, "Generalized beam parameters and transformation laws for partially coherent light", *Appl. Opt.* 27, 3696–3703 (1988).

[26] R. Gase, "The multimode laser radiation as a Gaussian Schell model beam", *J. Mod. Opt.* 38, 1107–1115 (1991).

[27] J. Serna, P.M. Mejias, and R. Martinez-Herrero, "Beam quality dependence on the coherence length of Gaussian Schell-model fields propagating through ABCD optical systems", *J. Mod. Opt.* 39, 625–635 (1992).

[28] P. DeSantis, F. Gori, G. Guattari, and C. Palma, "An example of a Collett-Wolf source", *Opt. Commun.* 29, 256–260 (1979).

[29] J. Deschamps, D. Courjon, and J. Bulabois, "Gaussian Schell-model sources: an example and some perspectives", *J. Opt. Soc. Am.* 73, 256–261 (1983).

[30] A. Gamliel and G.P. Agrawal, "Spectrum-enhanced spreading of partially coherent beams", *Opt. Commun.* 78, 203–207, (1990).

[31] W.H. Carter and E. Wolf, "Coherence and radiometry with quasihomogeneous planar sources", *J. Opt. Soc. Am.* 67, 785–796 (1977).

[32] Y. Li and E. Wolf, "Radiation from anisotropic Gaussian Schell-model sources", *Opt. Lett.* 7, 256–268 (1982).

[33] P. DeSantis, F. Gori, G. Guattari, and C. Palma, "Anisotropic Gaussian Schell-model sources", *Optica Acta* 33, 315–326 (1986).

[34] F. Gori, "Collett-Wolf sources and multimode lasers", *Opt. Commun.* 34, 301–305 (1980).

[35] A. Starikov and E. Wolf, "Coherent-mode representation of Gaussian Schell-model sources and of their radiation fields", *J. Opt. Soc. A.* 72, 923–928 (1982).

[36] E. Wolf and G.S. Agarwal, "Coherence theory of laser resonator modes", *J. Opt. Soc. Am. A* 1, 541–546 (1984).

[37] A. Starikov, "Effective number of degrees of freedom of partially coherent sources", *J. Opt. Soc. Am.* 72, 1538–1544 (1982).

[38] For the effects of coherence twists, see e.g. A.T. Friberg, "On the generalized radiometry of twisted Gaussian Schell-model sources and fields", (in this Proceedings).

[39] F. Gori, G. Guattari, and C. Pavadoni, "Modal expansion of J_0-correlated Schell-model sources", *Opt. Commun.* 64, 311–316 (1987).

[40] E. Wolf, "Completeness of coherent-mode eigenfunctions of Schell-model sources", *Opt. Lett.* 9, 387–389 (1984).

[41] A. Starikov and A.T. Friberg, "One-dimensional Lambertian sources and the associated coherent-mode representation", *Appl. Opt.* **23**, 4261–4268 (1984).

[42] F. Gori, "Mode propagation of the field generated by Collett-Wolf Schell-model sources", *Opt. Commun.* **46**, 149–154 (1983).

[43] E. Wolf, "Coherent-mode propagation in spatially band-limited wave fields", *Opt. Lett.* **3**, 1920–1924 (1986).

[44] J. Turunen, E. Tervonen, and A.T. Friberg, "Coherence-theoretic algorithm to determine the transverse-mode structure of lasers", *Opt. Lett.* **14**, 627–629 (1989).

[45] E. Tervonen, J. Turunen, and A.T. Friberg, "Transverse laser-mode structure determination from spatial coherence measurements: Experimental results", *Appl. Phys. B* **49**, 409–414 (1989).

[46] E. Tervonen, J. Turunen, and A.T. Friberg, "Transverse mode structure of laser beams determined from spatial coherence", in *Coherence and Quantum Optics VI*, eds. J.H. Eberly, L. Mandel, and E. Wolf (Plenum, New York, 1989), pp. 1141–1145.

[47] F. Gori and C. Palma, "Partially coherent sources which give rise to highly directional light beams", *Opt. Commun.* **27**, 185–188 (1978).

[48] F. Gori, "Directionality and optical coherence", *Optica Acta* **27**, 1025–1034 (1980).

[49] F. Gori and G. Guattari, "A new type of optical fields", *Opt. Commun.* **48**, 7–12 (1983).

[50] J. Turunen, E. Tervonen, and A.T. Friberg, "Acousto-optic control and modulation of optical coherence by electronically synthesized holographic gratings", *J. Appl. Phys.* **76**, 49–59 (1990).

[51] E. Tervonen, A.T. Friberg, and J. Turunen, "Gaussian Schell-model beams generated with synthetic acousto-optic holograms", *J. Opt. Soc. Am. A* **9**, 796–803 (1991).

[52] E. Tervonen, A.T. Friberg, J. Westerholm, J. Turunen, and M.R. Taghizadeh, "Programmable optical interconnections by multilevel synthetic acousto-optic holograms", *Opt. Lett.* **16**, 1274–1276 (1991).

[53] E. Tervonen, A.T. Friberg, and J. Turunen, "Acousto-optic conversion of laser beams into flat-top beams", *J. Mod. Opt.* **40**, 625–635 (1993).

[54] J. Turunen and A.T. Friberg, "Matrix representation of Gaussian Schell-model beams in optical systems", *Opt. Laser Technol.* **18**, 259–267 (1986).

[55] J. Turunen and A.T. Friberg, "Propagation of Gaussian Schell-model beams: A matrix method", in *Optical System Design, Analysis, and Production for Advanced Technology Systems*, eds. R.E. Fischer and P.J. Rogers, *Proc. SPIE* **655**, 60–66 (1986).

[56] A.T. Friberg and J. Turunen, "Imaging of Gaussian Schell-model sources", *J. Opt. Soc. Am. A* **5**, 713–720 (1988).

[57] Q. He, J. Turunen, and A.T. Friberg, "Propagation and imaging experiments with Gaussian Schell-model beams", *Opt. Commun.* **67**, 245–250 (1988).

[58] J. Durnin, "Exact solutions for nondiffracting beams. I. The scalar theory", *J. Opt. Soc. Am. A* **4**, 651–654 (1987).

[59] J. Durnin, J.J. Miceli, Jr., and J.H. Eberly, "Diffraction-free beams", *Phys. Rev. Lett.* **58**, 1499–1501 (1987).

[60] J. Turunen, A. Vasara, and A.T. Friberg, "Propagation invariance and self-imaging in variable-coherence optics", *J. Opt. Soc. Am. A* **8**, 282–289 (1990).

[61] A.T. Friberg and J. Turunen, "Spatially partially coherent Fabry-Perot modes", *J. Opt. Soc. Am. A* **11**, 227–235 (1994).

[62] A.T. Friberg, A. Vasara, and J. Turunen, "Partially coherent propagation-invariant beams: Passage through paraxial optical systems", *Phys. Rev. A* **43**, 7079–7082 (1991).

[63] E. Wolf, "Influence of source correlations on spectra of radiated fields", in *International Trends in Optics*, ed. J.W. Goodman (Academic Press, New York, 1991), pp. 221–232.

Proceedings of the

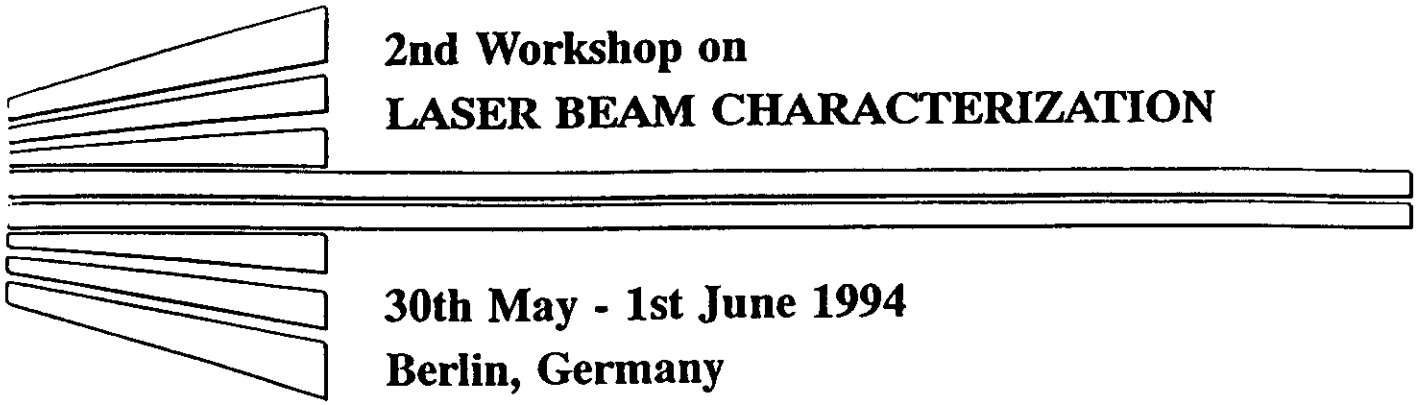

2nd Workshop on
LASER BEAM CHARACTERIZATION

30th May - 1st June 1994
Berlin, Germany

Editors:
H. Weber, N. Reng, J. Lüdtke, P. M. Mejías

This workshop was funded by the German Ministry of Research and Technology (BMFT).

ON THE GENERALIZED RADIOMETRY OF TWISTED GAUSSIAN SCHELL-MODEL SOURCES AND FIELDS

Ari T. Friberg

Department of Technical Physics, Helsinki University of Technology
Rakentajanaukio 2C, FIN-02150 Espoo, Finland

Abstract

A coherence-dependent twist phase alters the propagation of Gaussian Schell-model beams in free space and in optical systems. The modifications implied by this twist effect onto the generalized radiometric description of the planar Gaussian Schell-model sources and the fields they generate are discussed.

1. Introduction

It was recently shown [1] that partially coherent beam fields in rotationally symmetric optical systems allow a spectral, position-dependent phase that rotates the beam on propagation. This novel twist phase (handedness) has several remarkable properties that distinguish it from the customary phase curvature. For example, because of the non-negative definiteness of the cross-spectral density, the twist phase is bounded from above and it disappears in the limit of full spatial coherence (corresponding to usual lasers). Besides rotating the beam, the twist phase can further be viewed as decreasing the 'effective' degree of spatial coherence associated with the wave field. In free space this phenomenon obviously manifests itself in increased diffractive spreading, while in first-order systems it is expected to modify the various coherence-dependent propagation effects. For these reasons it appears natural to ask as to what are the effects of the additional coherence twist phase on the radiometric properties of the Gaussian Schell-model (GSM) sources and the fields they produce. This is the topic of the present paper.

After reviewing briefly the main characteristics and an experimental implementation to generate the twisted Gaussian Schell-model (TGSM) beams in free space, the exact radiant intensity produced by the planar TGSM sources is evaluated. The associated radiation efficiency and some physical twist-induced consequences of these results are discussed. The twist phase naturally also alters the source's generalized radiance and generalized radiant emittance, as well as the far-field spatial coherence as expressed by the extended van Cittert-Zernike theorem. Making use of the ABCD-matrix formalism the evolution of the TGSM beams can be analyzed in paraxial optical systems, and some twist-induced effects such as focus shift and changes in magnification have been observed. Certain propagation invariance theorems in passage through first-order systems can also be derived for the main definitions of the generalized radiance. The properties of the generalized radiance and some implications of these radiance (brightness) invariance laws e.g. in relation to the beam rotation are elucidated.

2. Twisted Gaussian Schell-model beams

Let us first recall the main properties of the twisted Gaussian Schell-model beams using the notation that has been applied when studying the paraxial wave propagation [1,2]. Across any plane z = constant the cross-spectral density [3] (at a frequency ω which is not shown) of a TGSM beam is

$$\begin{aligned} W(\rho_1,\rho_2;z) &= S_0 w^{-2}(z)\exp[-(\rho_1^2+\rho_2^2)/w^2(z)]\exp[-(\rho_1-\rho_2)^2/2\sigma^2(z)] \\ &\quad\times\exp[-ik(\rho_1^2-\rho_2^2)/R(z)]\exp[-ik\rho_1\cdot\epsilon\rho_2 u(z)], \end{aligned} \tag{1}$$

where S_0 is a positive constant (proportional to the on-axis spectrum), $\rho=(x,y)$ is a two-dimensional (column) vector, $k=\omega/c$ is the free-space wave number (c is the speed of light), and ϵ is an antisymmetric 2×2 matrix such that $\rho_1\cdot\epsilon\rho_2 = x_1y_2 - x_2y_1$. The real functions $w(z)$, $\sigma(z)$, $R(z)$, and $u(z)$ in Eq. (1) are

the beam's spot size, transverse coherence length, radius of wavefront curvature, and twist parameter, respectively. For a compact description of the evolution of these parameters in free space we need two propagation-invariant quantities, viz.

$$\beta = \{1 + [w(z)/\sigma(z)]^2\}^{-1/2}, \tag{2}$$

$$\eta = k\sigma^2(z)u(z), \tag{3}$$

of which the (usual) spatial coherence parameter β is obviously normalized between 0 (incoherent limit) and 1 (coherent limit). The (new) twist parameter η, on the other hand, is bounded [1] in such a way that $-1 \leq \eta \leq 1$; in view of Eq. (3) $\eta = 0$ corresponds to $u(z) = 0$ (no twist), while $|\eta| = 1$ represents the case of maximum (left-hand or right-hand) twist.

Taking the beam waist to be located in the plane $z = 0$ the four TGSM beam parameters obey, within the accuracy of the paraxial approximation (i.e. Fresnel diffraction), the free-space propagation laws

$$w(z) = w(0)[1 + (z/z_R)^2]^{1/2}, \tag{4}$$

$$\sigma(z) = \sigma(0)[1 + (z/z_R)^2]^{1/2}, \tag{5}$$

$$R(z) = z[1 + (z_R/z)^2], \tag{6}$$

$$u(z) = u(0)[1 + (z/z_R)^2]^{-1}, \tag{7}$$

where

$$z_R = \frac{\pi w^2(0)}{\lambda}\beta\left[1 + \eta^2\left(\frac{1-\beta^2}{2\beta}\right)^2\right]^{-1/2} \tag{8}$$

is the Rayleigh range of the TGSM beam ($\lambda = 2\pi/k$ is the wavelength). A measurement of the intensity distribution across any plane z = constant gives the spot size $w(z)$ but does not by itself reveal the presence of the twist. However, the influence of the twist is naturally indirectly included in the spot size through the η-dependence of the Rayleigh range. Calculation of the far-field diffraction angle from Eqs. (4) and (8) yields

$$\theta_d \approx \tan\theta_d = \lim_{z\to\infty} w(z)/z = \frac{\lambda}{\pi w(0)\beta}\left[1 + \eta^2\left(\frac{1-\beta^2}{2\beta}\right)^2\right]^{1/2}, \tag{9}$$

and we see that the beam spreading increases when the twist parameter $|\eta|$ increases.

The other characteristic effect of the twist, namely the beam rotation, cannot obviously be seen in a rotationally symmetric field but it can be demonstrated by suitable decompositions of the beam. Twisted GSM beams have been produced by passing a partially coherent, elliptic GSM beam field through a certain astigmatic lens system [2]. The unisotropic input field can be decomposed (exactly) into an integral of overlapping, mutually uncorrelated, Gaussian beams propagating in different directions, with a weighting function that is also a Gaussian. A sampled approximation of this superposition is efficiently generated using the acousto-optic coherence control technique [4], whereby a high-frequency Bragg carrier wave in an acousto-optic deflector is modulated with an optimized Raman-Nath grating (analogous to a synthetic hologram). The astigmatic lens consists of two groups of three cylindrical lenses, with each group performing imaging in one coordinate and Fourier transformation in the orthogonal coordinate (see Fig. 1). The focal lengths satisfy $f_x = 2f_y$, and the Rayleigh ranges z_R associated with both orthogonal coordinates of the elliptic input beam [cf. Eq. (8) with $\eta = 0$] are equal to f_x. When the latter lens group is rotated about the z-axis by 45 degrees with respect to the former group, the entire optical system converts the elliptic GSM beam into a rotationally symmetric twisted GSM beam.

If the elliptic GSM input beam is coherent in one direction while partially coherent in the other direction, a maximum degree of twist ($|\eta| = 1$) is obtained. Twisted GSM beams corresponding to this

situation have been produced and the rotation of the individual elliptic Gaussian component beams has been demonstrated experimentally and by simulation [2]. In free space the beam rotation reaches $\pi/4$ at $z = z_R$ and approaches $\pi/2$ in the far zone. Measurements of the TGSM beam spot-size evolution are presented in Fig. 2 as a function of the propagation distance from the waist, with $w(0) = 0.62$ mm, $\beta = 0.29$, and $\eta = -1$. The calculated theoretical TGSM beam profile, as well as the profiles for the corresponding ordinary GSM beam ($\eta = 0$) and coherent laser beam ($\beta = 1$) are shown for comparison.

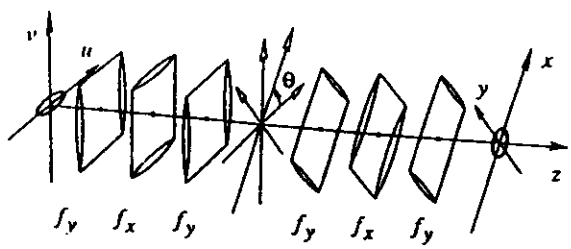

Figure 1. Illustration of an astigmatic lens system that converts an elliptic GSM input beam into a symmetric twisted GSM beam.

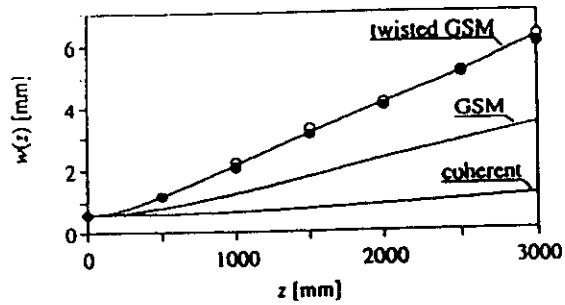

Figure 2. Measured TGSM beam spot sizes, compared with divergence of TGSM, ordinary GSM, and Gaussian laser beams.

We note that an analogous, although apparently different, practical superposition model of TGSM beams has been suggested and analyzed [5]. This model is expressed in terms of displaced and suitably inclined ordinary Gaussian beams, and it clarifies considerably the main physical properties of the twisted GSM beams. The mathematical coherent-mode decomposition associated with the cross-spectral density function (1) of TGSM beams has also been found [6], but it is not known how these modes could be realized in practice.

3. Radiometry of planar TGSM sources

Up to this point the discussion concerns only the twisted GSM wave fields in the paraxial approximation. In view of the observed phenomena it is of interest to analyze the situation in terms of the generalized radiometric theory that deals with energy-related quantities. We begin by considering the radiometry of planar TGSM sources using exact (i.e. non-paraxial) field propagation.

The main (observable) quantity associated with any fluctuating source is the radiant intensity $J(\mathbf{s})$, which is defined as the rate of energy (at frequency ω) emitted by the source per unit solid angle about the direction $\mathbf{s}$. For planar sources (located at $z = 0$) it can be expressed as [7,8]

$$J(\mathbf{s}) = (2\pi k)^2 \cos^2\theta\, \tilde{W}(-k\mathbf{s}_\perp, k\mathbf{s}_\perp; 0), \tag{10}$$

where $\mathbf{s}_\perp$ is the two-dimensional projection of the unit vector $\mathbf{s}$ onto the plane $z = 0$, i.e. $\mathbf{s} = (\mathbf{s}_\perp, s_z)$ with $s_z = \cos\theta$, and

$$\tilde{W}(\mathbf{f}_1, \mathbf{f}_2; 0) = (2\pi)^{-4} \iint W(\rho_1, \rho_2; 0) \exp[-i(\mathbf{f}_1 \cdot \rho_1 + \mathbf{f}_2 \cdot \rho_2)] \mathrm{d}^2\rho_1 \mathrm{d}^2\rho_2 \tag{11}$$

is the four-dimensional spatial Fourier transformation of the cross-spectral density function associated with the source. For a twisted GSM planar source the cross-spectral density is, from Eq. (1), given by the formula

$$W(\rho_1, \rho_2; 0) = W_0 \exp[-(\rho_1^2 + \rho_2^2)/2\sigma_S^2] \exp[-(\rho_1 - \rho_2)^2/2\sigma_g^2] \exp[-iku\rho_1 \cdot \epsilon\rho_2], \tag{12}$$

where we have introduced the abbreviations $W_0 = S_0/w^2(0)$, $\sigma_S = w(0)/2$, $\sigma_g = \sigma(0)$, and $u = u(0)$, and noted the fact that $R(0) = \infty$ [cf. Eq. (6)]. Making use of the identities $\rho \cdot \epsilon\rho = 0$, $\epsilon\rho \cdot \epsilon\rho = \rho^2$, and $s_\perp \cdot \epsilon\rho = -\epsilon s_\perp \cdot \rho$, as well as the integral [9]

$$\int_0^\infty e^{-qx^2} dx = \frac{1}{2}\sqrt{\frac{\pi}{q}}, \qquad (q > 0), \tag{13}$$

we find first, on substituting from Eq. (12) into Eq. (11), after considerable algebra that

$$\tilde{W}(-ks_\perp, ks_\perp; 0) = \frac{W_0}{(2\pi)^2[(4\sigma_S^4)^{-1} + (\sigma_S^2\sigma_g^2)^{-1} + k^2u^2]} \times \exp\left\{-\frac{k^2 s_\perp^2}{2\sigma_S^2[(4\sigma_S^4)^{-1} + (\sigma_S^2\sigma_g^2)^{-1} + k^2u^2]}\right\}. \tag{14}$$

Since the radiant intensity produced by a planar TGSM source is rotationally symmetric, we may then express $J(s)$ from Eqs. (10) and (14) in the form

$$J(\theta) = J(0)\cos^2\theta \exp(-\xi^2 \sin^2\theta), \tag{15}$$

$$J(0) = W_0(2\sigma_S^2)\xi^2, \tag{16}$$

where we have defined (with some foresight about the radiation efficiency) the quantity

$$\xi^2 = [1/2(k\sigma_S)^2 + 2/(k\sigma_g)^2 + 2(\sigma_S u)^2]^{-1}. \tag{17}$$

As anticipated in the introduction, the angular distribution of the radiant intensity depends also on the twist parameter u associated with the source. In the limit as $u \to 0$ (i.e. when the twist disappears), the result (15)–(17) reduces to that obtained before for the usual GSM sources [10].

If the radiation is confined (as a result of the parameter ξ) to small angles such that $\cos\theta \approx 1$ and $\sin\theta \approx \theta$, the exact radiant intensity (15) leads to the far-field diffraction angle (e^{-2} half-width)

$$\theta_d \approx \sqrt{2}(1/\xi), \tag{18}$$

which can be shown to be identical with that given by Eq. (9) for the twisted GSM beam-like fields. The proof is greatly facilitated by noting that $\xi = \sqrt{2}\, k\sigma_S\beta_{\text{eff}}$, i.e. the inclusion of the twist phenomenon in the GSM sources can be effected, as suggested by Eq. (8), by replacing the 'ordinary' coherence parameter β with the 'effective' coherence parameter β_{eff} according to

$$\beta \to \beta_{\text{eff}} = \beta\left[1 + \eta^2\left(\frac{1-\beta^2}{2\beta}\right)^2\right]^{-1/2}, \tag{19}$$

where β and η have been introduced in Eqs. (2) and (3), respectively.

Both the lack of full spatial coherence and the generation of evanescent waves are known to influence the amount of power radiated by optical sources. The radiation efficiency of a planar source of any state of coherence is defined as the ratio of the total hemispherical radiated power (flux) to the source-integrated spectral intensity (spectrum), i.e. [11]

$$C = \Phi/N, \tag{20}$$

where

$$\Phi = \int_{(2\pi)} J(s)d\Omega, \tag{21}$$

$$N = \int S(\rho, 0)d\rho, \tag{22}$$

and the spectrum is $S(\rho,0) = W(\rho,\rho;0)$. The radiation efficiency is known to satisfy the normalization relations $0 \le C \le 1$ for any planar source [11, 12]. On substituting from Eq. (15) into Eq. (21) (and applying the technique of integration by parts [13]), and from Eq. (12) into Eq. (22), we find that

$$C = 1 - D(\xi)/\xi, \tag{23}$$

where

$$D(\xi) = e^{-\xi^2} \int_0^{\xi} e^{t^2}\,dt \tag{24}$$

is the Dawson integral [14] and ξ is given by Eq. (17). Several special cases of Eqs. (23)–(24) corresponding to the ordinary untwisted GSM sources, including the coherent ($\sigma_g \to \infty$), quasihomogeneous ($\sigma_S \gg \sigma_g$), and homogeneous ($\sigma_S \to \infty$) limits, have been previously discussed [11–13]. In this paper we concentrate on the effects of the twist.

Since the magnitude of the normalized twist parameter η is bounded from above by unity, we obtain from Eq. (3) that $u^2 \le 1/k^2\sigma_g^4$. Considering for simplicity the quasihomogeneous TGSM sources only, the values of the parameter ξ in Eq. (17) lead e.g. to the following sequence

$$\xi^2 \approx \frac{k^2\sigma_g^2}{2} \ge \frac{k^2\sigma_g^2}{2(1+k^2\sigma_S^2\sigma_g^2u^2)} \ge \frac{k^2\sigma_g^2}{2(1+\sigma_S^2/\sigma_g^2)} \to \frac{k^2\sigma_g^2}{2}(\sigma_g^2/\sigma_S^2), \tag{25}$$

where the (in)equalities correspond to the homogeneous limit with no twist ($u = 0$), quasihomogeneous source with a twist (u), quasihomogeneous source with maximum twist ($|u| = 1/k\sigma_g^2$), and its limiting value. The radiation efficiency C decreases along this sequence, since according to Eqs. (23)–(24) C is a monotonously increasing function of ξ. Graphs of the radiation efficiency C as its parameters are varied continuously are shown in Fig. 3 both when there is no twist and when there is maximal twist.

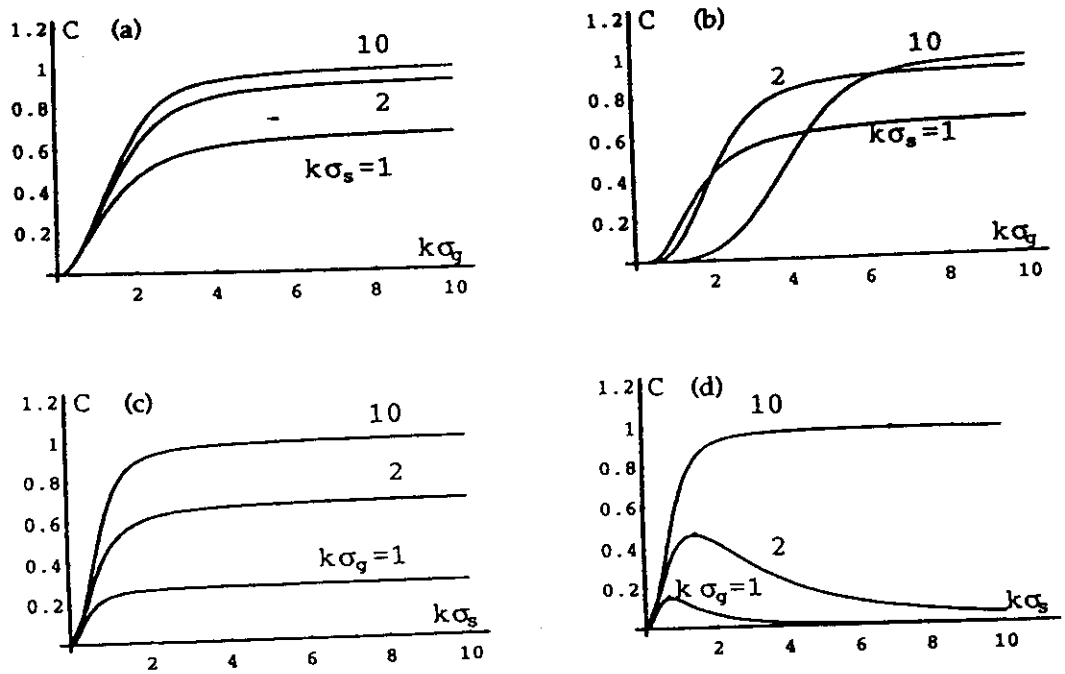

Figure 3. Radiation efficiency C as a function of $k\sigma_g$ for selected values of $k\sigma_S$ (a and b) and as a function of $k\sigma_S$ for selected values of $k\sigma_g$ (c and d), both in the no-twist case $u = 0$ (a and c) and in the maximum-twist case $|u| = 1/k\sigma_g^2$ (b and d).

Concerning the radiation from twisted GSM planar sources, a general equivalence relation in analogy with those discussed earlier [15–17] follows at once from Eqs. (15)–(16) and (23)–(24):

- Any two TGSM sources for which the parameters ξ in Eq. (17) are the same, produce identical angular distributions of the radiant intensity and their radiation efficiencies are equal. If, moreover, the quantities $J(0)$ are the same, then the entire radiant intensities are identical.

Relation (25) indicates that the coherence-induced twist may yield varied effects even among the class of quasihomogeneous sources. We also note that a quasihomogeneous ($\sigma_S \gg \sigma_g$) TGSM source has a higher radiation efficiency than a fully coherent Gaussian laser (rms width σ_L of spectral intensity) if

$$\sigma_g^2 > 4\sigma_L^2(1 + k^2\sigma_S^2\sigma_g^2u^2). \tag{26}$$

When the twist parameter $u = 0$, this result reduces to the corresponding relation obtained before for the ordinary GSM sources [12].

The radiance (brightness) is the principal quantity of a radiometric theory. The generalized radiance function associated with a planar source and compatible with the 'physical optics' expression (10) of the radiant intensity can be defined in several different ways [18]. The most commonly used definition, analogous in some respects with the Wigner distribution function, reads [7, 19]

$$B(\rho, \mathbf{s}_\perp; 0) = \left(\frac{k}{2\pi}\right)^2 \cos\theta \int W(\rho - \rho'/2, \rho + \rho'/2; 0) \exp[-ik\mathbf{s}_\perp \cdot \rho'] \mathrm{d}^2\rho', \tag{27}$$

where the integration is over the source plane. On substituting from Eq. (12) the integral in Eq. (27) can be performed in closed form as above. Expressed using the polar angles $\mathbf{s} = (\sin\theta\cos\phi, \sin\theta\sin\phi, \cos\theta)$, the result is

$$\begin{aligned} B(\rho, \mathbf{s}_\perp; 0) \;=\; & (2W_0/\pi)(k\zeta\sigma_S)^2 \cos\theta \\ & \times \exp[-(k\zeta\xi\rho)^2] \exp\{-2(k\zeta\sigma_S)^2 [\sin^2\theta + 2u\sin\theta(x\sin\phi - y\cos\phi)]\}, \end{aligned} \tag{28}$$

where ξ is given by Eq. (17) and we have also introduced the parameter $\zeta^2 = [1 + 4(\sigma_S/\sigma_g)^2]^{-1}$. It is seen that unlike the radiant intensity $J(\mathbf{s})$, the generalized radiance $B(\rho, \mathbf{s}_\perp; 0)$ associated with TGSM planar sources is not symmetric about the z axis. Because of the twist phenomenon the radiance function (28) contains, in addition to the ξ parameter, an exponential factor that depends both on θ and the azimuthal angle ϕ. When the contributions from the various parts of the source are combined so as to produce the radiant intensity in some given direction, the ϕ dependence disappears. In the limit as $u \to 0$, the usual rotationally symmetric radiance result pertaining to the ordinary GSM sources is recovered [10].

It is of interest to note that the cross-spectral density of light at any pair of points in the far zone can be obtained by suitable source integration of the generalized radiance function $B(\rho, \mathbf{s}_\perp; 0)$ in Eq. (27); this is the essence of the generalized van Cittert-Zernike theorem [20]. Alternatively, and physically more directly, the far-zone cross-spectral density may obviously be calculated simply by using Eq. (12) in conjunction with the appropriate far-field diffraction integral [10, 13]. We recall also that the generalized radiant emittance associated with a fluctuating planar source (counterpart to the generalized irradiance on illumination), consistent with the generalized radiance $B(\rho, \mathbf{s}_\perp; 0)$ in Eq. (27), is expressible in the form [7, 21]

$$E(\rho, 0) = (k^2/2\sqrt{2\pi}) \int W(\rho - \rho'/2, \rho + \rho'/2; 0) J_{3/2}(k\rho')/(k\rho')^{3/2} \mathrm{d}^2\rho', \tag{29}$$

where $J_{3/2}(x)$ is the Bessel function of the first kind and order 3/2. When the symmetrized form of the source cross-spectral density is substituted from Eq. (12), the expression for $E(\rho, 0)$ above can be written in an abbreviated notation as

$$E(\rho, 0) = C(\sigma_S, \sigma_g, u; \rho)\, S(\rho, 0), \tag{30}$$

where $S(\rho, 0)$ is the source spectral intensity and $C(\sigma_S, \sigma_g, u; \rho)$ is an extension of the 'transfer function' for TGSM sources [10, 13]. The quantity $C(\sigma_S, \sigma_g, u; \rho)$ is analogous to the radiation efficiency C and describes the flow of energy into the half-space $z > 0$, but we will not pursue these issues further.

To conclude this section we emphasize that apart from convenience in any particular case, there does not seem to exist any criteria to decide which one of the various generalized radiance functions should be used. Another widely used definition for the generalized radiance is [22,23]

$$B'(\rho, s_\perp; 0) = \left(\frac{k}{2\pi}\right)^2 \cos\theta \int W(\rho', \rho; 0) \exp[-iks_\perp \cdot (\rho - \rho')]\, d^2\rho'. \tag{31}$$

This function can be shown to be closely connected with the point and angle eikonals that characterize wave propagation in lenses, and so it too will be useful in problems of partially coherent radiance transfer through optical systems [23].

4. TGSM beams in optical systems

The passage of twisted GSM beams through an arbitrary rotationally symmetric paraxial system described by an ABCD ray-transfer matrix can readily be analyzed using the extended Fresnel diffraction integral for partially coherent fields. We may take, without any loss of generality, the beam waist $z = 0$ as the system input plane; the effect of free-space propagation between the waist and the actual input plane can always be included as part of the ray-transfer matrix. The parameters characterizing the TGSM beam on exit in the system output plane $z = z_{out}$ then are [24]

$$w(z_{out}) = w(0)(A^2 + B^2 z_R^{-2})^{1/2}, \tag{32}$$

$$\sigma(z_{out}) = \sigma(0)(A^2 + B^2 z_R^{-2})^{1/2}, \tag{33}$$

$$R(z_{out}) = (A^2 + B^2 z_R^{-2})/(AC + BDz_R^{-2}), \tag{34}$$

$$u(z_{out}) = u(0)(A^2 + B^2 z_R^{-2})^{-1}, \tag{35}$$

where z_R is the Rayleigh range given by Eq. (8). Apart from Eq. (35), which is unique to twisted beams, these expressions are the same as those obtained for ordinary GSM beams and Gaussian laser beams, when the appropriate modifications in z_R are taken into account. The ratio $w(z)/\sigma(z)$ (in the beam parameter β) and the product $\sigma^2(z)u(z)$ (in the twist parameter η) are seen to remain invariant.

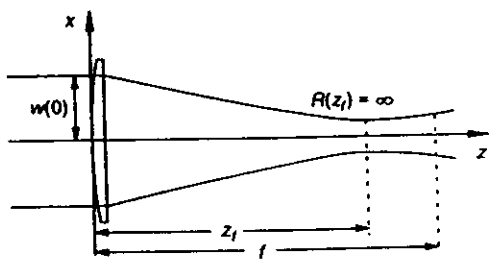

Figure 4. TGSM beam focusing geometry, with exit-beam waist defined by $R(z_f) = \infty$.

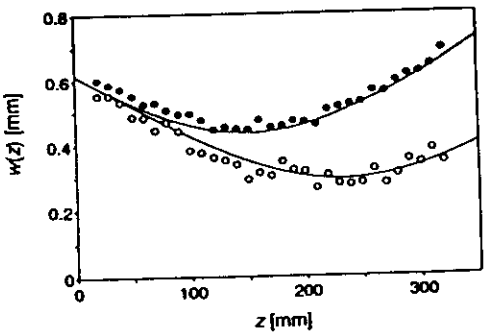

Figure 5. Focused TGSM (solid circles) and ordinary GSM (open circles) beam profiles.

We consider the standard focusing arrangement shown in Fig. 4 as an example. A thin positive lens of focal length f is placed at the input beam waist, and we are interested in the beam properties near the best focus at $z = z_f$ in the image space. Using $A = 1 - z/f$, $B = z$, $C = -1/f$, and $D = 1$ in the exit-beam waist condition $R(z_f) = \infty$, we first find from Eq. (34) that the image distance is [24]

$$z_f = f[1 + (f/z_R)^2]^{-1}. \tag{36}$$

The remaining beam parameters at the image beam waist then are, from Eqs. (32), (33), and (35),

$$w(z_f) = w(0)[1 + (z_R/f)^2]^{-1/2}, \tag{37}$$

$$\sigma(z_f) = \sigma(0)[1 + (z_R/f)^2]^{-1/2}, \tag{38}$$

$$u(z_f) = u(0)[1 + (z_R/f)^2]. \tag{39}$$

According to Eq. (36), the exit-beam waist is not in the geometrical image plane $z = f$, but rather it is closer to the lens. Moreover, since z_R is smaller for a twisted GSM beam than it is for the corresponding ordinary GSM beam [see Eq. (8) and Eq. (19)], the movement of the image waist location is larger for the TGSM beams. This effect is the twist-induced focus shift. In view of Eq. (37), the focused spot size $w(z_f)$ also depends on z_R and for a given $w(0)$ it is the larger the smaller z_R is, i.e. the twist increases the best attainable focal spot. If, for example, the focal length is $f = z_R$, the distance to the best focus is $z_f = f/2$ and $w(z_f) = w(0)/\sqrt{2}$.

In Fig. 5 we show spot-size measurements and theoretical beam profiles, both for the twisted GSM and the corresponding ordinary GSM beams described in Sec. 2, in the focal region of a lens for which $f = z_R(\text{twisted}) = 300$ mm. For the conventional GSM beam the Rayleigh range then accordingly is $z_R = 550$ mm. Theoretically, the position and size of the best focal spot in this case are $z_f = 150$ mm and $w(z_f) = 0.44$ mm for the twisted beam, and $z_f = 230$ mm and $w(z_f) = 0.29$ mm for the ordinary GSM beam. Good agreement between theory and experiment is observed. The rotation of the coherent elliptic Gaussian component beams that make up the TGSM field was also demonstrated. The beams have twisted about the z axis by $\pi/4$ at $z = z_f = 150$ mm and by $\pi/2$ at $z = f = 300$ mm [24].

The generalized radiance functions (27) and (31) are known to obey certain propagation invariance laws along geometric rays when traversing symmetric optical systems. More specifically, for any wavefield the quantity $B(\rho, s_\perp; z)$ remains constant along a paraxial ray within the extended Fresnel diffraction theory [1,25], while the quantity $B'(\rho, s_\perp; z)$ stays unchanged along a ray only in the short-wavelength limit (stationary phase calculation) [23]. Hence

$$B(\rho_o, s_{\perp o}; z_{\text{out}}) = B(\rho_i, s_{\perp i}; z_{\text{in}}), \qquad (\text{finite } \lambda), \tag{40}$$

$$B'(\rho_o, s_{\perp o}; z_{\text{out}}) = B'(\rho_i, s_{\perp i}; z_{\text{in}}), \qquad (\text{asymptotically as } \lambda \to 0), \tag{41}$$

where $(\rho_o, s_{\perp o})$ and $(\rho_i, s_{\perp i})$ are the output and input plane ray coordinates, respectively, connected in the usual way by the systems ABCD matrix. Regarding the twisted GSM beam fields that rotate in optical systems, it is evident that the polar and azimuthal-angle dependence of the generalized radiance [cf. Eq. (28)] is exactly compensated by the twist-induced radial beam evolution and field rotation.

5. Conclusions

The spatial coherence properties of a wavefield are known to influence its (spectral) radiometric behavior. In this paper we have shown that the twist phase associated with the GSM beams further modifies the wavefield's radiometry in a manner that is consistent with viewing the twist as effectively reducing the degree of coherence. The analyses pertained to the exact radiometric description of twisted GSM planar sources and to the paraxial evolution of twisted GSM beams in free space and in ABCD optical systems.

Acknowledgements

The author is a Senior Fellow with the Academy of Finland. Collaboration in parts of this research with J. Turunen and E. Tervonen is gratefully acknowledged.

References

[1] R. Simon and N. Mukunda, "Twisted Gaussian Schell-model beams", *J. Opt. Soc. Am. A* **10**, 95–109 (1993).

[2] A.T. Friberg, E. Tervonen, and J. Turunen, "Interpretation and experimental demonstration of twisted Gaussian Schell-model beams", *J. Opt. Soc. Am. A* (in press, 1994).

[3] For a discussion of coherence and beam concepts, see e.g. A.T. Friberg, "Partially coherent beams", (in this Proceedings).

[4] J. Turunen, E. Tervonen, and A.T. Friberg, "Acousto-optic control and modulation of optical coherence by electronically synthesized holographic gratings", *J. Appl. Phys.* **67**, 49–59 (1989).

[5] D. Ambrosini, V. Bagini, F. Gori, and M. Santarsiero, "Twisted Gaussian Schell-model beams: A superposition model", *J. Mod. Opt.* (in press, 1994).

[6] R. Simon, K. Kundar, and N. Mukunda, "Twisted Gaussian Schell-model beams. I. Symmetry structure and normal-mode spectrum", *J. Opt. Soc. Am. A* **10**, 2008–2016 (1993); "II. Spectrum analysis and propagation characteristics", *J. Opt. Soc. Am. A* **10**, 2017–2023 (1993).

[7] E.W. Marchand and E. Wolf, "Radiometry with sources of any state of coherence", *J. Opt. Soc. Am.* **64**, 1219–1226 (1974).

[8] E. Wolf, "The radiant intensity from planar sources of any state of coherence", *J. Opt. Soc. Am.* **68**, 1597–1605 (1978).

[9] I.S. Gradshteyn and I.M. Ryzhik, *Table of Integrals, Series, and Products* (Academic, New York, 1965), entry 3.321.

[10] H.P. Baltes and B. Steinle, "Radiometry with fields of large coherence area", *Nuovo Cimento* **41** B, 428–440 (1977).

[11] A.T. Friberg, "Effects of coherence in radiometry", *Opt. Eng.* **21**, 927–936 (1982).

[12] A. Gamliel, "Radiation efficiency of planar Gaussian Schell-model sources", *Opt. Commun.* **60**, 333–338 (1986).

[13] W.H. Carter and E. Wolf, "Coherence and radiometry with quasihomogeneous planar sources", *J. Opt. Soc. Am.* **67**, 785–796 (1977).

[14] M. Abramowitz and I.A. Stegun, eds. *Handbook of Mathematical Functions* (National Bureau of Standards, U.S. Government Publishing Office, Washington, D.C., 1964), p. 319.

[15] E. Collett and E. Wolf, "Is complete spatial coherence necessary for the generation of highly directional light beams?", *Opt. Lett.* **2**, 27–29 (1978).

[16] E. Wolf and E. Collett, "Partially coherent sources which produce the same far-field intensity distribution as a laser", *Opt. Commun.* **25**, 293–296 (1978).

[17] F. Gori and C. Palma, "Partially coherent sources which give rise to highly directional light beams", *Opt. Commun.* **27**, 185–188 (1978).

[18] G.S. Agarwal, J.T. Foley, and E. Wolf, "The radiance and phase-space representations of the cross-spectral density operator", *Opt. Commun.* **62**, 67–72 (1987).

[19] A. Walther, "Radiometry and coherence", *J. Opt. Soc. Am.* **58**, 1256–1259 (1968).

[20] E. Wolf and W.H. Carter, "A radiometric generalization of the van Cittert-Zernike theorem for fields generated by sources of arbitrary state of coherence", *Opt. Commun.* **16**, 297–302 (1976).

[21] W.H. Carter, "Four definitions for the term emittance", *Appl. Opt.* **19**, 3419–3420 (1980). Errata: *Appl. Opt.* **20**, 735 (1981).

[22] A. Walther, "Radiometry and coherence", *J. Opt. Soc. Am.* **63**, 1622–1623 (1973).

[23] A. Walther, "Propagation of the generalized radiance through lenses", *J. Opt. Soc. Am.* **68**, 1606–1610 (1978).

[24] A.T. Friberg, E. Tervonen, and J. Turunen, "Focusing of twisted Gaussian Schell-model beams", *Opt. Commun.* **106**, 127–132 (1994).

[25] A.T. Friberg, "Propagation of a generalized radiance in paraxial optical systems", *Appl. Opt.* **30**, 2443–2446 (1991).